CLONING AND CHARACTERIZATION OF NOVEL ISOFORMS OF THE HUMAN RECEPTOR FOR PROSTAGLANDIN F2 ALPHA

by

George A. Vielhauer

A Dissertation Submitted to the Faculty of the

DEPARTMENT OF PHARMACOLOGY & TOXICOLOGY

In Partial Fulfillment of the Requirements
For the Degree of

DOCTOR OF PHILOSOPHY

In the Graduate College

THE UNIVERSITY OF ARIZONA

2004

The University of Arizona ®
Graduate College

As members of the Final Examination Committee, we certify that we have read the dissertation prepared by George A. Vielhauer

entitled CLONING AND CHARACTERIZATION OF NOVEL ISOFORMS OF THE HUMAN RECEPTOR FOR PROSTAGLADIN F2 ALPHA

and recommend that it be accepted as fulfilling the dissertation requirement for the Degree of Doctor of Philosophy

John W. Regan	3/12/04 date
Richard R. Vaillancourt	March 12, 04 date
John W. Bloom	3/12/04 date
Patricia B. Hoyer	Mar 12 2004 date
Ronald Heimark	3/12/04 date

Final approval and acceptance of this dissertation is contingent upon the candidate's submission of the final copies of the dissertation to the Graduate College.

I hereby certify that I have read this dissertation prepared under my direction and recommend that it be accepted as fulfilling the dissertation requirement.

Dissertation Director: 3/12/04 date

STATEMENT BY AUTHOR

This dissertation has been submitted in partial fulfillment of requirements for an advanced degree at The University of Arizona and is deposited in the University Library to be made available to borrowers under rules of the Library.

Brief quotations from this dissertation are allowable without special permission, provided that accurate acknowledgment of source is made. Requests for permission for extended quotation from or reproduction of this manuscript in whole or in part may be granted by the head of the major department or the Dean of the Graduate College when in his or her judgment the proposed use of the material is in the interests of scholarship. In all other instances, however, permission must be obtained from the author.

SIGNED: 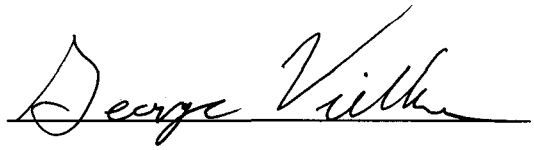

ACKNOWLEDGEMENTS

First, I would like to thank Dr. John W. Regan for the support and guidance he has provided throughout my doctoral studies. Dr. Regan has given me many opportunities to expand my horizons by allowing me to participate in outside collaborations from which I have gained a tremendous amount of knowledge and experience. I venerate Dr. Regan's intelligence, work ethic, scientific integrity as well as attention to detail; they are second to none and it is easy to see why he is very successful.

I would also like to thank my committee members Doctors Richard R.Vaillancourt, Pat Hoyer, John Bloom, and Ronald Heimark for their scientific and professional support.

I would like to thank Dr. Hiromichi Fujino for his time and experience in helping me with my studies. Hiromichi has always been available to listen to ideas and offer valuable advice throughout my graduate experience.

I would like to thank all the other folks in the Regan and Vaillancourt labs; Alfred, Wei, Samit, Tony, Dinesh, Todd, Angela, Kim, Chi-ling, Xiau-Bo, Chris, Vicki, Zach, Nancy, Dee, Ursula, and Ann for their help over the years.

I would like to thank Nancy Hart and Dave Alberts (University of Arizona, Cancer Center) for their help with immunohistochemical staining and Achyut K. Bhattacharyya and Mark Nelson (University of Arizona, Dept. of Pathology) for their help with histological interpretation of the placenta staining data.

I would like to thank Tom Fritz, Terry Matsunaga, Rajan Ramanswami, and Terry R.Barrett for their help early on in my research career. It was a result of their strong influence on me that I participated in the Pharm.D./Ph.D. program.

Last, and certainly not least, I would like to thank my parents, James and Janet as well as my siblings, Katy, Wally, Andy, Matt, and Charlie for their support over the years.

DEDICATION

This dissertation is dedicated to my family, especially my parents, who over the years have supported my efforts with great patience, support, many prayers (mom) and love. I would like to thank my wife and children, of which I have neither, for their lack of support; I am sure that one day they will appreciate the fruits of my labor that have painstakingly taken me twelve years of hard work to accomplish.

TABLE OF CONTENTS

TABLE OF CONTENTS-Continued

LIST OF FIGURES

LIST OF FIGURES-Continued

LIST OF TABLE

LIST OF ABBREVIATIONS

COX-1 = Cyclooxygenase 1

COX-2 = Cyclooxygenase 2

GPCR = G-protein coupled receptor

NSAID = Non-steroidal anti-inflammatory

PCR = Polymerase chain reaction

PGD_2 = Prostaglandin D_2

PGE_2 = Prostaglandin E_2

$PGF_{2\alpha}$ = Prostaglandin $F_{2\alpha}$

PGG_2 = Prostaglandin G_2

PGH_2 = Prostaglandin H_2

PGI_2 = Prostaglandin I_2

PKC = Protein kinase C

PLA_2 = Phospholipase A_2

TM = Transmembrane

TXA_2 = Thromboxane A_2

RT-PCR = Reverse transcriptase polymerase chain reaction

PKA = Protein kinase A

OTR = Oxytocin receptor

GAPDH = Glyceraldehyde-3-phosphate

PI3K = Phosphatidyl inositol 3-kinase

APC = Adenomatous polyposis coli

GSK-3β = Glycogen synthase kinase-3

ABSTRACT

Prostaglandin F2 alpha ($PGF_{2\alpha}$) regulates physiological responses including lowering of intraocular pressure, luteolysis, and parturition. FP prostanoid receptors are GPCRs mediating the actions of $PGF_{2\alpha}$. mRNA splice variants exist for the ovine FP receptor gene and are designated FP_A and FP_B. Thus far, receptor heterogeneity for the human FP receptor gene has yet to be established. This dissertation identifies human FP receptor isoforms and their pharmacological significance.

Utilizing PCR, a putative human FP_B (hFP_B) ortholog from placenta and CX-1 (colon adenocarcinoma) cDNA was identified. These clones produced similar cDNA sequence both containing inverted repeat sequences. However, the mechanism by which the hFP_B is produced appears different from alternative mRNA splicing and remains unexplained. Pharmacological characterization of the hFP_B ortholog is ongoing and its significance remains unknown.

Additionally, we report the cloning of a FP receptor mRNA splice variant from human heart and placenta cDNA, named human FP sevenless (hFP_S). The cDNA encoding hFP_S has a 71 base pair insert that produces a frame shift resulting in a truncated receptor lacking transmembrane-7 and a carboxyl tail. This sequence is identified as a distinct exon localized on the human FP receptor gene. hFP_S mRNA are expressed in human skeletal muscle, heart and placenta. Immunohistochemical staining showed positive immunoreactivity in vascular endothelium, trophoblast, and decidual cells from placenta. hFPs represents the first confirmed alternative splice variant of the human FP prostanoid receptor gene, however, its function is unknown.

Pharmacological characterization of hFP_S demonstrated no significant $PGF_{2\alpha}$ binding or $PGF_{2\alpha}$-mediated inositol phosphate hydrolysis. FLIPR high throughput screening membrane potential assays yielded four potential agonists for hFP_S activation that were not observed in (-)293-EBNA cells; oxytocin, PGB_2, AGNA9B9, and AGNA10B10. These potential agonists require further investigation for hFP_S selectivity and until such data is determined, hFP_S should continue to be considered an orphan receptor.

In conclusion, these studies demonstrate one FP receptor splice variant of the six transmembrane (6TM) nature exists in humans. In addition, preliminary evidence suggests the existence of a hFP_B receptor ortholog potentially generated from a mechanism other than traditional mRNA splicing and could contribute to the development of colon carcinogenesis.

CHAPTER ONE:

INTRODUCTION

Portions of this chapter have appeared previously in Vielhauer G.A., Fujino H., Regan J.W. (2004) Cloning and localization of hFPs: a six-transmembrane mRNA splice variant of the Human FP Prostanoid Receptor. Archives of Biochemistry and Biophysics 421: 175-185.

1.1 Introduction

Prostaglandins are a group of ubiquitously released autacoids that have a history dating back to 1930 where Kurzrok and Lieb observed that human semen can cause either uterine contraction or relaxation (Kurzrok and Lieb 1930). Around that same time at the Karolinska Institute in Sweden, Goldblatt (Goldblatt 1933) and von Euler (Euler 1934) noted that semen extracts could display hypotensive effects leading von Euler to coin the term "prostaglandin" (Euler 1935, Euler 1937). After World War II, Bergstrom and Sjovall (1957) described these extracts to contain various hydroxylated fatty acids that were non-nitrogenous and biologically active. These observations, made 68 years ago, led to the birth of the prostaglandin field and ultimately their adoption into the autacoid family.

Autacoids are biologically active hormones that are locally released in many tissues to exert their physiologic or pathologic effects at multiple receptor subtypes. Eicosanoids are a class of autacoids produced by oxygenation of polyunsaturated long chain fatty acids. Arachidonic acid, a 20-carbon aliphatic acid containing four double bonds, is the most abundant precursor utilized for eicosanoid biosynthesis. Arachidonate is primarily mobilized from membrane phospholipids via phospholipase A_2 (PLA_2) and can be further metabolized by lipoxygenases, epoxygenases, cyclooxygenases and free radicals to form leukotrienes, epoxides, prostaglandins, and isoprostanes, respectively. Figure 1.1 depicts the mobilization of arachidonate from phospholipids and subsequent enzymatic or non-enzymatic (free radical) metabolism to the various eicosanoids.

Prostanoids are formed from unstable intermediates prostaglandin G_2 and H_2 (PGG_2 and PGH_2, respectively) produced by the metabolism of arachidonate via cyclooxygenase isozymes (COX-1 and COX-2). COX-1 (formerly PGH synthase-1) is ubiquitously expressed and has been detected in nearly every cell type (O'Neill and Ford-Hutchinson 1993). Conversely, COX-2 (formerly PGH synthase-2) is nearly undetectable in unstimulated cells yet is capable of being induced (Crofford, Pillemer et al. 1994). Nonsteroidal anti-inflammatory drugs (NSAIDS) can inhibit COX enzymes either irreversibly (e.g. aspirin) or reversibly (e.g. ibuprofen) resulting in a decrease in prostanoid production. COX-1 is thought to serve as a housekeeping protein (e.g., gastric cytoprotection), whereas COX-2 is capable of being induced 10 to 18 fold by specific promoters and is thought to be upregulated in inflammatory, as well as pathological, conditions. This upregulation corresponds to an increase in inflammatory prostaglandins *in vivo* (Masferrer, Zweifel et al. 1994). There are five naturally occurring prostanoid metabolites produced *in vivo*; PGD_2, PGE_2, PGI_2, $PGF_{2\alpha}$, and TXA_2. Interestingly, PGI_2 and TXA_2 are highly unstable compared to the other prostanoids with a half-life of approximately 30 seconds. The specific thromboxane and prostaglandins are produced by their respective isomerase (synthase) from the PGH_2 intermediate. For example, PGH_2 is acted upon by PGD synthase to produce PGD_2. In addition to its own synthase, $PGF_{2\alpha}$ can also be created from PGE_2 by PGE 9-ketoreductase. The prostanoid nomenclature is characterized first by their backbone structure, prostanoic acid, then by their substitution pattern on the cyclopentane ring and finally by the number of double bonds contained within their backbone.

Prostanoids play important roles in several physiological processes. In the female reproductive system PGE_2 and $PGF_{2\alpha}$ have potent oxytocic actions. When given in the first two trimesters, these prostaglandins efficiently terminate pregnancy and are used to prime or ripen the cervix before abortion. However, when administered towards the end of a pregnancy, PGE_2 and $PGF_{2\alpha}$ facilitate labor and have a similar efficacy compared to oxytocin. In the male reproductive system, alprostadil (PGE_1 analog) is used in the treatment of erectile dysfunction. In fetal development, local PGE_2 and PGI_2 production are believed to be required for maintaining patency of the ductus arteriosus. In congenital heart disease, neonatal patency of the ductus arteriosus is maintained by administering PGE_1 before surgery. Conversely, failure of the ductus arteriosus to close after birth is treated with indomethacin to inhibit PGE_2 and PGI_2 production. In the respiratory system, PGE_2 is a bronchodilator and selective PGE_2 agonists are currently under development for the treatment of asthma. Misoprostol, a PGE_1 analog, is used for its cytoprotective effect in the gastrointestinal tract. $PGF_{2\alpha}$ and TXA_2 are strong bronchoconstrictors and were once thought to play a role in the pathophysiology of asthma. However, their clinical efficacy remains questionable. In the immune system, prostanoids play a central role in signaling lymphocytes and macrophages in either an inhibitory or stimulatory fashion depending on the individual agonist. NSAIDS are commonly used in the treatment of many arthritic conditions to block prostaglandin production. In the treatment of glaucoma, $PGF_{2\alpha}$ analogs have been shown to be equally potent at lowering intraocular pressure when compared to beta-blockers. Since prostanoids display diverse functions, investigating prostanoids and their receptors may

not only yield new physiologic roles, but also new target identification.

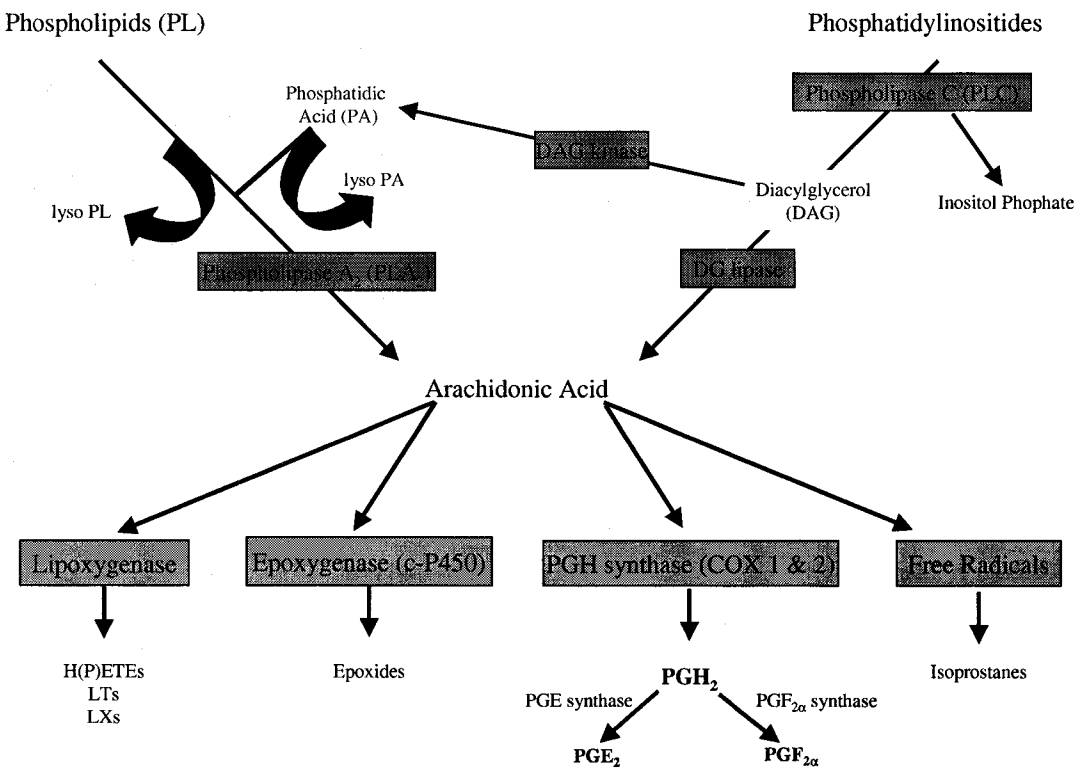

Figure 1.1 Schematic pathways of eicosanoid synthesis from arachidonic acid release and metabolism. Arachidonate is produced from either phospholipids (PL) or phosphatidylinositides by PLA_2 or PLC, respectively. Arachidonic acid is then subjected to further metabolism by lipoxygenases, epoxygenases, cyclooxygenases, or free radicals to produce the various classes of eicosanoids. Individual isomerases (e.g. $PGF_{2\alpha}$ synthase) convert unstable PGH_2 to the five major prostanoid subclasses, PGD_2, PGE_2, PGI_2, $PGF_{2\alpha}$, and TXA_2.

1.2 Prostanoid receptors

Prostanoid receptors are heptahelical proteins spanning seven transmembrane domains with an extracellular amino terminus and an intracellular carboxyl tail. The overall homology between these receptors is low (30%) indicating that they arise from different genes. However, some amino acids, especially the putative transmembrane domains, are highly conserved (Thierauch, Dinter et al. 1994). The 7TM domain displays the highest degree of homology between the prostanoid receptors (Narumiya, Sugimoto et al. 1999). Prostanoid receptors are classified G-protein coupled receptors (GPCR) given that they couple to intracellular heterotrimeric G-proteins. Binding of agonist leads to a receptor conformational change resulting in G-protein dissociation, via an exchange of the guanine nucleotide GDP for GTP, resulting in a second messenger downstream signaling cascade.

Prostanoid receptors are classified by the endogenous ligand that results in their activation. Of the five major naturally occurring prostanoids, PGD_2, PGE_2, $PGF_{2\alpha}$, PGI_2 and TXA_2, each has its own endogenous G-protein coupled receptor that has been pharmacologically defined. Thus, the DP, EP, FP, IP and TP receptors bind PGD_2, PGE_2, $PGF_{2\alpha}$, PGI_2 and TXA_2, respectively (Coleman, Smith et al. 1994). Several key features on the prostanoids are important for their ability to bind to these receptors. First, the substitution pattern on the cyclopentane ring is important for discrimination between the prostanoid receptors and their specific prostaglandin. Second, the C-1 carboxylic acid and the 15-hydroxyl group have been shown to be important functional moieties for interacting with the ligand binding domain. Specifically, the negatively charged C-1

carboxylic acid is thought to have hydrogen and ionic interactions with the positively charged arginine located at the distal end of TM-7. This arginine residue is conserved throughout all prostanoid receptors and mutation of this amino acid results in a dramatic loss of ligand binding shown by analysis of EP_3 and TP receptors (Funk, Furci et al. 1993; Chang, Negishi et al. 1997). Third, stereochemical changes in a single bond on the carbon backbone can cause a complete loss in binding. The naturally occurring isoprostane, 8-iso-$PGF_{2\alpha}$, is produced by non-enzymatic free radical peroxidation of arachidonic acid that changes the stereochemistry at the C-8 position resulting in a complete loss of binding. The five major classes of prostanoid receptors can be further categorized by their ability to display receptor heterogeneity and their second messenger signaling.

Molecular biology identified the individual subtypes and splice variant isoforms encoding all the prostanoid receptors and their subsequent activation and signal transduction (Pierce and Regan 1998). Each of the prostanoid receptors as well as the multiple EP receptor subtypes have been shown to arise from distinct genes. Each of these EP receptor subtypes, designated EP_1, EP_2, EP_3, and EP_4, display differential signaling in response to PGE_2. With respect to signal transduction, the DP, EP_2, EP_4 and IP receptors all couple to G_s resulting in activation of adenylate cyclase and accumulation of cyclic adenosine monophosphate (cAMP). The EP_3 receptors couple to G_i and inhibit adenylate cyclase. The EP_1, FP, and TP receptors couple to G_q and stimulate phospholipase C (PLC), liberating inositol triphosphate and diacylglycerol from phosphatidylinositides.

By mechanism of alternative mRNA splicing within a distinct gene, receptor heterogeneity has been established for the EP_1, EP_3, FP and TP receptors. The prostanoid receptor gene, in general, has two known splice donor sites that allow for alternative splicing to occur. The first is located near the latter half of TM-6 while the second is located in the carboxyl tail approximately ten amino acids from TM-7. Figure 1.2A depicts a schematic representation of the general splicing pattern for the prostanoid genes. Heteronuclear RNA alternative splicing at the first location occurs in all prostanoid receptor pre-mRNAs, with the exception of EP_1 and FP receptors, which do not lead to alternative transcripts. The rat EP_1-variant and bovine 6TM FP variants arise from an insertion at the TM-6 splice site, causing a frame shift in the coding sequence, which results in a truncated receptor lacking an intracellular carboxyl tail. mRNA splicing at the second location generates carboxyl terminal isoforms of the EP_3, FP and TP receptors. These receptors and their respective isoforms demonstrate alternative splicing at the second splice site with identical nucleotide sequence throughout their seven transmembrane domains. Thus, divergence of the nucleotide sequence at this site results in receptor isoforms with intracellular carboxyl tails of different lengths. Phylogenetic analysis of the cloned prostanoid receptors, based on their signal transduction and existence of receptor isoforms, reveals two main branches shown in figure 1.2B. In this analysis, receptors that share the same second messenger coupling are more closely related than receptors that share the same endogenous ligand (Pierce and Regan 1998). The upper branch contains the DP, EP_2, EP_4, and IP receptors due to their coupling to the G_S transduction pathway and lack of receptor isoforms. The lower branch

consists of the prostanoid receptors that display receptor heterogeneity, EP_1, EP_3, FP and TP, coupling to either the G_q transduction pathway (EP_1, FP, and TP) or the G_i inhibitory pathway (EP_3). These analyses suggest that the ancestral prostanoid receptor was of EP origin from which all other prostanoid receptors evolved (Pierce and Regan 1998). To date, the ligand binding properties of the prostanoid receptor isoforms produced by mRNA splicing remain intact. It is interesting to note that even the r-EP_1-variant, lacking an intracellular carboxyl terminus, demonstrates significant binding to PGE_2 (Okuda-Ashitaka, Sakamoto et al. 1996). Conversely, the effects of mRNA alternative splicing appear to have a more pronounced effect on the differential signaling exhibited by each isoform rather than the endogenous ligand they bind (Breyer, Bagdassarian et al. 2001). Each of these receptors will be discussed further individually with special attention to the FP receptor isoforms in relation to their human significance.

A)

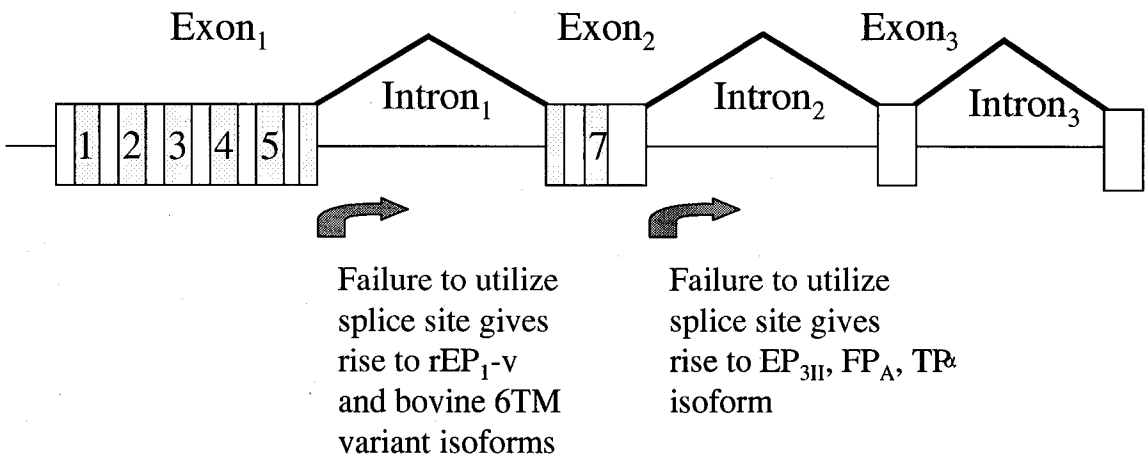
Exon1
Exon2
Exon3
Intron1
Intron2
Intron3
1
2
3
4
5
7
Failure to utilize splice site gives rise to rEP1-v and bovine 6TM variant isoforms
Failure to utilize splice site gives rise to EP3II, FPA, TRα isoform

B)

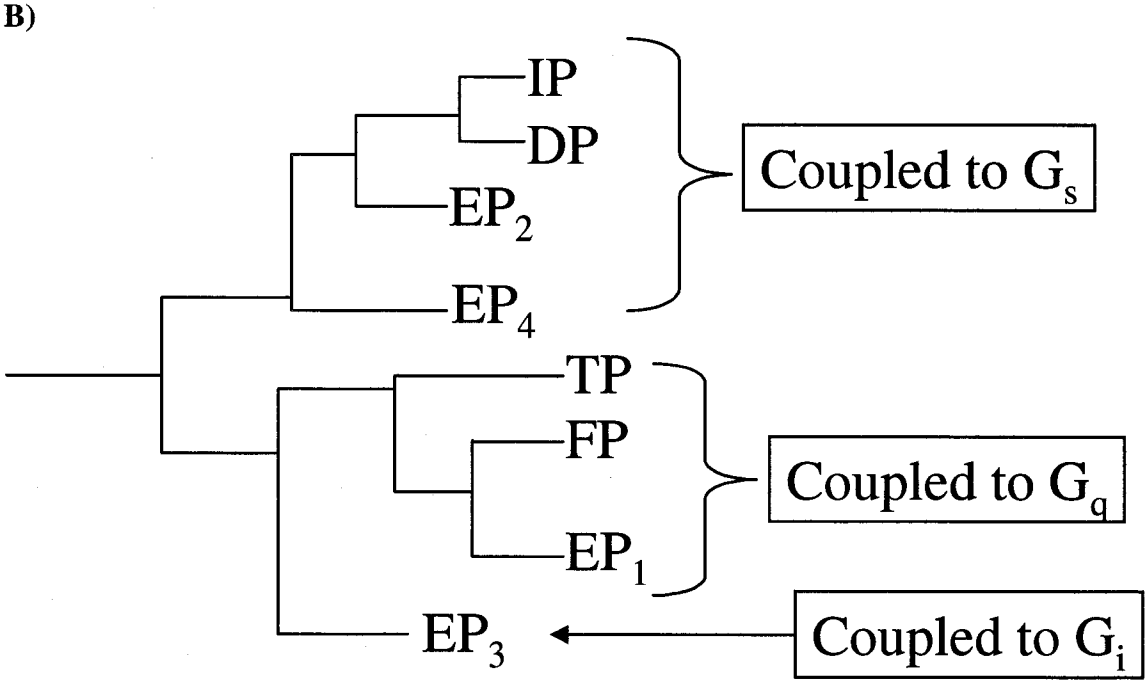
IP
DP
EP2
EP4
TP
FP
EP1
EP3
Coupled to Gs
Coupled to Gq
Coupled to Gi

Figure 1.2 General structure of the prostanoid receptor gene (*A*) and phylogenetic analysis of the prostanoid receptors (*B*). *A*) General model for the exon-intron organization of the prostanoid receptor gene. The numbers refer to the regions encoding transmembrane domains while open boxes depict the amino terminus, intracellular and extracellular loops as well as the carboxy terminus. Arrows depict the two known splice donor sites where alternative splicing results in prostanoid receptor genes. *B*) Phylogenetic schematic of the two main branches of the prostanoid receptors. Receptors that share the same second messenger are more closely related than receptors that share the same endogenous ligand. Therefore, the upper branch containing the DP, EP_2, EP_4 and IP receptors are more closely related given their coupling to stimulation of adenylate cyclase. In the lower branch, EP_1, FP and TP receptors, which couple to stimulation of inositol phosphate turnover as well as calcium mobilization and are more closely related than the EP_3 receptor which is coupled to inhibition of adenylate cyclase (Pierce and Regan 1998).

1.3 TP receptors

The human thromboxane A_2 (TP) receptor was the first eicosanoid receptor to be cloned encoding a 343 amino acid protein (Hirata, Hayashi et al. 1991). This receptor has also been isolated from rat, monkey and mouse. Two alternative splice variants of the TP receptor have been described to exist, designated TP_α and TP_β and were initially cloned from the placenta and endothelium, respectively (Raychowdhury, Yukawa et al. 1994). These two isoforms are identical through their seventh transmembrane domain diverging in their amino acid sequence at the carboxyl terminal of the receptor. The TP_β receptor encodes for a 407 amino acid protein resulting in a longer intracellular carboxyl tail relative to the TP_α isoform. In other species, alternative splicing of the TP receptor have not been described. However, the apparent lack of homology in the variant region between the mouse TP receptor carboxy terminus and either of the human isoforms has been proposed as evidence for the possible existence of further undiscovered splice variants (Narumiya, Sugimoto et al. 1999). Several synthetic TXA_2 analogs have been designed to investigate TP_α and TP_β specific binding due to the unstable nature of the endogenous ligand, TXA_2. The synthetic compound SQ29548 demonstrates a similar K_d, 10 and 12.4 nM, for the TP_α and TP_β isoforms. TP receptors typically couple to the G_q protein resulting in mobilization of Ca^{2+} and DAG. However, recent evidence suggests the TP receptor can also couple to G_{11}, G_{12}, G_{13} and the transglutaminase G_h. Northern blot analysis of mouse tissue revealed the highest levels of TP mRNA to be expressed in the thymus, followed by spleen, lung, and kidney, with lower levels observed in the heart, uterus, and brain (Namba, Sugimoto et al. 1992).

TXA_2 is a potent mediator of platelet aggregation as well as smooth muscle contraction and proliferation. Increased production of TXA_2 has been linked to cardiovascular disease that includes acute myocardial ischemia, heart failure, and renal disease. Acetylsalicylic acid prevents the formation of TXA_2 by inhibiting COX in platelets, thereby reducing morbidity of thrombotic and vascular diseases. In knockout mice, TP receptor deficient mice demonstrated an increased bleeding tendency, and were resistant to cardiovascular shock induced by intravenous infusion of a TP agonist and arachidonic acid (Thomas, Mannon et al. 1998). Considering the involvement of TXA_2 in the pathophysiology of certain diseases, TP receptor antagonists have the potential for therapeutic agents.

1.4 EP_1 receptors

EP_1 receptors mediate the contraction of smooth muscle in various tissues including the gastrointestinal tract, respiratory tract, vas deferens, myometrium and iris sphincter muscle (Coleman and Kennedy 1985). Additionally, EP_1 receptors mediate neurotransmitter release (Ehrenpreis, Greenberg et al. 1973). The cloned human EP_1 receptor cDNA encodes a 402 amino acid protein isolated from an erythroleukemia cell line (Funk, Furci et al. 1993). Initially, activation of the EP_1 receptors was thought to be mediated by G_q leading to phosphatidyl inositol hydrolysis and increased intracellular Ca^{2+}. However, agonist stimulation of the cloned mouse EP_1 receptor causes a robust increase in intracellular Ca^{2+} but only a modest increase in inositol-3, 4, 5-triphosphates (IP_3) suggesting that the EP_1 receptor might not couple to G_q signaling. In subsequent experiments, the PGE_2 stimulated increase in intracellular Ca^{2+} by EP_1 receptors

expressed in Chinese hamster ovary (CHO) cells was abolished by the removal of extracellular Ca^{2+} (Negishi, Sugimoto et al. 1995). Similarly, any PGE_2 stimulated phosphoinositide metabolism was also completely removed by the absence of extracellular Ca^{2+} (Katoh, Watabe et al. 1995).

EP_1 receptors were the first prostanoid receptor to demonstrate alternative splicing at the TM-6 site. The rat EP_1-variant arises from a 425 bp insert in the TM-6 splice site, giving rise to a frame shift, and resulting in a protein of 366 amino acids that was cloned from uterine cDNA and shown to be highly expressed in the kidney (Okuda-Ashitaka, Sakamoto et al. 1996). This EP_1-variant was shown to bind PGE_2 with similar dissociation constant (K_D) and maximal binding (B_{max}) to that of the rat EP_1 receptor. However no signal transduction could be identified. Okuda-Ashitaka et al. (1996) went on to demonstrate that coexpression of the EP_1-variant along with either the EP_1 or endogenous EP_4 receptors in CHO cells could antagonize their respective signal transduction pathway. The pharmacological significance of this truncated EP_1 alternative variant remains unclear.

1.5 EP_3 receptors

The EP_3 receptors display the most diversity of all the prostanoid receptors when generating multiple alternative splice variants. Currently, there are eight human isoforms of the EP_3 receptor, all of which are produced at the carboxyl-terminal splice site. EP_3 receptors mediate various physiological responses including contraction of the uterus (Krall, Barrett et al. 1984), inhibition of gastric acid secretion (Chen, Amirian et al. 1988), modulation of neurotransmitter release (Ohia and Jumblatt 1990), lipolysis in

adipose tissue (Richelsen, Eriksen et al. 1984), sodium and water reabsorption in kidney tubules (Garcia-Perez and Smith 1984), and stimulation of catecholamine release from adrenal chromaffin cells (Tanaka, Yokohama et al. 1990). Recently, EP_3 receptors were implicated in acid-induced duodenal bicarbonate secretion, which is physiologically relevant in the mucosal defense against acid injury (Takeuchi, Ukawa et al. 1999).

An essential question that a number of studies have attempted to answer is the pharmacological significance of these alternative splice variants. Potential functional differences between EP_3 isoforms include signal transduction, receptor phosphorylation, receptor desensitization, and intracellular localization. These splice variants normally inhibit cAMP production through a pertussis toxin-sensitive G_i-coupling. However, supplementary signaling mechanisms coupling to G_s as well as calcium release appear to be differentially activated by different carboxy-terminal tails. The Rho-dependent signal transduction pathway can be initiated by constitutively active forms of the G_{12}, G_{13}, or G_q proteins (Katoh, Aoki et al. 1998). Studies of the bovine EP_3 isoform implicate downstream activation of the Rho-dependent signal transduction pathway suggesting the EP_3 receptor may activate these G-proteins (Aoki, Katoh et al. 1999). The EP_3 receptor also activates PKC and cAMP-independent cAMP-response element (CRE) mediated gene transcription in HEK-293 cells. In canine kidney cells, different patterns of EP_3 receptor localization were shown depending on which mouse EP_3 isoform was expressed, suggesting that splice variants may direct receptors to the nuclear membrane versus the plasma membrane *in vivo* (Hasegawa, Katoh et al. 2000). Currently, the physiological significance of the EP_3 receptor isoforms remains uncertain.

1.6 FP receptors

$PGF_{2\alpha}$ receptors (FP) have been shown to subsist in numerous tissues from a variety of different species. Northern blot analysis of 12 human tissues revealed mRNA expression in the heart, skeletal muscle, colon, kidney, small intestine, placenta and lung (unpublished data). Functional expression of FP receptors has been shown in human granulosa cells and osteoblasts. These receptors are expressed at a high level in the corpus luteum, where they mediate luteolysis. In the myometrium as well as smooth muscle, FP receptors have been shown to elicit contractile responses. The human eye represents the tissue most widely scrutinized for FP receptor expression and function. To date, molecular biology, including functional studies, *in situ* and *in vitro* have shown FP receptor expression in trabecular meshwork (Anthony, Pierce et al. 1998), lens epithelium (Mukhopadhyay, Bhattacherjee et al. 1999), ciliary epithelial and ciliary muscle (Mukhopadhyay, Geoghegan et al. 1997), as well as the iris sphincter muscle (Mukhopadhyay, Bian et al. 2001).

The FP receptor has been cloned from several different species including human, bovine, mouse and ovine (Abramovitz, Boie et al. 1994; Sakamoto, Ezashi et al. 1994; Sugimoto, Hasumoto et al. 1994; Graves, Pierce et al. 1995). The human ortholog of the FP receptor was cloned from kidney cDNA encoding a 359 amino acid protein that has seven putative transmembrane domains. The ovine ortholog was isolated from a large luteal cell cDNA library (prepared from day 10 mid-luteal phase RNA) and encodes a protein of 362 amino acids. Similar to the EP_1, EP_3, and TP receptors, FP receptors display mRNA alternative splicing.

Within the branch of prostanoid receptors that display receptor isoforms, the FP receptors are unique in that they demonstrate alternative splicing at both splice donor sites in the prostanoid receptor gene. The first FP isoform to be unveiled was the ovine FP_B alternative splice variant (Pierce, Bailey et al. 1997). Using a combination of homology-based screening with the original ovine FP receptor as a probe and PCR amplification, Pierce et al. (1997) cloned a carboxyl-terminal isoform from the same ovine mid-cycle large cell corpus luteum library. The strategy for cloning this receptor was based on two important facts. First, prostanoid receptors (EP_1 and TP at the time) of the same phylogeny and signal transduction pathway demonstrated receptor isoforms. Second, Northern blot analysis showed the overall abundance of mRNA for the FP receptor in the mid-cycle corpus luteum library to be unusually high at 0.1% of the total message (Graves, Pierce et al. 1995). Therefore, it was hypothesized that splice variants of the FP receptor exist and could be identified using a library with high FP receptor expression. The resulting isoform discovered from this strategy was designated FP_B compared to the original isoform, which was further defined as FP_A. The ovine FP splice variants are identical in amino acid sequence until they diverge at a tyrosine residue nine amino acids into the carboxy tail. The FP_A isoform continues for 46 amino acids downstream of the splice site while the FP_B has only one additional residue (isoleucine) resulting in a truncated receptor relative to the FP_A (Figure 1.3). Recently, a third FP receptor isoform was cloned from bovine corpus luteum that is created from alternative mRNA splicing at the 6TM site (Ishii and Sakamoto 2001). The bovine 6TM FP receptor splice variant arises from an insertion, which like the 6TM EP_1 variant, causes a frame

shift and premature stop. Unlike the EP_1 variant, however, the bovine 6TM FP variant is not likely to form a seventh TM domain and its carboxyl terminus is probably extracellular. Pharmacological characterization of these isoforms demonstrated common as well as unique properties. Additionally, five bovine FP receptor isoforms have been isolated from corpus luteum cDNA demonstrating alternative mRNA splicing at both the 6TM (2 isoforms) and 7TM (3 isoforms) splice donor sites (Sakamoto, Ishii et al. 2002). However, their protein expression and pharmacology remain to be characterized.

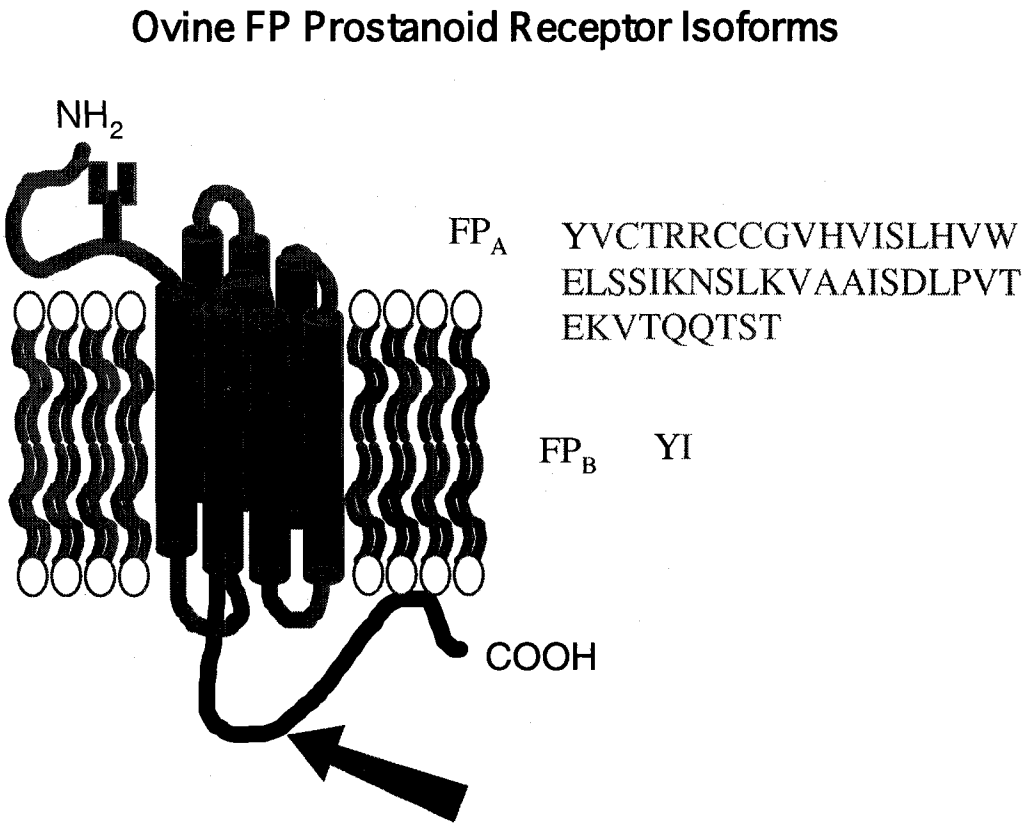

Figure 1.3 Generalized schematic of the ovine FP carboxyl tail receptor isoforms. The arrow indicates where alternative mRNA splicing produces divergence of amino acid sequence for the respective FP_A and FP_B receptor isoforms. Shown at the right is the last conserved tyrosine residue (**Y**) followed by the unique amino acid sequences for each receptor isoform.

Of the three FP receptor isoforms that have been pharmacologically investigated, the bovine 6TM variant is the least characterized. In COS-7 cells, Ishii et al (2001) demonstrated that coexpression of the 6TM variant with the original FP receptor resulted in a suppression of PKC activity stimulated by $PGF_{2\alpha}$. No PKC activity was observed in cells only expressing the 6TM variant and $PGF_{2\alpha}$ radioligand binding of this truncated bovine FP receptor was not reported.

Evidence for functional activation of the original FP receptor, FP_A, by $PGF_{2\alpha}$ via coupling to the G_q signaling cascade is widely present throughout the literature. Initial pharmacological characterization comparing the FP_A and the FP_B isoforms revealed that both isoforms stimulate PKC activation, IP accumulation and calcium mobilization through coupling to the G_q/G_{11} protein subunits (Pierce, Bailey et al. 1997). It was noted in these initial experiments that the FP_B isoform, at the basal level, had IP accumulation that was ~130% of the FP_A isoform. This result was interpreted as the FP_B isoform being more constitutively active relative to the FP_A isoform. The constitutive activity, defined as activity independent of agonist, was observed in COS-7 as well as human embryonic kidney 293-EBNA cells suggesting that this result was not cell specific.

After establishing that both receptors link to G_q signal transduction, efforts were directed at investigating the differences between these isoforms. It was discovered that $PGF_{2\alpha}$-stimulated cardiomyocytes induced hypertrophy and atrial natriuretic factor expression independent of PKC activation (Adams, Migita et al. 1996). The lack of sensitivity of PKC inhibitors to $PGF_{2\alpha}$-stimulated cardiac hypertrophy brought attention to the fact that $PGF_{2\alpha}$ could potentially activate additional transduction pathways other

than the G_q and G_{11} pathways. Furthermore, linking the effects of $PGF_{2\alpha}$ specific signal transduction to the FP_B isoform in cardiomyocytes could produce significant evidence for the presence of a human FP_B ortholog. Likewise, understanding the relationship of $PGF_{2\alpha}$ signaling as it relates to the pathophysiology of cardiac hypertrophy could be useful for potential therapeutic drug targets. To identify the unique signal transduction pathways activated by the FP_A and FP_B receptor isoforms, 293-EBNA stable cell lines were generated expressing each of the respective isoforms.

Early on, subtle differences in cell morphology between the FP_A and FP_B receptor expressing cell lines could be observed under a microscope. Unexpectedly, $PGF_{2\alpha}$ treatment of the FP_A or FP_B cell lines led to the retraction of filapodia, cell rounding, and a cobblestone appearance of the cells (Pierce, Fujino et al. 1999). This result was not observed in untransfected 293-EBNA cells and could not be blocked by inhibiting PKC using bisindolylmaleimide I (BIM). Eventually, phalloidin labeling of the FP receptor expressing cells treated with $PGF_{2\alpha}$ identified the induction of stress fibers by binding to filamentous actin that was not observed in untransfected 293-EBNA cells. Utilizing a specific inhibitor of the small G-protein Rho, C3-exoenzyme, the morphological shape change observed in transfected FP receptor cells was blocked. Correspondingly, p125 focal adhesion kinase (FAK), downstream of the Rho pathway, demonstrated an increase in tyrosine phosphorylation by $PGF_{2\alpha}$ stimulation, which could be largely inhibited by pretreatment with C3-exoenzyme. These data suggest that FP_A and FP_B receptors are capable of coupling to both the G_q and Rho signal transduction pathways. Currently, the pathway from FP receptor to Rho remains undefined. However, the most likely effectors

linking the FP receptors to the Rho pathway are G_{12} and G_{13}. Previously, these two G-proteins have been implicated in the formation of stress fibers and FAK phosphorylation (Needham and Rozengurt 1998). However, thus far no discernible differences could be determined between these FP isoforms.

The first functional differences between the FP_A and FP_B receptors signaling were observed in their differential regulation by PKC (Fujino, Srinivasan et al. 2000). The FP_A and FP_B cell lines stimulate IP formation with maximal response and similar EC_{50} values. However, when pretreated with BIM, the FP_A expressing cells demonstrate enhanced $PGF_{2\alpha}$–stimulated IP accumulation and maximal response in the dose response curve not observed in the FP_B expressing cells. The differential sensitivity to the PKC inhibitor could be explained by the presence of four potential PKC phosphorylation sites in the unique amino acids of the FP_A carboxyl tail. Whole cell lysate along with a GST/FP_A fusion protein utilized in phosphorylation assays demonstrated that the FP_A isoform undergoes a large degree of phosphorylation, while the FP_B isoform demonstrates minimal phosphorylation (Fujino, Srinivasan et al. 2000). Therefore, the inhibition of PKC by BIM results in a decrease of FP_A receptor phosphorylation, thereby preventing its desensitization (negative feedback) causing enhanced $PGF_{2\alpha}$–stimulated total IP formation in the dose response curve. These data represent the first evidence for differential regulation of second messenger signaling by the FP receptor isoforms mediated through PKC dependent phosphorylation. Later pharmacological differences between the FP_A and FP_B receptors were identified with respect to their ability to activate Ca^{2+} dependent Cl^- conductance when expressed in xenopus oocytes (Anthony, Fujino et

al. 2002). More recently, fundamental differences between these isoforms were identified in that the FP_A receptor undergoes a classic agonist-induced and clathrin-dependent internalization, whereas the FP_B receptor undergoes an agonist-independent constitutive internalization that does not involve clathrin (Srinivasan, Fujino et al. 2002).

The $PGF_{2\alpha}$ induced morphological shape change of these isoforms was further investigated leading to a reversal of cell rounding and receptor resensitization discovery. The cell rounding that occurs in cell lines stably expressing each of the FP receptor isoforms were shown to revert back to its original shape more quickly in the FP_A expressing cells than in the FP_B cells. The FP_A cells reversal of cell rounding appears to be complete in an hour whereas the FP_B cells demonstrate no reversal of cell rounding even after two hours (Fujino, Pierce et al. 2000). Figure 1.4 illustrates the differences between the FP_A and FP_B isoforms with regard to reversal of cell rounding after either vehicle or $PGF_{2\alpha}$ treatment for one hour followed by washing of the cells. Correspondingly, the disappearance of stress fibers and dephosphorylation of p125 FAK following removal of agonist are much slower in FP_B expressing cells versus FP_A cells. This result can potentially be explained by a mechanism of receptor resensitization following removal of $PGF_{2\alpha}$. Whole cell radioligand binding as well as functional studies showing agonist induced phosphatidyl inositol hydrolysis and intracellular Ca^{2+} release demonstrate the FP_B isoform resensitizes more slowly than the FP_A isoform. The results of these studies suggest that the carboxyl terminus of the FP_A receptor is critical for resensitization and that the delayed resensitization of the FP_B receptor results in

prolonged signaling. These findings also establish clear pharmacological differences in the activation of these FP receptor alternative splice variants.

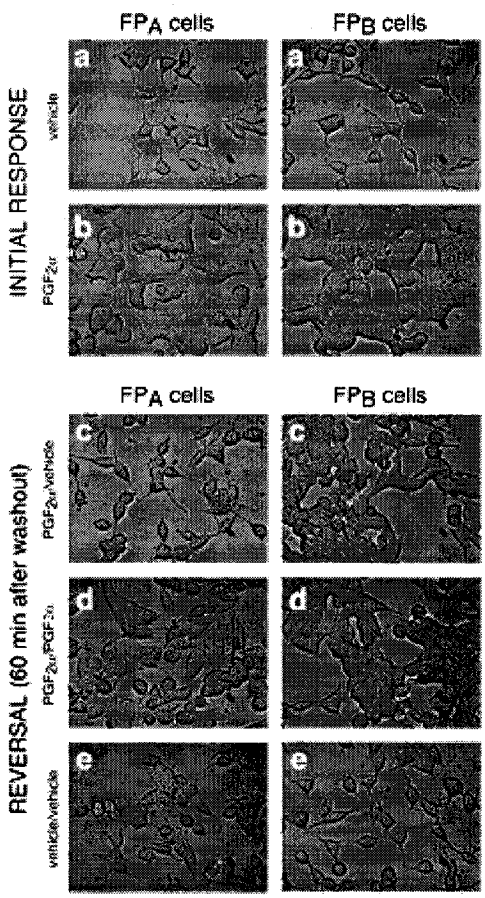

Figure 1.4 $PGF_{2\alpha}$-induced cell rounding (*top*) and its reversal following agonist wash-out (*bottom*) in 293-EBNA cells stably expressing the ovine FP_A and FP_B prostanoid receptor isoforms. Two plates each of FP_A- and FP_B-expressing cells were treated with either vehicle (*panels a*) or 1 μM $PGF_{2\alpha}$ (*panels b*) for 60 min at 37 °C and were then examined for their initial response to these treatments (*top*). Three plates each of FP_A- and FP_B-expressing cells were subjected to the same initial treatment with either vehicle (one plate) or 1 μM $PGF_{2\alpha}$ (two plates) and were washed out by rinsing three times with Opti-MEM followed by the addition of media containing either vehicle alone (*panels c* and *panels e*) or 1 μM $PGF_{2\alpha}$ (*panels d*). After a 60 minute incubation at 37°C, the cells were examined for reversal of cell rounding. The notation to the *left* of the *bottom panels* refers to the initial treatment/treatment after washout (*e.g.* in *panels c*, the initial treatment was with 1 μM $PGF_{2\alpha}$, and the treatment after wash-out was with vehicle). Images were obtained at a magnification of x75. These results are all from one experiment that was repeated over 10 times with virtually identical results. (Reproduced with permission from Fujino and Pierce et al., 2000)

The most significant finding demonstrating differential FP receptor isoform signal transduction involved a molecular mechanism that links the constitutive agonist-independent internalization of the FP_B isoform with the selective activation of T-cell factor (Tcf)/β-catenin signaling by the FP_B isoform and not the FP_A isoform (Fujino and Regan 2001). An important finding from this study was agonist-induced Tcf/β-catenin transcriptional activation could be blocked by inhibiting the Rho-mediated cellular shape change pathway. In a second report, several additional findings were reported describing the cellular conditioning of the FP_B expressing cells, involving phosphatidyl inositol-3-kinase (PI3K), β-catenin and E-cadherin (Fujino, Srinivasan et al. 2002). The FP_B receptor interacts with the p85 subunit of PI3K that can be disrupted upon receptor activation by $PGF_{2\alpha}$. Inhibiting PI3K blocks the basal constitutive internalization of the FP_B receptor, which results in an accumulation of receptor on the plasma membrane. It also results in an increase in membrane-associated expression of E-cadherin, β-catenin, and PI3K. Together with the FP_B receptor, these proteins form a macromolecular complex that undergoes constitutive internalization, in the absence of $PGF_{2\alpha}$, that can be blocked by wortmannin, a specific PI3K inhibitor (Fujino, Srinivasan et al. 2002). It is important to note that the expression of E-cadherin and β-catenin are significantly greater in FP_B expressing cells when compared to FP_A cells. Upon $PGF_{2\alpha}$ stimulation of FP_B cells, increased expression of β-catenin was also observed to undergo a major reorganization along the regions of cell to cell contact, not observed in FP_A cells (Fujino and Regan 2001). As a result of this work, a two step mechanism was proposed in which FP_B expressing cells first undergo an agonist-independent conditioning step involving

constitutive internalization of the FP_B receptor followed by an agonist-dependent activation step leading to Tcf transcriptional activation through a β-catenin signaling pathway. Figure 1.5 represents a schematic of the common, as well as unique, signal transduction pathways for the FP receptor isoforms. It also has been reported that the FP_B isoform stimulates COX-2 promoter activity in 293-EBNA cells suggesting the potential for increased COX-2 expression, which may result in increased prostaglandin production (Fujino and Regan 2003a). Interestingly, it has been established that abnormal activation of Tcf/β-catenin signaling is associated with the development of colorectal cancer (Korinek, Barker et al. 1997; Morin, Sparks et al. 1997; Peifer and Polakis 2000) and that inhibition of COX by NSAIDs can slow tumor progression (Smalley and DuBois 1997). Given the recent data published on the ovine FP_B receptor and the evidence surrounding the etiology of colorectal cancer, colon cancer cells represent a potential target for the identification of a human FP_B ortholog.

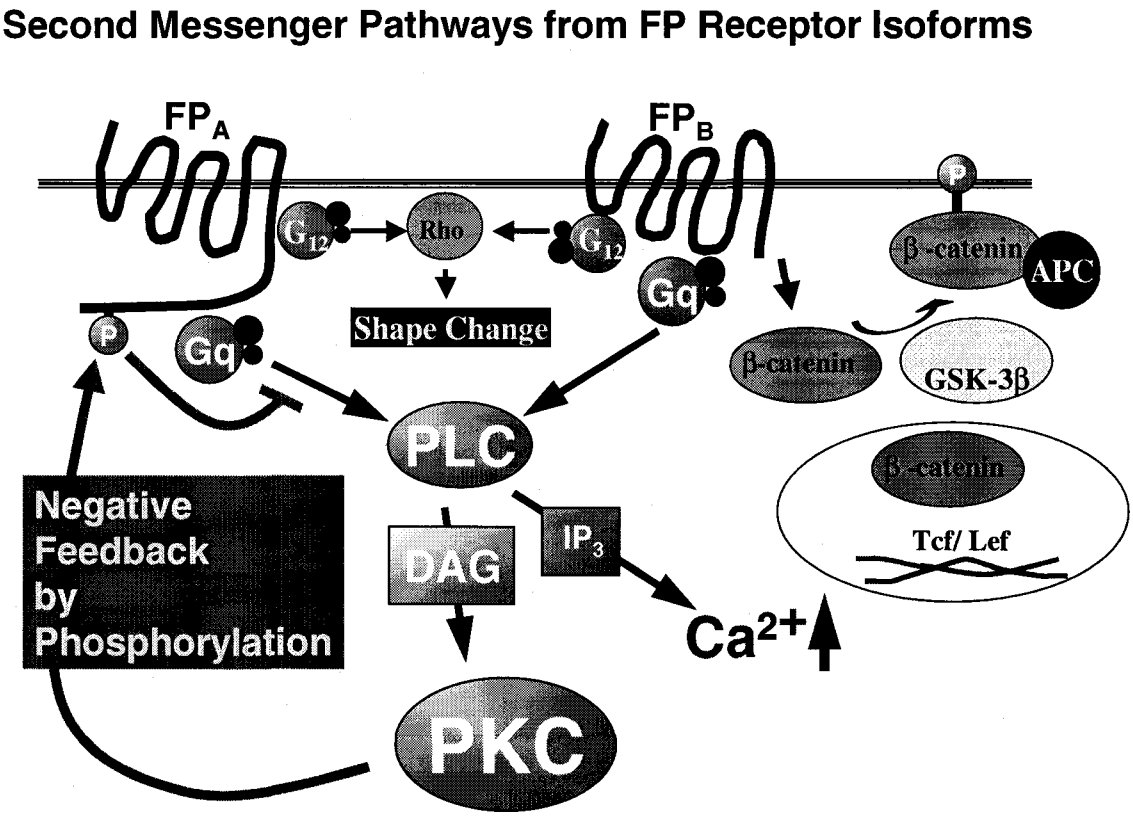

Figure 1.5 Common and unique signal transduction pathways for the FP receptor isoforms. Both FP_A and FP_B receptor isoforms are capable of coupling to the G_q protein hydrolyzing phosphatidylinositol lipids resulting in activation of PKC and Ca^{2+} mobilization. Individually, the FP_A receptor isoform undergoes a negative feedback desensitization through a PKC mediated phosphorylation while the FP_B receptor activates Tcf/β-catenin signal transduction. Both isoforms activate the small G-protein Rho resulting in a morphological change that can be reversed in FP_A expressing cells but not FP_B. APC: adenomatous polyposis coli, GSK-3β: glycogen synthase kinase-3, PLC: phospholipase C.

1.7 Hypothesis and aims

Alternative mRNA splice variants have been demonstrated for the EP_1, EP_3, FP, and TP prostanoid receptors. To date, only the EP_3 and TP receptors have displayed receptor heterogeneity in human. With respect to FP receptors, the bovine and ovine species demonstrate alternative mRNA receptor isoforms at two separate splice donor sites within the FP prostanoid receptor gene. The bovine isoforms display alternative splicing at both the 6TM and carboxyl tail splice donor sites while the ovine generates its receptor isoforms utilizing the carboxy terminal splice site. **The overall hypothesis of my dissertation is that human FP receptor mRNA alternative splice variants in the coding region exist and demonstrate physiological and pharmacological differences relative to the known FP receptor.**

To examine this hypothesis, molecular biology techniques will be utilized to identify unique cDNA clones, which will be further scrutinized using an array of pharmacological assays to identify its pharmacological and physiological relevance. These assays will employ the use of a stable cell line created in 293-EBNA cells as well as any human tissue and cell line that may endogenously express an FP alternative splice variant. The pharmacological assays will include identification of ligand (endogenous or exogenous) and characterization of signal transduction with an emphasis on second messenger signaling, gene transcription, and mobilization of intracellular ions as well as membrane phospholipids. If possible, specific antibodies will be generated to the unique amino acid sequence displayed by newly identified FP receptor isoform(s) for the

purpose of distinguishing differences in localization, internalization and desensitization from the known FP receptor.

CHAPTER TWO:

CLONING OF A PUTATIVE HUMAN FP_B ORTHOLOG FROM CX-1 COLON ADENOCARCINOMA AND PLACENTA cDNA

2.1 Introduction

To date, alternative splice variants of the human FP receptor have yet to be identified, although bovine and ovine receptor isoforms have been established. The ovine isoforms demonstrate alternative mRNA splicing in the carboxy terminus of the FP prostanoid receptor gene resulting in a truncated FP_B splice variant. It is important to note that the FP_A and FP_B receptor isoforms are identical in amino acid sequence up to the tyrosine residue in the carboxyl terminus. After the tyrosine residue, alternative splicing produces the truncated FP_B isoform that continues for one additional amino acid, an isoleucine, while the FP_A isoform continues for 46 additional amino acids producing a longer intracellular carboxyl tail (Figure 1.3).

Previously, in 293-EBNA cells stably expressing the FP_B receptor, activation of the Tcf/β-catenin signaling pathway was observed (Fujino and Regan 2001). Activation of this pathway is believed to be an important event in the development of colon cancer (Srivastava, Verma et al. 2001). Furthermore, mutations in either β-catenin or the adenomatous polyposis coli (APC) protein resulting in unregulated Tcf/β-catenin signaling are responsible for 65% of patients with hereditary nonpolyposis colorectal cancer (Srivastava, Verma et al. 2001). Early adenoma markers demonstrate increases in cytosolic β-catenin and successive formation of a β-catenin/Tcf complex leading to the induction of COX-2 expression that is characteristic of late adenoma and carcinoma (Srivastava, Verma et al. 2001). Another characteristic marker of colon cancer cells is a robust expression of PI3K (Petiot, Ogier-Denis et al. 2000). Similarly, cells expressing the FP_B receptor show a constitutive PI3K activity that may lead to an increase role of β-

catenin expression (Fujino, Srinivasan et al. 2002). Clinical studies have demonstrated PI3K activity that was approximately four-fold higher in colorectal tumor tissue as compared with normal tissue from the same patient (Phillips, St Clair et al. 1998), which strikingly resembles the four-fold increase in PI3K activity observed in FP_B cells relative to control FP_A cells (Fujino, Srinivasan et al. 2002). The FP_B expressing cells also demonstrate a Rho-dependent $PGF_{2\alpha}$ activation of a COX-2 promoter (Fujino and Regan 2003a). Collectively, the unique pharmacological signal transduction of the FP_B expressing cells, but not the FP_A cells, demonstrates remarkable similarities to those observed in human colon cancer cell lines. Therefore, the pharmacological demonstration of the FP_B receptor as well as the effects of NSAIDS as chemopreventive agents against colon cancer provides a possible link to cancer.

In humans, it is my hypothesis that a human FP_B ortholog exists demonstrating a similar carboxy terminus splice donor site (near the tyrosine residue) and amino acid sequence resulting in a truncated receptor. Alternatively, it is important to note that the FP_B isoform may be generated by a means independent of alternative mRNA splicing. It is feasible for a human FP_B ortholog to be produced by post-translational proteolytic cleavage of the FP_A receptor or by post-transcriptional alteration of the FP_A mRNA.

In this chapter we report the identification of a human FP_B ortholog that was cloned from placenta as well as a CX-1 human colon cancer cell line. However, the mechanism by which it is produced appears to be different from alternative mRNA splicing and remains difficult to explain. Furthermore, attempts at functional characterization of this receptor will be presented.

2.2 Experimental procedures

2.2.1 cDNA cloning

Human heart, uterus, placenta and CX-1 colon adenocarcinoma Marathon Ready™ cDNA was obtained from Clontech Laboratories (Palo Alto, CA). PCR reactions were performed according to the manufacturer's protocol using the Advantage Taq polymerase from Clontech (product #8417-1). The initial PCR program used was 95°C for 5 min, 95°C for 1 min, 70°C for 1 min, 72°C for 6 min repeat steps 2-4 for five cycles, then 95C° for 1 min, 68°C for 1 min, 72°C for 6 min repeat steps 6-8 for five cycles, then 95°C for 1 min, 66°C for 1 min, 72°C for 6 min repeat steps 10-12 for 20 cycles then 72°C for 15 min followed by a 4°C hold. This reaction utilized a FP sense primer, corresponding to Genbank accession no. L24470 nucleotide 613, GGCAGTGTGATGGCCATTGAGCGGTGTATTGG, with the anti-sense adaptor primer (AP1). All adaptor primers, AP1 and AP2, used in the Rapid Amplification of Complimentary Ends (RACE) PCR were included in the Marathon Ready™ cDNA kit. The resulting placenta PCR reaction was diluted 1:5 in water and nested PCR was performed. The colon adenocarcinoma amplified products were directly ligated into pGEM-T (below), as nested PCR was not required. The nested placenta PCR was identical to the previous program, except the total number of cycles was decreased to 20. The nested PCR reaction utilized a FP sense primer, corresponding to Genbank accession No. L24470 nucleotide 736, GCTTTGCTGCCCATCCTTGGACATCGAGAC, with the anti-sense nested adaptor primer (AP2). Products from the entire PCR amplification

were purified using Gene Clean II according to the manufacturer's instructions (BioRad product #1001-200).

Purified PCR products were ligated into the pGEM-T vector using a cloning kit (Promega #Q5601; Madison, WI) and the instructions provided therein. Following the ligation, bacteria were transformed and positive colonies were selected for the preparation of plasmid DNA using a crude alkaline lysis protocol (Zhou, Yang et al. 1990).

Purified plasmid DNA was digested with restriction enzymes specific to the multiple cloning site and electrophoresed on 1.2% agarose gels to separate the PCR inserts from the pGEM-T backbone. The gel was then denatured, neutralized and DNA was transferred to a nylon membrane by blotting overnight using 20x SSC. Following transfer the membrane was washed and baked for 2 hr at 80°C in preparation for Southern blot analysis.

2.2.2 Southern blot analysis

A 228 bp probe, starting in the third intracellular loop and spanning the 7TM, was prepared by digesting $hFP_A/pcDNA_3$ with *BglII* and *HindIII* and radiolabeled with [^{32}P]dCTP using a nick translation kit (Gibco product #18160-010). Following purification with an Amicon spin column (Millipore product #42409), the probe was used for Southern blot analysis according to standard protocols (Maniatis, Fritsch et al. 1982). Clones containing positive inserts were digested with *BglII* and *HindIII*, which yielded a single 228 base pair product corresponding to the previously cloned human FP receptor.

Positive clones that did not yield this product were sent for DNA sequencing. The resulting DNA sequences were analyzed (Macvector 7; Accelrys, Burlington, MA) and compared to the previously cloned human FP receptor. This strategy yielded four out of 44 clones from placenta and nine out of 12 clones from colon adenocarcinoma of putative hFP_B/pGEM-T. To avoid confusion, the previously cloned human FP receptor will hereafter be referred to as hFP_A.

2.2.3 Construction of a putative hFP_B expression vector

$hFP_B/pcDNA_3$, a full-length clone encoding human FP_B, was prepared by digesting the $hFP_A/pcDNA_3$ and hFP_B/pGEM-T clones with *BglII* that cuts at nucleotide 958 (Fig. 2.1, double underline) in the coding sequence of both hFP_A and hFP_B. The digests were then treated with *NotI* which cuts in the multiple cloning site of $pcDNA_3$ and pGEM-T. The larger fragment from the digest of $hFP_A/pcDNA_3$ (containing the 5' end of the hFP_A receptor) and the smaller fragment from the digest of hFP_B/pGEM-T (containing the 3' end of the hFP_B clone) were purified using Gene Clean II, then ligated and subcloned to yield $hFP_B/pcDNA_3$.

2.2.4 Transient transfection protocol and cell culture

293-EBNA cells used for radioligand binding, IP accumulation and Tcf/lymphocyte enhancer binding factor (Lef) reporter gene assays were all transfected in the same fashion. Cells were split into 10 cm dishes and the next day were transiently transfected using FuGENE-6 (Roche Molecular Biochemicals) with 10 μg/dish of the respective cDNA plasmid for each of the individual experiments. Untransfected as well

as transiently transfected 293-EBNA cells were maintained in Dulbecco's modified Eagle's medium (DMEM, Life Technologies, Inc.) containing 10% fetal bovine serum (FBS), 250 μg/ml Geneticin and 100 μg/ml gentamicin. 293-EBNA cells stably expressing the ovine FP_B receptor were maintained in the same media as untransfected 293-EBNA cells only hygromycin (200 μg/ml) was included to maintain receptor expression. CX-1 cells were maintained in RPMI 1640 with 10% FBS (Life Technologies, Inc.) and 1% pen/strep antibiotic (L-glutamine, 100 units/ml penicillin G, and 100 mg/ml of streptomycin; Life Technologies, Inc.)

2.2.5 Membrane enrichment and whole cell radioligand binding

Radiolabeled [^{3}H]$PGF_{2\alpha}$ (218 Ci/mmol) and unlabeled $PGF_{2\alpha}$ were obtained from Amersham and Cayman Chemical, respectively. CX-1 cells were first membrane enriched as previously reported (Woodward, Fairbairn et al. 1995). Briefly, cells were washed with PBS, trypsinized and neutralized with media. Cells were centrifuged for 10 minutes at 400 x g using a Beckman tabletop centrifuge with swinging buckets and resuspended in 2 ml homogenization buffer (0.25 M sucrose, 5 mM MES, 1 μM indomethacin, pH 7.4). The cells were then homogenized using a polytron homogenizer layered onto an equal volume of 1 M sucrose then centrifuged at 112,700 x g for 22 minutes using a Beckman ultracentrifuge and NVT 100 rotor. The pellet fraction was collected and resuspended in homogenization buffer and centrifuged at 304,000 x g for 9 min using the same centrifuge. The pellet was collected and resuspended in MES working buffer (10 mM MES, 0.4 mM EDTA and 10 mM $MnCl_2$) containing 1 μM indomethacin. Protein assay were performed to determine the amount of protein added to

each tube and membranes were subsequently used for radioligand binding. Total and nonspecific binding was determined in triplicate for each experiment. Total and nonspecific binding samples contained 100 µl enriched membrane added to a final assay volume of 200 µl containing MES working buffer (diluent), 2.5 n M [^{3}H]$PGF_{2\alpha}$ alone (total binding) or 2.5 nM [^{3}H]$PGF_{2\alpha}$ plus 10 µM unlabeled $PGF_{2\alpha}$ (nonspecific binding), respectively. Samples were incubated for 1 hr at room temperature then reactions were terminated by filtration through Whatman GF/C glass filters using a cell harvester (M-24R, Brandel) and washed in ice cold MES working buffer. Samples were then determined on the scintillation counter and specific binding calculated

Cells, used for whole cell radioligand binding, were washed in PBS, trypsinized, gently centrifuged and washed once more in MES working buffer. Following the final wash, cells were resuspended in MES working buffer at a concentration of 10^7 cells/ml, and 100 µl was added to a final assay volume of 200 µl containing MES working buffer (diluent), 2.5 nM [^{3}H]$PGF_{2\alpha}$ alone (total binding) or 2.5 nM [^{3}H]$PGF_{2\alpha}$ plus 10 µM unlabeled $PGF_{2\alpha}$ (nonspecific binding), respectively. Incubations were for 1 hr at room temperature and reactions were terminated as previously described. Filters were washed five times with ice-cold MES working buffer, and radioactivity was determined on the scintillation counter and specific binding calculated.

2.2.6 Inositol phosphate (IP) assay

293-EBNA cells were transfected with either the human FP_A/$pcDNA_3$ or FP_B/$pcDNA_3$ receptor plasmid and grown to a confluence of approximately 90-100%. Cells were maintained as previously described, and the night before the experiment 0.2

uM myo-[2-^{3}H]Inositol (Amersham, 16.6 Ci/mmol) were added to the cells in regular DMEM containing no serum. The following morning cells were washed with PBS then trypsinized and 10^6 cells were aliquoted per sample. Cells were then centrifuged in a Beckman tabletop centrifuge and resuspended in DMEM containing 10 mM LiCl (Sigma) to prevent breakdown of IPs. Cells were allowed to equilibrate for 10 min at 37°C/5% CO_2. Treatment groups were performed in duplicate with each sample receiving either vehicle (0.002% $NaCO_3$) or 1 μM $PGF_{2\alpha}$ for one hour. After 1 hr, samples were centrifuged and washed with PBS followed by total inositol extraction by adding 2.5 ml of methanol/chloroform/water (1:1:0.5). Samples were then vortexed and centrifuged (4°C). After centrifugation, the aqueous phase was added to H_2O and loaded onto the elution columns. Poly-Prep chromatography columns 0.8 x 4 cm (Bio-Rad) were loaded with 10% AG 1-X8 resin (Bio-Rad) and washed with H_2O. The columns were then washed three times with H_2O and two times with five mM sodium tetraborate (borax, Sigma)/60 mM sodium formate (Sigma). The ^{3}H-IP were eluted with 0.2 M ammonium formate/0.1 M formic acid (Sigma) and radioactivity determined by liquid scintillation counting. Data analyzed using PRISM software.

2.2.7 RNA collection

CX-1 cells were collected and centrifuged at 4°C, then suspended in ice-cold lysis buffer and placed on ice. Lysis buffer contained 140 mM NaCl, 1.5 mM $MgCl_2$, 10 mM Tris-HCl (pH 8.6), 0.5% Nonidet P-40 (NP40), and 10 mM vanadyl ribonucleotide complexes (RNase inhibitor). The cell mixture was slowly loaded onto an equal volume of sucrose lysis buffer then centrifuged at 4°C for 10 min. Sucrose lysis buffer contained

24% sucrose, 140 mM NaCl, 1.5 mM $MgCl_2$, 10 mM Tris-HCl (pH 8.6), 0.5% Nonidet P-40 (NP40), and 10 mM vanadyl ribonucleotide complexes (RNase inhibitor). The supernatant was mixed with an equal volume 0.2 M Tris-HCl (pH 7.5), 25 mM EDTA, 0.3 M NaCl, 2% sodium dodecyl sulfate (SDS) and 200 µg/ml of proteinase K, incubated at 37°C for 40 minutes, extracted with phenol then precipitated with sodium acetate and ethanol.

2.2.8 Northern blot analysis

For each sample 30 µg total RNA were added to an equal volume of 4x sample buffer (6.4 M formaldehyde, 40 mM sodium-phosphate buffer pH 7.4, 2 mM EDTA (pH 8.0) in DEPC-H_2O) and 2x the volume of formamide. RNA samples were denatured at 65°C for 5 min then ¼ the volume of sample application buffer (0.5% SDS, 0.025% bromophenolblue dye, 25% glycerol, 25 mM EDTA in H_2O) was added to each sample. Samples were electrophoresed in a 1% formaldehyde/sodium-phosphate agarose gel (2.2 M formaldehyde, 0.02 M phosphate buffer (pH 7.4), in DEPC- H_2O) at 70 V. The gel was transferred overnight onto a nylon membrane (BioRad) using 20x SSC and subsequently cross-linked by baking at 80°C for 2 hours. A hybridization solution containing 50% formamide, 1x SSC, 0.1% SDS, Denhardt's Reagent, and DNA salmon sperm was prepared to block the membrane overnight at 42°C. A 228 base pair probe, starting in the third intracellular loop and spanning the 7TM, was prepared by digesting $hFP_A/pcDNA_3$ with *BglII* and *HindIII* and was radiolabeled with [^{32}P]dCTP using a nick translation kit (Gibco product #18160-010). Probes were purified utilizing an Amicon spin column (Millipore product #42409). Membranes were blocked, hybridized and

washed in a low salt buffer (0.01x SSC, 0.1% SDS) then exposed to X-ray film and developed.

2.2.9 CX-1 colon adenocarcinoma and normal human colon RT-PCR

Two micrograms of either CX-1 RNA from above or normal human colon RNA (Stratagene, #735009) were treated with DNase (Life Technologies, Inc.) then 25 mM EDTA was added and the reaction was inactivated at 65°C for 10 min. Oligo(dT) were added and first strand synthesis carried out by adding half of the above RNA mix to two tubes along with the reverse transcription (RT) mix. The RT mix contained 5 µl first strand buffer (250 mM Tris-HCl, pH 8.3, 375 mM KCl, 15 mM $MgCl_2$), 1 µl dNTP (10 mM), 2 µl DTT (0.1 M), and DEPC-H_2O per 10 µl RNA. For each sample, two treatment groups were performed, one with reverse transcriptase (RT+) and one without (RT-). The samples were then incubated for 50 min at 42°C followed by 15 min at 70°C and ice for 5 min. RNase H (4 units) was added to each tube and incubated for 20 min at 37°C.

CX-1 cDNA PCR was performed using primers designed to the human FP receptor as well as glyceraldehyde-3-phosphate (GAPDH). The FP primers consisted of two generic sets (FP_{gen1}, FP_{gen2}) capable of amplifying any FP receptor isoform and a specific set (FP_A) discriminating the known human FP receptor. The first set of generic primers (FP_{gen1}) consisted of a sense primer, GGCAGTGTGATGGCCATTGAGCGGTGTATTGG and an anti-sense primer, ATTCCATGTTGCCATTCGGAGAGC, corresponding to Genbank accession no. L24470 nucleotides 613 and 1124, respectively. The second set of generic primers (FP_{gen2}) consisted of sense primer, AACAGCCTTGCCATCGCCATTCTC, and anti-

sense primer, GGTTTTGTGACTCCAATACACCGCTC, corresponding to Genbank accession no. L24470 nucleotides 367 and 656, respectively. The FP_A specific set used the same FP_{gen1} sense primer from above (nt 613) and a FP_A specific anti-sense primer, CTAGGTGCTTGCTGATTTCTCTGCAACTGG, corresponding to nucleotide 1317. Human GAPDH primer pair included the following sequences; GAPDH sense TGGGTGTGAACCATGAGAAG; and GAPDH anti-sense, TCTACATGGCAACTGTGAGG. Each PCR reaction contained 0.4 μM of the respective primer sets (FP_A, FP_{gen1}, FP_{gen2} or GAPDH), 0.2 mM dNTP, 1.5 mM $MgCl_2$, 1x PCR buffer [20 mM Tris-HCl (pH 8.4), 50 mM KCl], 0.5 U Taq polymerase (Gibco) and nuclease free water per 50 μl reaction. The PCR amplification were run under the following conditions 95°C for 5 min initial denaturing step, followed by 95°C for 1minute, 58°C for 1 min, 72°C for 1 min for 35 cycles and ending with 72°C for 15 min. PCR reactions were electrophoresed on a 1.2% agarose gel and visualized for FP_{gen1}, FP_{gen2}, FP_A and GAPDH specific PCR product sizes of 511, 289, 704 and 736 base pairs, respectively.

Human colon cDNA PCR was performed utilizing two sets of primers designed to the human FP receptor as well as GAPDH. The FP primer sets consisted of a generic set (FP_{gen1}) and a specific FP_A set discriminating the known human FP receptor. Primer sequences are as follows: the FP generic PCR reaction utilized the same primer set listed above (FP_{gen1}), while the FP_A specific set used the same FP_{gen1} sense primer from above (nt 613) and a FP_A specific anti-sense primer, GCAACTGGTGACTCAGAAATAGCAGC (nt 1295). Human GAPDH primers were

the same as previously stated. Each PCR reaction was set up as previously reported. The PCR amplification cycle consisted of 95°C for 5 min initial denaturing step, followed by 95°C for 1 min, 62°C for 1 min, 72°C for 1 min for 45 cycles and ending with 72°C for 15 min. PCR reactions were electrophoresed and visualized for FP_{gen1}, $FP_{A,}$ and GAPDH specific PCR product sizes of 511, 682, and 736 base pairs, respectively.

2.2.10 Tcf/Lef reporter gene assay

CX-1 cells or 293-EBNA cells stably expressing the ovine FP_B receptor were split into 10 cm dishes and the next day were transiently transfected as previously described with either the wildtype Tcf/Lef reporter plasmid TOPflash or the mutant plasmid FOPflash. FOPflash differs from TOPflash by the mutation of its Tcf binding sites and serves to differentiae Tcf/β-catenin-mediated signaling from background (Upstate Biotechnology, Inc.). Cells were incubated overnight then treated for 1 hr at 37°C with either vehicle or 1 μM $PGF_{2\alpha}$. They were then rapidly washed three times each with Opti-MEM (Life Technologies, Inc.) as described previously (Fujino and Regan 2001) and incubated for 16 h at 37°C in 10 ml of their respective media. Cells were placed on ice, rinsed twice with ice-cold PBS and extracts were prepared using the Luciferase Assay System (Promega). Luciferase activity in the extracts (~500 ng protein/ sample) was measured using a Turner TD-20/20 luminometer and was corrected for background by subtraction of FOPflash values from corresponding TOPflash values.

2.3 Results

A combination of RACE PCR, Southern blot analysis, restriction enzyme mapping and DNA sequencing were used to identify potential human FP mRNA

alternative splice variants screened from human heart, uterus, placenta and colon adenocarcinoma cDNA libraries. Two cDNA's, one from placenta and one from CX-1 colon adenocarcinoma cDNA libraries were cloned that encode a human ortholog of the ovine FP_B receptor, Figure 2.1 and Figure 2.2, respectively. These figures depict the partial cDNA and amino acid sequences obtained from placenta and CX-1 colon adenocarcinoma starting at nucleotide 900 of the GenBank accession no. L24470. The human FP_A and placenta FP_B isoform are identical up to nucleotide1183, at which point there is a divergence in the FP_B receptor nucleotide sequence relative to the FP_A. The FP_B isoform continues for only 37 nucleotides before reaching its poly-A tail resulting in a 7TM truncated receptor with a significantly shorter intracellular carboxyl tail. Comparing the ovine FP receptor isoforms to human, the splice donor site is in the exact location that would be predicted, nine amino acid residues into the carboxyl tail with tyrosine being the last conserved residue. Following this tyrosine residue, the ovine FP_B isoform continues on for one amino acid (isoleucine) while the human ortholog (317 amino acids.) contains three additional amino acids, proline, arginine, and isoleucine before reaching its stop codon. For the human FP_A (359 amino acids), it continues for 40 additional amino acids downstream of the tyrosine residue resulting in the longer intracellular carboxyl tail. The rectangular boxes indicate an inverted repeat region that appears to be responsible for the unique coding of the hFP_B receptor isoform and may indicate that this isoform is generated by a means different than that of alternative mRNA splicing. The unique 37 nucleic acids in the human FP_B sequence shown, downstream of the putative splice donor site (gray and italics), are comprised of 33 bp from the inverted

repeat region and four bp outside the inverted repeat region making up the final portion of the 3´UTR before the poly-A tail.

The FP_B cDNA sequence from colon CX-1 adenocarcinoma is very similar to the placenta in that it produces a similar unique amino sequence downstream of the carboxyl terminal splice donor site and also contains an inverted repeat region. However, the nucleotide sequence and inverted repeat region in the CX-1 sequence display some differences when compared to the placenta FP_B sequence. Figure 2.2 depicts the partial cDNA and amino acid sequence starting at nucleotide 900 of the GenBank accession no. L24470. The cDNA sequence is identical to that of the previously cloned hFP_A (Abramovitz, Boie et al. 1994) up to nucleotide 1147 where the FP_B isoform diverges resulting in a 7-TM truncated receptor. Similarly, the last four residues of the CX-1 FP_B are conserved compared to the placenta FP_B. The CX-1 FP_B also contains an inverted repeat sequence shown in boxes that is in the same region relative to the placenta FP_B but is three nucleotides shorter. The CX-1 FP_B receptor differs from the placenta FP_B receptor nucleotide sequence at positions 1147-1149, 1156-1173 and 1180-1182. Interestingly, in both hFP_B cDNA sequences the inverted repeat region surrounds nucleotides 1147-1149 as well as 1180-1182. It seems unlikely that in two distinct tissues, placenta (healthy specimen) and CX-1 (diseased specimen) that these virtually identical sequences could be produced at this exact location as a result of inefficient mRNA processing either naturally or artificially. If these data were artifact, it seems more likely that the mechanism by which they arise would differ slightly with respect to their location. Therefore it can be hypothesized that these two nucleotide sequences

(1147-1149 and 1180-1182) are very important for the generation of the hFP_B ortholog and should be subsequently investigated further to support the presence of a hFP_B ortholog. The pharmacological significance of the hFP_B ortholog will be determined by utilizing the placenta cDNA sequence to construct a plasmid.

Interestingly from the cDNA cloning studies, mRNA expression levels of hFP_A: FP_B receptor isoforms from placenta yielded a ratio of approximately 9:1 upon *in silico* DNA analysis. However, in the CX-1 colon adenocarcinoma *in silico* DNA analysis the ratio of hFP_A: FP_B receptor isoform mRNA was estimated to be 0:9. To further investigate this result, RNA was collected from a CX-1 cell line and analyzed by Northern blot analysis as well as RT-PCR.

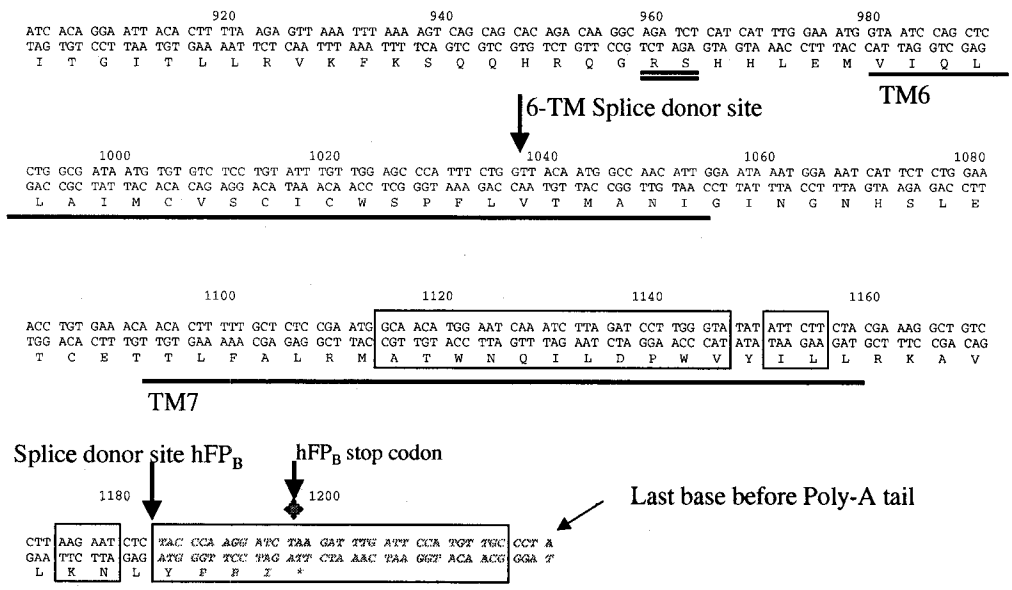

Figure 2.1 Partial cDNA and deduced amino acid sequences of the placenta human FP$_B$ isoform. The cDNA sequence is based on the previously cloned human FP receptor (Abramovitz, Boie et al. 1994) and starts with nucleotide 900 of the Genbank accession no. L24470. These FP receptor isoforms have identical nucleotide sequence up to nucleotide 1183 where the FP$_B$ isoform diverges at the carboxy terminus splice site (*large arrow*) resulting in a 7-TM truncated receptor with a shorter carboxyl tail. The transmembrane domains (TM) are underlined and numbered TM6 and TM7. The unique nucleotide as well as amino acid sequence appear as gray, bold and italics (nt. 1183). The double underline represents the *BglII* site (nt. 958) that was utilized to create a full-length hFP$_B$ coding sequence. The boxes depict the inverted repeat sequence that is responsible for generating the human FP$_B$ ortholog.

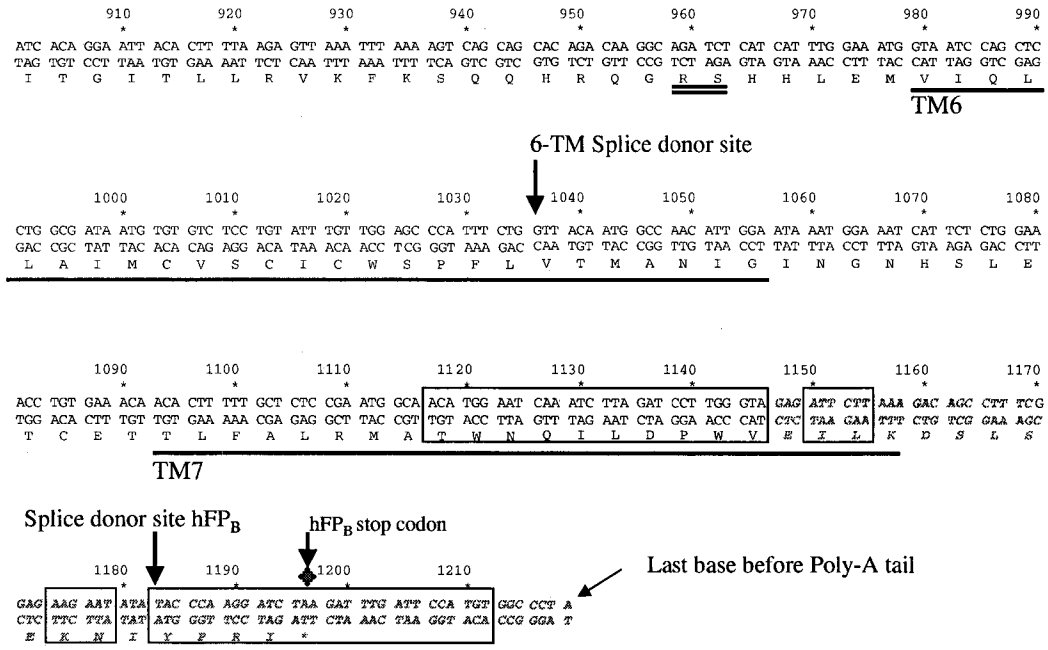

Figure 2.2 Partial cDNA and deduced amino acid sequences of the CX-1 colon adenocarcinoma human FP$_B$ isoform. The cDNA sequence is based on the previously cloned human FP receptor (Abramovitz, Boie et al. 1994) and starts with nucleotide 900 of the Genbank accession no. L24470. These FP receptor isoforms have identical nucleotide sequence up to base nucleotide 1147 where the FP$_B$ isoform diverges resulting in a 7-TM truncated receptor with a shorter carboxyl tail. The transmembrane domains (TM) are underlined and numbered TM6 and TM7. The unique nucleotide as well as amino acid sequence appear as gray, bold and italics (nt. 1147). The boxes depict the inverted repeat sequence that is responsible for coding the human FP$_B$ ortholog.

Northern blot analysis of CX-1 RNA utilizing a generic probe recognizing any FP receptor isoform failed to yield any conclusive results (data not shown). One explanation is that the message level of the hFP_B ortholog is below the limits of detection by northern blot analysis.

Utilizing hFP_A specific primers and two different sets of generic primers (hFP_{gen1} and hFP_{gen2}) capable of amplifying any hFP isoform, RT-PCR was performed with CX-1 RNA shown in Figure 2.3 (top and middle panels). If the CX-1 cells express only a hFP_B ortholog as predicted by the cDNA cloning data, then PCR with the above primers should produce only a product with the hFP_{gen} primers. In Figure 2.3, lane 1 in the top (n=2) and middle panels (n=1) shows a PCR product obtained with the two separate sets of hFP_{gen1} and hFP_{gen2} primers corresponding to the correct sizes of 511 bp and 289 bp, respectively. Conversely, lane 4 shows no products were observed of the expected size, 704 bp, in either the top or middle panel utilizing the hFP_A specific primers. Lane 7 depicts a product (736 bp) of the expected size for the GAPDH positive control primers. Lanes 2, 5, and 8 correspond to negative controls in which CX-1 cDNA template was omitted for the reaction while lanes 3, 6, and 9 represent negative controls reactions where RT was not used.

To confirm expression of the hFP_A receptor in normal colon tissue, the same RT-PCR strategy described for the CX-1 tissue was utilized. Figure 2.3 (bottom panel) depicts RT-PCR utilizing the hFP_{gen}, hFP_A and GAPDH primers sets. Lane 1, in the bottom panel, shows a PCR product obtained with the hFP_{gen1} primers corresponding to the correct size of 511 bp. Lane 4 depicts the PCR product (685 bp) obtained with the

hFP_A specific primers described in experimental procedures. Lane 7 illustrates the PCR product (736 bp) obtained with the GAPDH specific primers. Lanes 2, 5, 8 and 3, 6, 9 represent the corresponding negative controls as previously described above. The cDNA cloning data, along with the observations from the CX-1 PCR reactions, suggest mRNA for the human FP_A receptor are expressed in normal human colon tissue but not in at least one type of cancerous colon tissue.

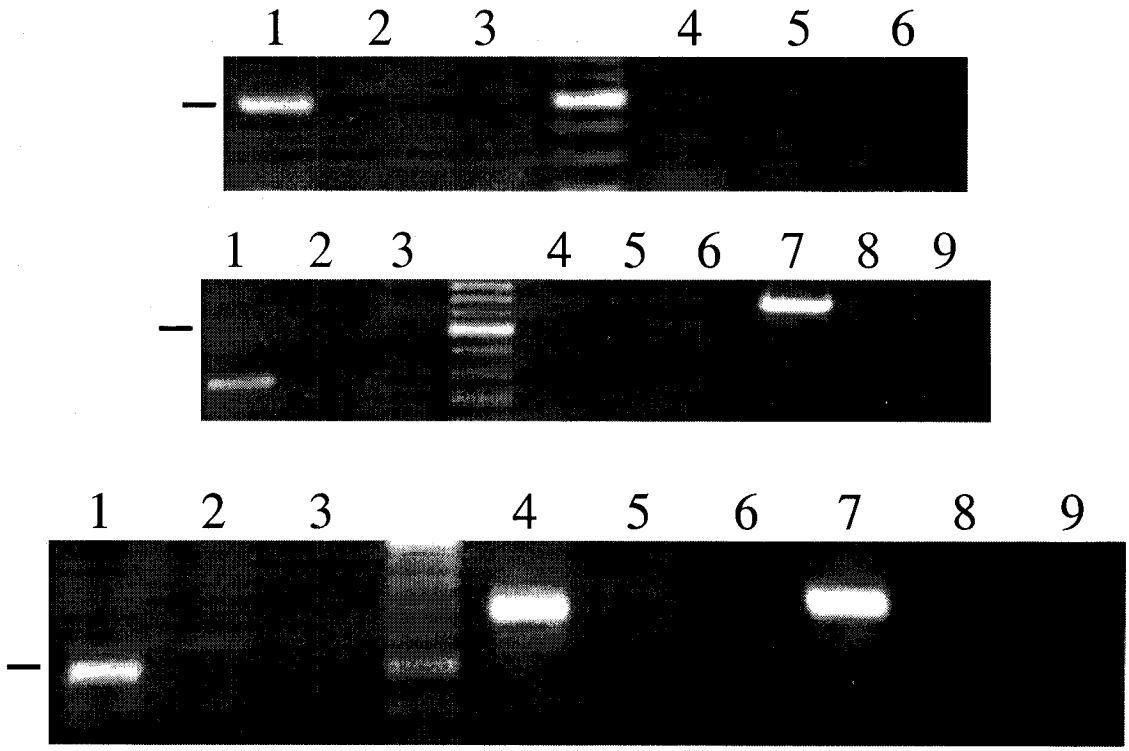

Figure 2.3 RT-PCR of CX-1 (colon adenocarcinoma) cell RNA (*top and middle panels*) and human colon RNA (*bottom panel*) utilizing hFP_{gen1} and hFP_{gen2} primers (*lanes 1-3*), hFP_A primers (*lanes 4-6*) and GAPDH primers (*lanes 7-9*). *Lane 1* (*top and bottom panels*) depicts a PCR product (511 bp) using a hFP_{gen1} (nt 613-1124) primer set. *Lane 1* (*middle panel*) shows a PCR product (289 bp) obtained with a second set of hFP_{gen2} (nt. 367-656) primers. *Lane 4* (*top, middle, and bottom panels*) illustrates the absence (*top and middle panel*, 704 bp) and presence (*bottom panel*, 682 bp) of PCR products utilizing hFP_A specific primer sets. Lane 7 (*middle and bottom panels*) demonstrates PCR products (736 bp) for the GAPDH primer set. *Lanes 2,5 and 8* are corresponding negative controls lacking cDNA template, while *lanes 3, 6, and 9*, represent negative control reactions where RT was not used. A 100 bp ladder is shown between *lanes 3 and 4*. Tick marks indicate the location of the 500 bp standard.

The placenta hFP_B cDNA sequence was placed in a $pcDNA_3$ expression vector to investigate the radioligand binding properties as well as its pharmacological significance. Radioligand binding of $[^3H]PGF_{2\alpha}$ was performed on 293-EBNA cells transiently transfected with vector, hFP_B, or hFP_A plasmid. Likewise, CX-1 cells were investigated for $[^3H]PGF_{2\alpha}$ radioligand binding to corroborate the endogenous expression of the hFP_B receptor. Figure 2.4 depicts total and non-specific binding for the CX-1 adenocarcinoma cells as well as the transiently transfected 293-EBNA cells. Panel A depicts the total and non-specific binding of 293-EBNA cells transfected with (left to right) vector alone, hFP_B or hFP_A receptor. The total binding in these studies is the difference between the total and nonspecific radioligand activity. Both the hFP_A and hFP_B receptors display significant specific $PGF_{2\alpha}$ binding, however these results are from a single experiments and could not be further repeated. Panel B shows the radioligand binding of endogenous putative hFP_B receptor thought to be expressed in CX-1 cells as compared to mouse JB6 epidermal cells used as a positive control for expression of an endogenous FP receptor. These data represent a single experiment and suggest a small amount of specific binding when compared to the JB6 cell line.

A)

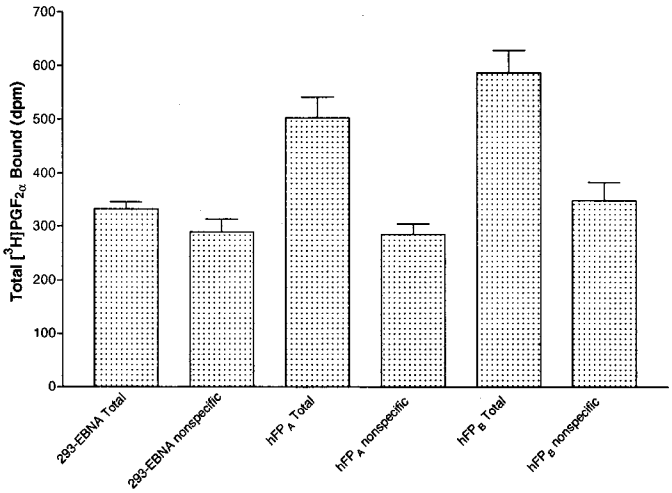

B)

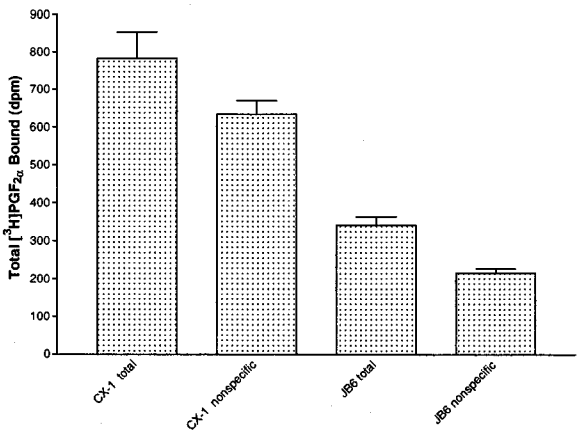

Figure 2.4 [^{3}H]PGF$_{2\alpha}$ Radioligand binding competition studies of transiently transfected 293-EBNA or CX-1 cells. *A*) Whole cell radioligand binding as described in *EXPERIMENTAL PROCEDURES* of 293-EBNA cells transiently transfected with vector, hFP$_B$, or hFP$_A$ plasmid. *B*) Membrane enriched radioligand binding of CX-1 and mouse JB6 epidermal cells (positive control). Data are a means ± of a single experiment for each panel performed in duplicate.

CX-1 colon adenocarcinoma cells were further investigated for a $PGF_{2\alpha}$ functional response by evaluating phosphatidylinositol hydrolysis. CX-1 cells were pretreated with indomethacin (right) or vehicle (left) overnight to block any endogenous prostaglandin production via the COX pathway. Cells were then stimulated with $PGF_{2\alpha}$ and total IP accumulation was determined. Figure 2.5 shows a moderate IP accumulation in both $PGF_{2\alpha}$ treatment groups compared to vehicle treated controls. Pretreatment with indomethacin did not appear to have any effect on increasing IP accumulation in these cells. The data suggest the possible presence of an endogenous FP receptor within this cell line.

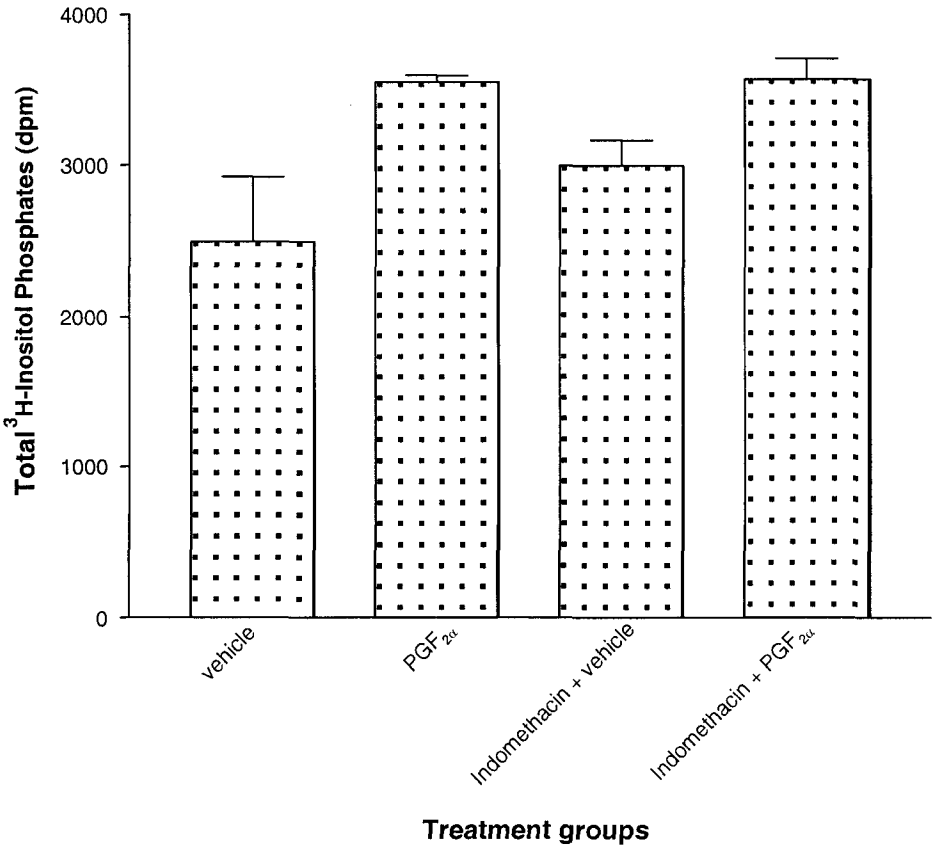

Figure 2.5 $PGF_{2\alpha}$ stimulated IP accumulation in cells endogenously expressing the putative hFP_B isoform. *Columns three and four* (left to right) were pretreated with indomethacin overnight while *columns one and two* received only vehicle. The next day CX-1 cells were subsequently treated with either vehicle (Na_2CO_3) or $PGF_{2\alpha}$ and total IP accumulation were determined. Data are a means $\pm$ of a single experiment for each column and treatment groups were performed in triplicate.

Previously it has been demonstrated that the ovine FP_B expressing cells, upon $PGF_{2\alpha}$ stimulation, activate Tcf/β-catenin mediated signaling (Fujino and Regan 2001). Aberrant activation of Tcf/β-catenin signaling is associated with the development of colorectal cancer (Korinek, Barker et al. 1997; Morin, Sparks et al. 1997; Peifer and Polakis 2000). It is plausible, therefore, to hypothesize that if an hFP_B ortholog exists in the CX-1 cell line, as the data suggest, it should activate a Tcf/Lef β-catenin reporter construct upon $PGF_{2\alpha}$ stimulation. To test this hypothesis, CX-1 cells or ovine FP_B expressing cells were transiently transfected with a Tcf/Lef reporter gene construct then stimulated with $PGF_{2\alpha}$. Figure 2.6 depicts β-catenin mediated reporter gene activation of CX-1 and ovine FP_B cells upon $PGF_{2\alpha}$ stimulation.

A)

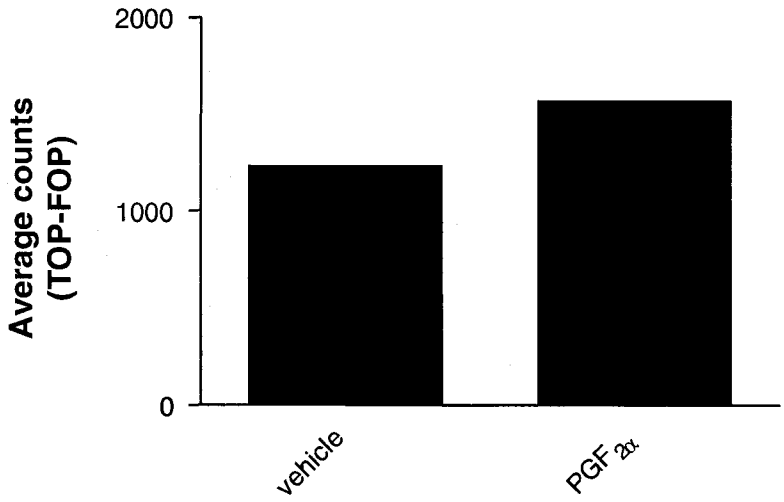

B)

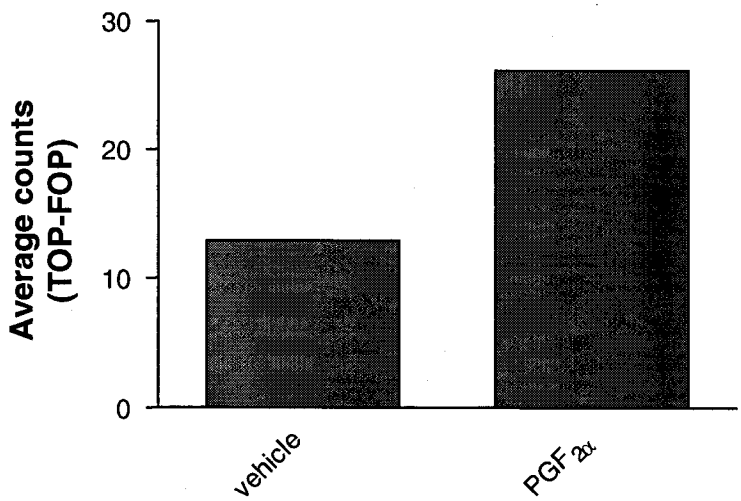

Figure 2.6 $PGF_{2\alpha}$ stimulation of Tcf/Lef-responsive luciferase reporter gene activity in ovine FP_B and CX-1 adenocarcinoma cells. *A*) Ovine FP_B expressing cells and *B*) CX-1 cells after 1 hr treatment with either vehicle or $PGF_{2\alpha}$, then washed extensively and incubated for 16 hr at 37°C in drug-free media. Luciferase data represent a single experiment each performed in duplicate.

2.4 Discussion

Previously, FP receptor mRNA alternative splice variants were identified from a ovine mid-cycle large cell luteal library and were named FP_A and FP_B (Graves, Pierce et al. 1995; Pierce, Bailey et al. 1997). Recently, six bovine FP receptor isoforms were cloned from a bovine corpus luteal library (Sakamoto, Ishii et al. 2002). These isoforms display mRNA alternative splicing at both splice donor sites previously described, three diverge their nucleotide sequence at the 6TM site and three at the carboxyl terminal splice site. It is feasible that one of these three splice variants at the carboxyl terminal splice site could be a bovine FP_B ortholog. Interestingly, in looking at the amino acid sequence of these three isoforms, one clone (FP-α) has two conserved residues at the end similar to the human FP_B. Where the hFP_B ends with the amino acid sequence proline, arginine, and isoleucine the bovine FP-α ends with an arginine, isoleucine, and asparagine. However, the bovine carboxy terminal splice variants physiological and pharmacological significance remains uncertain, as only their cDNA sequence has been reported. Likewise, since these isoforms have not been submitted to GenBank, it is not possible to investigate the carboxy terminal splice variant's for the presence of an inverted repeat in their respective cDNA sequence. Two cDNAs, one from placenta and one from a CX-1 colon adenocarcinoma, were cloned encoding a putative human FP_B receptor isoform. The placenta ortholog bears a more striking resemblance to the ovine FP_B than the CX-1 isoform in that it diverges at the exact location, a tyrosine residue in the carboxyl tail, as do the ovine FP isoforms. Both human FP_B clones share similar properties, in that the last four amino acid residues are conserved and they both contain

an almost identical inverted repeat that is responsible for generating their unique amino acid sequence. The CX-1 ortholog nucleotide sequence diverges upstream of the tyrosine residue resulting in a slightly different amino acid sequence relative to the placenta hFP_B. The differences between the putative hFP_B receptors in CX-1 and placenta nucleotide sequence can be explained by two possibilities. First, the CX-1 unique nucleotide sequence could result from DNA aberrations or recombination that are commonly seen in a malignant cell lines. Second, the amino acid sequence within the region of the inverted repeat may not be as important as the actual truncation of the receptor itself, for protein function, resulting in small but insignificant differences in amino acid sequence. The inverted repeat in each of these cDNA clones causes some concern and suggest two possibilities for their occurrence. First, they are generated by a mechanism other than mRNA alternative splicing, possibly post-transcriptional modification of the original human FP receptor (hFP_A) message RNA. Second, these orthologs are simply a cloning artifact produced from PCR or a result of an engineered cDNA library. The former seems to be the most likely scenario to be the most likely for the following reasons: first, the chances that an FP_B ortholog could be produced as an artifact diverging its sequence at the exact location that was predicted from the ovine FP isoforms seem highly unlikely. Second, the fact that the hFP_B isoform was cloned from two separate cDNA libraries and produces virtually the same sequence further strengthens the arguments that it exists. Finally, the unique amino acid sequence and truncated carboxyl tail closely resemble the ovine FP_B isoform in that of the three unique amino acids, the last is an isoleucine residue that is conserved between human and ovine species. Interestingly, there are reports in the

literature of 3' UTR terminal inverted repeat mRNA sequences that have been hypothesized to function in a capacity that increases stability or represses protein translation of specific mRNA.

Attempts to functionally characterize these two clones were made by transiently transfecting the placental hFP_B clone or using the CX-1 cell line as an endogenous system to gain a functional response to $PGF_{2\alpha}$. While, initial studies in radioligand binding, IP accumulation and Tcf/Lef reporter gene activation of this receptor were successful; repeat studies are required to determine their reproducibility. One concern for the reproducibility in these experiments lie in the fact that the inverted repeat hairpin sequence prevents complete translation of the protein thereby rendering it inactive. It seems plausible to suggest that the hFP_B inverted repeat sequence may require some sort of regulatory protein to dissociate the hairpin structure facilitating proper translation. In addition, in-vitro translation experiments can be performed utilizing the hFP_B plasmid to determine if it is capable of being expressed as a full-length protein.

RT-PCR on CX-1 cells using a strategy of hFP generic and hFP_A specific primers seemed to suggest the presence of an FP isoform other than hFP_A indicating that the cDNA cloning data may be significant. It is interesting to note that the hFP_A receptor mRNA is expressed in normal human colon tissue but not in the CX-1 diseased colon tissue as observed from the cloning ratio of hFP_A:hFP_B and RT-PCR studies. It could be hypothesized that post-transcriptional transformation of hFP_A mRNA message to the hFP_B isoform may lead to the pathophysiology of colorectal cancer. As previously noted, the ovine FP_B receptor has been linked to increased PI3K basal activity that mediates

Tcf/β-catenin signal transduction and demonstrates potential for increased COX-2 expression (Fujino and Regan 2003a; Fujino and Regan 2003b). Interestingly, virtually identical characteristics of colon cancer include; increased basal PI3K activity, increased Tcf/β-catenin signaling, increased COX-2 expression and increased prostaglandin synthesis (Phillips, St Clair et al. 1998; Petiot, Ogier-Denis et al. 2000; Srivastava, Verma et al. 2001). Collectively, the data presented here, as well as by Dr. Hiromichi Fujino and colleagues with respect to the ovine FP_B isoform, strongly suggest the presence of an hFP_B ortholog. However, whether or not the actual hFP_B DNA sequence is that which has been identified herein remains circumspect.

CHAPTER THREE:

CLONING AND LOCALIZATION OF hFP_S: A SIX-TRANSMEMBRANE mRNA SPLICE VARIANT OF THE HUMAN FP PROSTANOID RECEPTOR

Portions of this chapter have appeared previously in Vielhauer G.A., Fujino H., Regan J.W. (2004) Cloning and localization of hFPs: a six-transmembrane mRNA splice variant of the Human FP Prostanoid Receptor. Archives of Biochemistry and Biophysics 421: 175-185.

3.1 Introduction

Prostanoids are locally acting hormones synthesized from arachidonic acid via the cyclooxygenase pathway (Goodman, Gilman et al. 1996). There are five primary metabolites of arachidonic acid, which include prostaglandin D_2 (PGD_2), PGE_2, $PGF_{2\alpha}$, PGI_2 (prostacyclin), and thromboxane A_2 (TXA_2). Pharmacologically the receptors for these hormones are classified by the endogenous prostanoid they bind. Therefore, PGD_2 activates the DP receptors, PGE_2 activates the EP receptors and $PGF_{2\alpha}$, PGI_2 and TXA_2 respectively activate the FP, IP and TP receptors (Coleman, Smith et al. 1994; Sugimoto, Ushikubi et al. 1999). Prostanoid receptors are typically seven transmembrane (TM) G-protein coupled receptors (GPCR) that have an extracellular amino terminus and intracellular carboxyl terminus. Prostanoid receptors can be subdivided into two major groups based upon phylogenic analysis (Regan, Bailey et al. 1994; Toh, Ichikawa et al. 1995). The first group consists of the EP_2, EP_4, DP and IP receptors, which all couple to G_S and stimulate intracellular cAMP formation. The second group, consists of the EP_1, EP_3, FP, and TP receptors, all of which couple to either G_q or G_i and either stimulate phosphatidyl inositol hydrolysis or inhibit cAMP formation. Interestingly, all the members of this second group exist as multiple isoforms, which are generated by alternative mRNA splicing (Pierce and Regan 1998). This alternative mRNA splicing occurs at two distinct locations in the prostanoid receptor genes. The first location corresponds to the middle of TM-6 and the second is approximately 10 amino acids downstream of TM-7 in the carboxyl terminus. Splicing at the first location occurs in all prostanoid receptor pre-mRNA, but with the exception of the EP_1 and FP receptors does

not lead to alternative transcripts (Okuda-Ashitaka, Sakamoto et al. 1996; Ishii and Sakamoto 2001). mRNA splicing at the second location generates carboxyl terminal isoforms of the EP_1, FP and TP receptors (Pierce and Regan 1998).

The first prostanoid receptor isoform to be characterized involving splicing at the TM-6 site was an EP_1 variant that was cloned from rat uterus cDNA and shown to be highly expressed in the kidney (Okuda-Ashitaka, Sakamoto et al. 1996). This EP_1 variant arises from a 425 base pair insert in the TM6 splice site giving rise to a frame shift resulting in a protein of 366 amino acids. The amino acid sequence of this variant up to the splice site is the same as the original rat EP_1 isoform, however because of the insert and frame shift, the amino acid sequence downstream of the splice site is divergent. Although the EP_1 6TM isoform appears to be capable of forming a 7TM domain, it does not share any homology with the 7TM domains of other prostanoid receptors.

Previously two FP receptor isoforms were cloned from ovine corpus luteum that represent alternative mRNA splicing at the C-terminal site (Graves, Pierce et al. 1995; Pierce, Bailey et al. 1997). These two isoforms, termed FP_A and FP_B, are identical up to and including tyrosine 317, which are nine amino acids downstream of TM-7 in the intracellular carboxy terminus. In the FP_A receptor isoform there are 46 additional amino acids downstream of tyrosine 317, while in the FP_B isoform there is just one amino acid (an isoleucine) following tyrosine 317 (Pierce, Bailey et al. 1997). This leads to a truncated version of the FP_A receptor with a shortened intracellular carboxy terminus. Recently, a third FP receptor isoform was cloned from the bovine corpus luteum that is created from alternative mRNA splicing at the 6TM site (Ishii and Sakamoto 2001). This

bovine 6TM FP receptor splice variant arises from an insertion, which like the 6TM EP_1 receptor variant causes a frame shift and premature stop. Unlike the 6TM EP_1 variant, however, the bovine 6TM FP variant is unlikely to form a seventh TM domain and its carboxyl terminus is probably extracellular.

To date only one human FP receptor has been cloned which represents the human ortholog of the ovine FP_A (Abramovitz, Boie et al. 1994), the bovine FP (Sakamoto, Ezashi et al. 1994) and the mouse FP (Sugimoto, Hasumoto et al. 1994). To identify possible isoforms of the human FP prostanoid receptor we used PCR to screen human cDNA libraries for the presence of potential FP receptor mRNA splice variants. In this chapter, we report the cloning and characterization of a 6TM alternative mRNA splice variant of the human FP receptor. This variant, named hFP_S (sevenless) has a 71 base pair insert in the 6TM splice site that results in a frame shift and premature stop much like the bovine 6TM FP variant. The hFP_S mRNA is present in several human tissues and appears to be expressed as a protein but it does not bind $PGF_{2\alpha}$ and its function is presently unknown.

3.2 Experimental procedures

3.2.1 cDNA cloning

Human placenta, heart, uterus, and colon adenocarcinoma Marathon Ready™ cDNA was obtained from Clontech Laboratories (Palo Alto, CA). PCR reactions were performed according to the manufacturer's protocol using the Advantage Taq polymerase from Clontech (product #8417-1). The initial PCR program used was 95°C for 5 min,

95°C for 1 min, 70°C for 1 min, 72°C for 6 min repeat steps 2-4 for five cycles, then 95°C for 1 min, 68°C for 1 min, 72°C for 6 min repeat steps 6-8 for five cycles, then 95°C for 1 min, 66°C for 1 min, 72°C for 6 min repeat steps 10-12 for 20 cycles then 72°C for 15 min followed by a 4°C hold. This reaction utilized a FP sense primer (nt. 613), GGCAGTGTGATGGCCATTGAGCGGTGTATTGG, with the anti-sense adaptor primer (AP1). All adaptor primers used in the RACE PCR were included in the Marathon Ready™ cDNA kit. The resulting PCR reaction was diluted 1:5 in water and a nested PCR reaction was performed. The nested PCR was identical to the previous program, except the total number of cycles was decreased to 20. The nested PCR reaction utilized a FP sense primer (nt. 736), GCTTTGCTGCCCATCCTTGGACATCGAGAC, with the anti-sense nested adaptor primer (AP2). Products from the entire PCR reaction were purified using Gene Clean II according to the manufacturer's instructions (BioRad product #1001-200; Hercules, CA).

Purified PCR products were ligated into the pGEM-T vector using a cloning kit (Promega #Q5601; Madison, WI) and the instructions provided therein. Following the ligation, JM109 cells were transformed and positive colonies were selected for the preparation of plasmid DNA using a crude alkaline lysis protocol (Zhou, Yang et al. 1990).

Purified plasmid DNA was digested with restriction enzymes directed to the multiple cloning site and electrophoresed on 1.2% agarose gels, to separate the PCR inserts from the pGEM-T backbone. The gel was then denatured and neutralized and the DNA was transferred to a nylon membrane by blotting overnight using 20x SSC.

Following transfer the membrane was washed and baked for two hours at 80°C in preparation for Southern blot analysis.

3.2.2 Southern blot analysis

A 228 bp probe, starting in the third intracellular loop and spanning the 7TM, was prepared by digesting human FP/pcDNA$_3$ with *BglII* and *HindIII* and was radiolabeled with [^{32}P]dCTP using a nick translation kit (Gibco product #18160-010; Carlsbad, CA). Following purification with an Amicon spin column (Millipore product #42409; Billerica, MA), the probe was used for Southern blot analysis according to standard protocols (Maniatis, Fritsch et al. 1982). Clones containing positive inserts were digested with *BglII* and *HindIII*, which will yield a single 228 base pair product with the previously cloned human FP receptor. Positive clones that did not yield this product were sent for DNA sequencing. The resulting DNA sequences were analyzed (Macvector 7; Accelrys, Burlington, MA) and compared to the previously cloned human FP receptor. This yielded two clones of hFP$_S$/pGEM-T, one from the heart library and one from the placenta. To avoid confusion, the previously cloned human FP receptor will hereafter be referred to as hFP$_A$.

3.2.3 Construction of an hFP$_S$ expression vector and stable cell line

hFP$_S$/pcDNA$_3$, a full-length clone encoding human FP$_S$, was prepared by digesting the hFP$_A$/pcDNA$_3$ and hFP$_S$/pGEM-T clones with *BglII* that cuts at nucleotide 958 (Fig. 1, double underline) in the coding sequence of both hFP$_A$ and hFP$_S$. The digests were then treated with *NotI* which cuts in the multiple cloning site of pcDNA$_3$ and

pGEM-T. The larger fragment from the digest of $hFP_A/pcDNA_3$ (containing the 5' end of the hFP_A receptor) and the smaller fragment from the digest of hFP_S/pGEM-T (containing the 3' end of the hFP_S clone) were purified using Gene clean II, and were then ligated and subcloned to yield $hFP_S/pcDNA_3$. To prepare a plasmid for stable expression of hFP_S in 293-EBNA cells, *NheI* and *XhoI* sites were introduced by PCR of $hFP_S/pcDNA_3$ with the following primers: sense, CAGCTAGCATGAACAATTCCAAA; anti-sense, TTCTCGAGTTGTTCTAAGCCCCACAC. The product was isolated and subcloned into pGEM-T to yield hFP_SNX/pGEM-T. The later was digested with *NheI* and *XhoI* and the fragment encoding hFP_S was isolated and ligated with FLAG-FP_A/pCEP4, which had been digested with *NheI* and *XhoI* to remove the fragment encoding ovine FP_A. The resulting plasmid, FLAG-hFP_S/pCEP4, was then used to stably transfect 293-EBNA cells by limiting dilution and hygromycin selection as previously described (Fujino, Srinivasan et al. 2000).

3.2.4 Immunoprecipitation & immunoblot analysis

Cells were plated at a low density and grown to confluence then washed with 1x phosphate-buffered saline (PBS). The cells were scraped and sonicated in a lysis buffer consisting of 20 mM Tris-HCl (pH 7.5), 10 mM EDTA, 2 mM EGTA, 2 mM phenylmethylsulfonyl fluoride, 0.1 mg/ml leupeptin, and 2 mM sodium vanadate. Samples were centrifuged (16,000 x g) for 15 min at 4°C, the supernatant (cytosolic fraction) was removed and the pellet (particulate fraction) was solublized with lysis buffer containing 0.05% Triton X-100 and centrifuged again to remove insoluble debris as previously described (Fujino and Regan 2001). Protein concentrations were

determined using a Bio-Rad assay kit (Bio-Rad Laboratories, Hercules, CA) and samples were immunoprecipitated overnight utilizing a FLAG-M2 agarose antibody (Sigma product #A-2220; St. Louis, MO). Samples were then centrifuged for 3 min at 3000 rpm and washed with lysis buffer. Laemmli buffer (5x) was added and the samples were heated for 10 min at 55°C then placed on ice for 5 min and centrifuged. Samples were then separated on a 10% SDS-polyacrylamide gels, transferred to nitrocellulose membranes, and blocked with 1.5% nonfat milk in Tris-buffered saline (TBS) containing 0.1% polyoxyethylenesorbitan monolaurate (TBST) for one hour at room temperature with rotation. The membrane was then incubated with anti-FLAG-M2 antibodies (1:1000, Sigma #F-3165) overnight at 4°C with rotation. The membranes were washed in TBST and incubated with anti-mouse secondary antibodies conjugated to horseradish peroxidase (1:10,000, Jackson Laboratories) for one hour at room temperature. The membranes were washed, and visualized by enhanced chemiluminescence (SuperSignal; Pierce).

3.2.5 Immunofluorescence microscopy

293-EBNA cells untransfected or stably expressing the hFP_S receptor were grown in six-well plates containing 22-mm round glass cover slips for 3-4 days. Cover slips were washed, fixed, and incubated with either hFP_S polyclonal (1:500 dilution) or FLAG-M2 monoclonal primary antibodies (1:500, Sigma #F-3165) in 5% Blotto (nonfat dry milk in TBS). They were then washed and incubated (1:1000 dilution) with either a fluorescein isothiocyanate (FITC) conjugated goat anti-rabbit secondary antibody (Sigma # F-1262) for the hFP_S antibody, or a tetramethylrhodamine isothiocyanate (TRITC) goat

anti-mouse secondary antibody (Sigma # T-7782) for the FLAG-M2 antibody. Cover slips were subsequently washed, mounted on slides, and examined with a 60x PlanApo oil objective, by epifluorescence microscopy using an Olympus IX70 microscope. Images were obtained and processed using an Olympus Magna Fire camera and software (model #S99806).

3.2.6 Human heart and placenta PCR

To confirm specific mRNA expression of the hFP_S we performed PCR and RT-PCR utilizing hFP_S and hFP_{gen} (generic region) specific primers. Primers to glyceraldehyde-3-phosphate dehydrogenase (GAPDH) served as a positive control. The PCR utilized the heart and placenta RACE cDNA from above and the following primers: hFP_S sense, TTTCTGGGATACAGAATAATTTTG; hFP_{gen} sense, GCTCCTGGCGATAATGTGTGTCTC; hFP_{gen} anti-sense, GCAACTGGTGACTCAGAAATAGCAGC; GAPDH sense, TGGGTGTGAACCATGAGAAG; and GAPDH anti-sense, TCTACATGGCAACTGTGAGG. The PCR reaction was run under the following conditions 95°C for five min, 95°C for one min, 62°C for one min, 72°C for one min repeat steps two to four for 45 cycles, 72°C for 15 min and 4°C hold. PCR reactions were amplified using heart or placenta RACE cDNA. Each PCR reaction contained 10 mM of the respective primers (hFP_S, hFP_{gen} or GAPDH), 0.2 mM dNTP, 1.5 mM $MgCl_2$, 1x PCR buffer (20 mM Tris-HCl, pH 8.4, 50 mM KCl), 2.5 units Taq polymerase (Gibco) and nuclease free water.

3.2.7 Human umbilical vein endothelial cell RT-PCR

Cytoplasmic RNA (4.5 μg) was prepared as previously described and treated with DNase for 15 min at room temperature, then 25 mM EDTA was added and the reaction inactivated at 65°C for 10 min. Oligo (dT) were added and the reaction heated for 10 min at 70°C. First strand synthesis was carried out by adding half of the above RNA mix to two tubes along with the RT mix. The RT mix contained first strand buffer 5 μl (250 mM Tris-HCl, pH 8.3, 375 mM KCl, 15 mM $MgCl_2$), 1 μl dNTP (10 mM), 2 μl DTT (0.1 M), and diethyl pyrocarbonate (DEPC)-H_2O per 10 μl RNA. For each sample, two treatment groups were performed, one with RT+ and one without RT-. The samples were then incubated for 50 min at 42°C followed by 15 min at 70°C and ice for 5 min. RNase H (4 units) was added to each tube and incubated for 20 min at 37°C.

PCR was performed using the same primers described above for the hFP_S, hFP_{gen} and GAPDH nucleotide sequences except the hFP_{gen} sense primer was replaced with the following sense primer, GCTTTGCTGCCCATCCTTGGACATCGAGAC, corresponding to nucleotide 736 of the Genbank accession no. L24470. PCR reactions were amplified using cDNA from the above RT reaction. Each PCR reaction contained 0.2 mM of the respective primers (hFP_S, hFP_{gen} or GAPDH), 0.2 mM dNTP, 1.5 mM $MgCl_2$, 1x PCR buffer (20 mM Tris-HCl, pH 8.4, 50 mM KCl), 2.5 units Taq polymerase (Gibco) and nuclease free water. The PCR amplification cycle consisted of 95°C for 5 min, initial denaturing step, followed by 95°C for 1 min, 55°C for 1 min, 72°C for 1 min for 45 cycles and ending with 72°C for 15 min for the hFP_S specific reaction. The PCR amplification cycle for the hFP_{gen} specific reaction consisted of 95°C for 5 min, initial

denaturing step, followed by 95°C for 1 min, 63°C for 1 min, 72°C for 1 min for 45 cycles and ending with 72°C for 15 min. Due to the differences in annealing temperature of the hFP_S and hFP_{gen} specific primers two separate reactions were performed and thus the corresponding GAPDH reaction for each. PCR products were analyzed by electrophoresis on an agarose gel. All reagents utilized for RT-PCR were from Gibco/ Invitrogen.

3.2.8 Northern blot analysis

A multiple human tissue northern blot was obtained from Clontech (#7780-1) and was hybridized with either hFP_S or hFP_{gen} specific probes or with a probe to GAPDH. The hFP_S specific probes consisted of four 20-bp synthetic oligonucleotides that were end-labeled with [^{32}P]γATP and together spanned the entire 71 bp exon that is unique to hFP_S. The hFP_{gen} probe consisted of a 948 bp cDNA fragment produced by cutting hFP_A/ $pCDNA_3$ plasmid with *Nhe1* and *HindIII* restriction enzymes. The hFP_{gen} and GAPDH probe was prepared utilizing a standard nick translation kit (Gibco). The hybridization solution for the hFP_S northern blot was 20% formamide (Sigma), 10% dextran sulfate (Sigma), 1% SDS-DEPC, 1 M NaCl-DEPC, 0.1 mg/ml sonicated DNA salmon sperm (Sigma). The hybridization solution for the GAPDH northern blot was identical to that for the hFP_S except 50% formamide was substituted for 20%. Membranes were blocked, hybridized and washed at 39-42°C. The hFP_S northern was washed with only a high salt buffer (2x SSC, 0.1% SDS) while the GAPDH northern was washed with a high salt buffer as well as a low salt buffer (0.01x SSC, 0.1% SDS). Membranes were then exposed to X-ray film and developed.

3.2.9 Preparation of hFP_S antibodies and immunohistochemical staining

Rabbit polyclonal antibodies were prepared by Covance (Princeton, N.J.) to a GST-hFP_S fusion protein containing the 31 amino acids that are unique to hFP_S (267-297, Fig. 1). The antibodies were purified by affinity chromatography using a pMAL-hFP_S fusion protein containing the same 31amino acids that had been immobilized to agarose beads.

Human placenta was obtained from the University of Arizona, University Medical Center Labor and Delivery Unit. Tissue samples were formalin fixed, paraffin embedded, and four-micron slices were placed on glass slides. Slides were then deparaffinized and subjected to antigen retrieval in 0.01 M citrate buffer, (citric acid and sodium citrate, pH 8.0, Sigma). They were then blocked in series with 3% H_2O_2/97% MeOH, a Vector lab blocking kit (product #SP-2001; Burlingame, CA), and finally by 10% goat serum (Sigma) with a PBS wash between each blocking agent. Primary antibodies were added overnight at 4°C and slides received either a negative control rabbit primary IgG isotype antibody (Zymed #08-6199), the hFP_S polyclonal antibodies (1:100 dilution in 2% goat serum/PBS) or the hFP_S antibody incubated overnight with the GST-hFP_S fusion protein. Slides were washed and a secondary goat anti-rabbit IgG antibody added (1:300, Vector labs #BA-1000) at room temperature. The slides were washed and a Vectastain elite ABC kit was utilized (PK-6100) according to manufacturer instructions. Following another wash, slides were placed in 250 μg/ml diaminobenzidine tetrahydrochloride (DAB, Simga), rinsed in H_2O and counterstained with a 1:4 dilution of VMS hematoxylin (diluent; 30% polyethylene glycol, 64.2% distilled H_2O, and 5.8%

glacial acetic acid). Slides were dehydrated and glass coverslips were attached using Cytoseal.

3.3 Results

Human heart, placenta, uterus and colon adenocarcinoma cDNA libraries were screened by a combination of PCR, Southern blot analysis, restriction enzyme mapping and DNA sequencing to identify potential alternative mRNA splice variants of the human FP prostanoid receptor. Two identical cDNAs, one from the heart and one from the placenta, were cloned that encoded a novel splice variant, which we have named hFP_S to distinguish it from the previously cloned human FP receptor that we will refer to as hFP_A. Figure 3.1 shows the cDNA and deduced amino acid sequences of the hFP_S isoform. The hFP_A and hFP_S isoforms are identical up to nucleotide 1036, at which point there is an insertion of 71 nucleotides relative to the hFP_A sequence. This 71 bp insert causes a frame shift and results in a premature stop 24 nucleotides past the end of the insert (nt. 1131). There are several consequences of this in terms of the primary and secondary structure of hFP_S. First, the amino acid sequence of hFP_S diverges from that of hFP_A at leucine-266, which is close to the predicted carboxyl terminal end of TM-6. Second there are only 31, mostly hydrophilic, amino acids before the end of the predicted amino acid sequence. For the hFP_A there are a total of 93 amino acids downstream of leucine-266 that constitute the third extracellular loop (~19 amino acids), TM-7 (~22 amino acids) and the intracellular carboxyl terminus (~52 amino acids). We predict based on the number of hydrophilic residues and the absence of a contiguous stretch of 20-24 hydrophobic residues that hFP_S does not have a 7TM domain and that its carboxy

terminus is extracellular. Furthermore, even if this divergent sequence was capable of forming a 7TM segment, it lacks any amino acid homology to the 7TM domain of other prostanoid receptors. Except for this 71 bp insert the nucleotide sequence of hFP_S and hFP_A are the same, including the 3'-untranslated region.

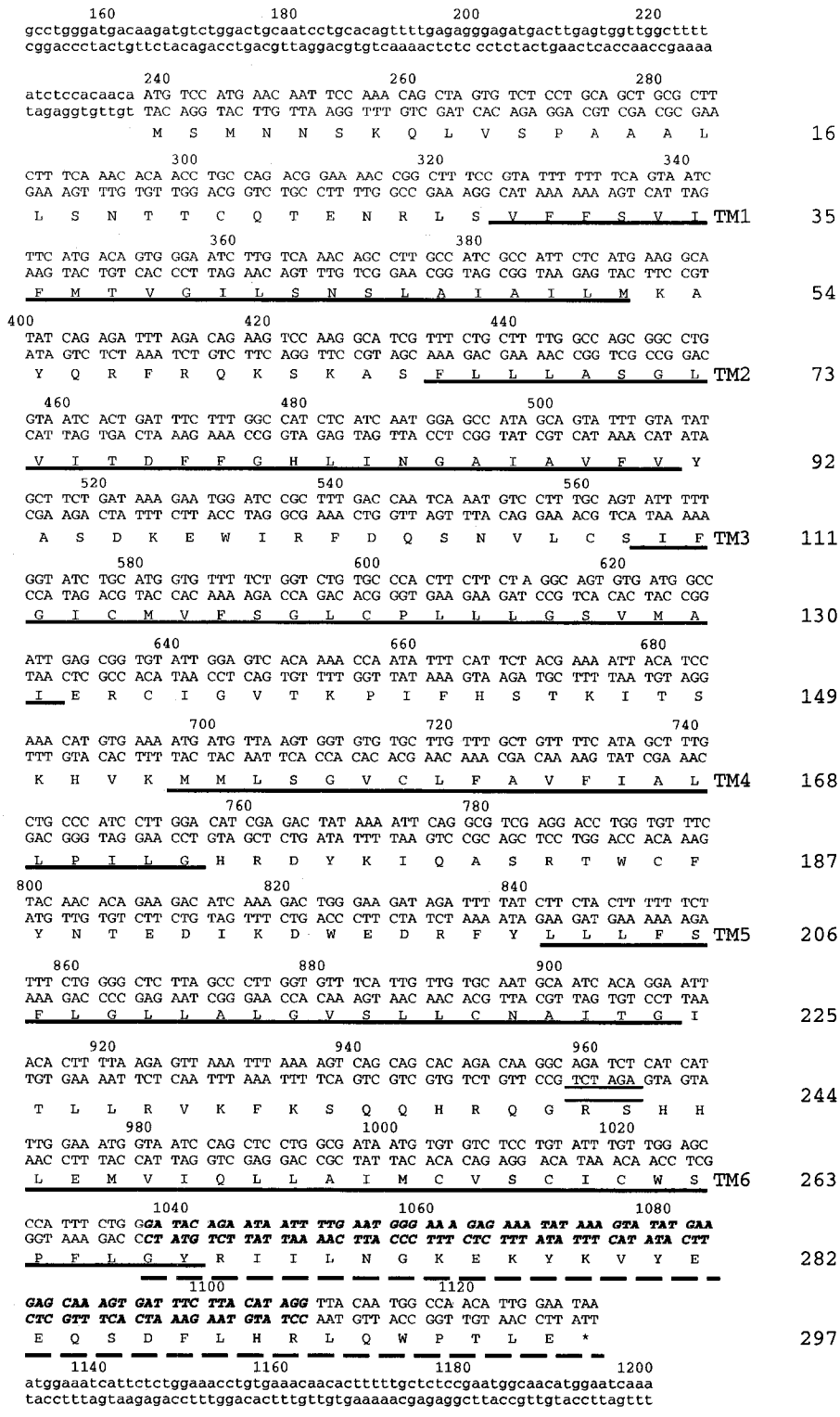
TM1
TM2
TM3
TM4
TM5
TM6

Figure 3.1 cDNA and deduced amino acid sequences of the human FP_S isoform. The cDNA sequence is based on the previously cloned human FP receptor (Abramovitz, Boie et al. 1994) and starts with nucleotide 151 of GenBank accession No. L24470. The GenBank accession number of hFP_S is AY485530. Numbering of the amino acid sequence is shown on the far right. The transmembrane (TM) domains are underlined (solid) and are numbered TM1-TM6 on the right. The 31 hFP_S specific amino acids are indicated with a dashed underline and the corresponding cDNA sequence is in bold italics. The *Bgl*II site (nt. 958) that was utilized to create a full-length hFP_S coding sequence is shown as a double underline.

In silico analysis was used to locate the hFP_S specific 71 bp insert in the human genome. A perfect match was found on chromosome-1 (1p22.3-31.2) within an approximate 135 kilobase sequence containing the FP prostanoid receptor gene. The hFP_S specific 71 bp sequence was flanked by an upstream splice acceptor site (AG) and a downstream splice donor site (GT). The presence of these splice donor and acceptor sites are typical of intron/exon boundaries and indicate that this 71 bp insert represents a previously unknown exon in the FP receptor gene. Figure 3.2 shows the organization of the human FP gene as it is presently known. There are at least four exons. The first encodes most of the 5'-UTR while the second encodes the remaining 5'-UTR and the coding sequence up to leucine 266 near the end of TM6. The third exon represents the hFP_S specific 71 bp insert and the fourth encodes the rest of the coding sequence and the 3'-UTR.

RT-PCR with hFP_S specific primers and with a generic set of primers (hFP_{gen}) that could amplify either hFP_S or hFP_A was used to verify the expression of hFP_S message in cDNA from human heart (Figure 3.3, top panel) and placenta (Figure 3.3, bottom panel). Lane 1 shows that a product of the expected size (326 bp) was obtained with both heart and placenta cDNA using hFP_S specific primers. On the other hand, lane 3 shows the generic set of primers yielded a major product of the size expected for the hFP_A (308 bp) and a minor product of the size expected for hFP_S (379 bp). The data are consistent with the presence of mRNA encoding hFP_A and hFP_S in both the human heart and placenta.

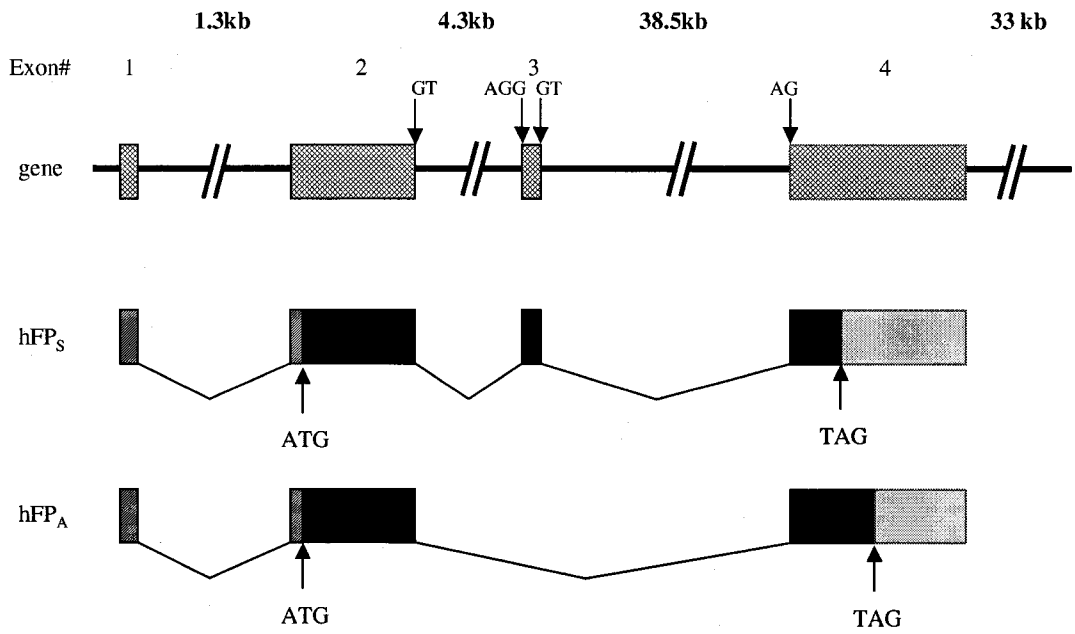

Figure 3.2 Organization of the human prostaglandin $F_{2\alpha}$ receptor gene. Comparison of the human FP gene and the two FP isoforms generated by mRNA alternative splicing. There are four exons located on the gene indicated by the *crossed boxes*. The diagonal and gray shaded boxes represent the 5'-UTR and 3'-UTR regions, respectively. The black boxes indicate the coding sequence for the FP receptor isoforms. The hFP_S isoform consists of all four exons while the hFP_A consists only of exons 1, 2, and 4. Exon-3, which is specific for hFP_S consists of 71 base pairs. Sizes of the boxes are not to scale.

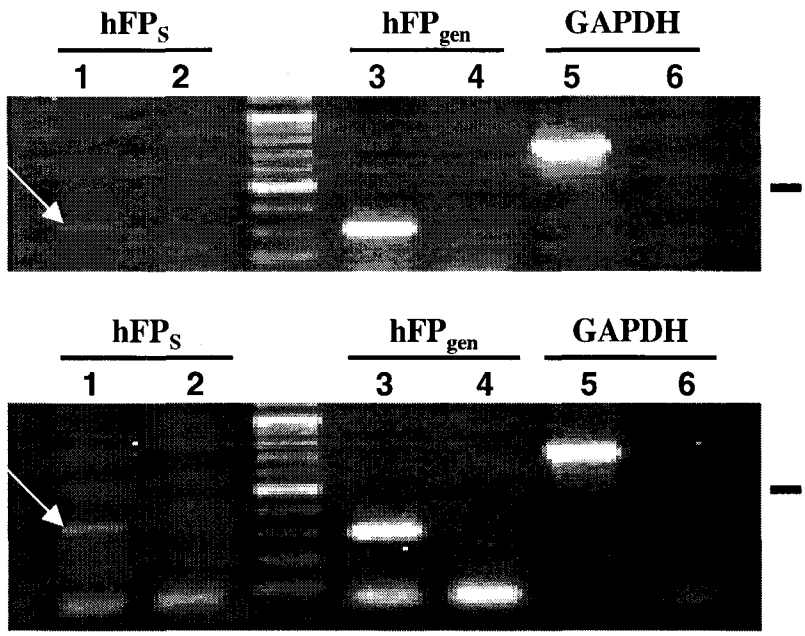

Figure 3.3 Photograph of PCR products following agarose gel electrophoresis utilizing hFP$_S$ specific and hFP generic (hFP$_{gen}$) primers. The *top panel* shows the PCR products obtained using human heart cDNA while the *bottom panel* shows the products obtained with placenta cDNA. *Lane 1* (*top and bottom*) shows the hFP$_S$ specific product with *lane 2* being the corresponding negative control (H_2O). *Lane 3* shows the hFP$_{gen}$ products with its negative control in *lane 4*. *Lane 5* shows GAPDH as a positive internal control with its negative control in *lane 6*. The size of the expected products are as follows: hFP$_S$, 326 bp; hFP$_{gen}$, 308 bp, and 379 bp; and GAPDH, 736 bp. A 100 bp DNA ladder is shown between *lanes 2 and 3*. Tick marks indicate the location of the 500 bp standard.

Northern blotting was used to further examine the expression of mRNA encoding hFP_S in twelve human tissues. As shown in Figure 3.4 (top, left panel), an hFP_S specific probe detected two major transcripts of approximately 6.8 and 4.9 kb in RNA from human heart and skeletal muscle (lane 2 and 3, respectively). The hybridization of the hFP_S probe was not related simply to the amount of RNA loaded on the gel as reflected by the amount of GAPDH message (bottom, right panel). For example, hybridization of the hFP_S probe was much greater to RNA from the heart as compared to the skeletal muscle, whereas the GAPDH probe showed the opposite. In addition, as shown in the bottom left panel, the hFP_S probe was very specific for hFP_S cDNA and did not cross react with hFP_A cDNA even at the highest amounts applied. Northern blot with a hFP_{gen} specific probe (top, right panel) depicts the presence two major FP_{gen} transcripts similar in size to that observed with the hFP_S specific probes, 4.9 and 6.8 kb, respectively. It is important to note that the FP_{gen} probe will hybridize to hFP_S, hFP_A or any other hFP splice variant containing RNA sequence up to and including TM7. In the skeletal muscle, colon, kidney, small intestine and placenta both major transcripts are observed while only the 4.9 kb transcript is clearly observed in the heart and lung.

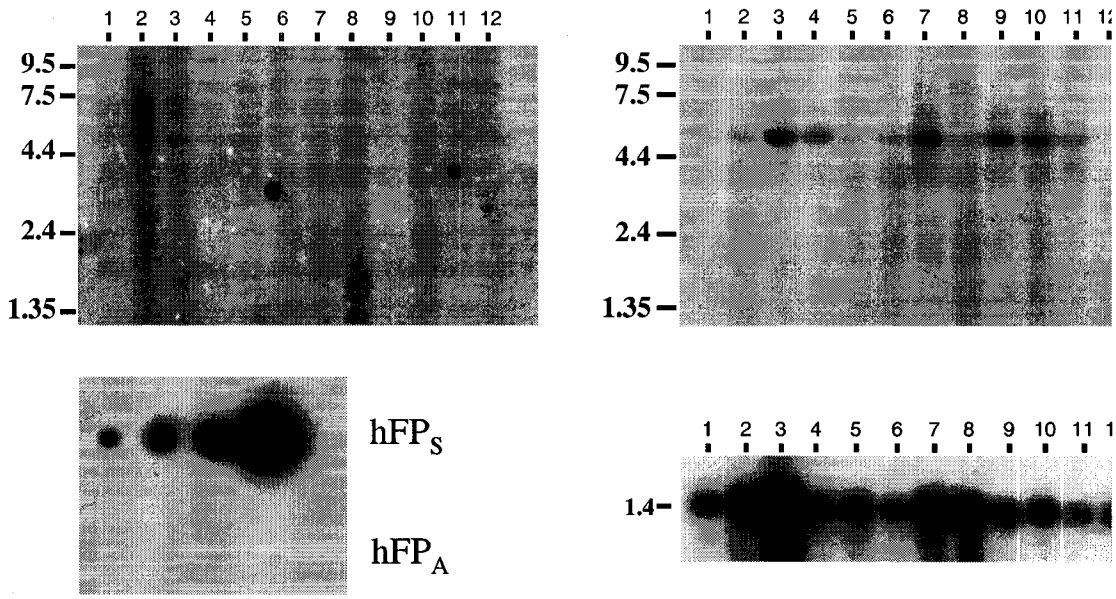

Figure 3.4 Northern blot of mRNA from 12 human tissues using hFP_S (top, left panel), hFP_{gen} (*top, right panel*) and GAPDH (*bottom, right panel*) radioactive probes. Tissues are as follows: *lane 1*, brain; *lane 2*, heart; *lane 3*, skeletal muscle; *lane 4*, colon; *lane 5*, thymus; *lane 6*, spleen; *lane 7*, kidney; *lane 8*, liver; *lane 9*, small intestine; *lane 10*, placenta; *lane 11*, lung; *lane 12*, peripheral blood leukocyte. The *bottom left panel* shows a positive control membrane spotted left to right with 4, 40, 400 and 4,000 μg of either hFP_S or hFP_A plasmid cDNA. Shown at the left are molecular weight markers (kb).

To examine the functional expression of hFP_S, 293-EBNA cells were stably transfected with a recombinant hFP_S construct containing a FLAG-epitope on the amino terminus. A clonal cell line was chosen based upon positive immunofluorescence staining with both FLAG and hFP_S specific antibodies and was further confirmed by immunoblot analysis with anti-FLAG antibodies. Figure 3.5 (top panel) shows that in cells stably transfected with FLAG-hFP_S a band of the expected size (32.7 kDa) was present in the particulate fraction, but not in the cytosolic fraction (lanes 2). Furthermore, a band of this size was not present in either untransfected 293-EBNA cells (lanes 1) or in 293-EBNA cells stably transfected with the ovine FLAG-FP_A (lanes 3). Immunofluorescence labeling of the FLAG-hFP_S cell line with either FLAG-M2 monoclonal antibodies (panels A-D) or hFP_S polyclonal antibodies (panels E-H) clearly show hFP_S specific immunoreactivity (white arrows). As shown in panels A, C, E, and G, hFP_S immunoreactivity was not observed in the untransfected 293-EBNA cells. Panels C, D, G and H represent a 3x magnification of the area within the white boxes shown in panels A, B, E and F, respectively. These magnified images show that the predominant expression of hFP_S is in the perinuclear region within the cell, most likely in association with the endoplasmic reticulum and/or Golgi apparatus. Overall these findings, along with the immunoprecipitation data, indicate that the hFP_S cDNA can be expressed as a membrane associated protein in these stably transfected 293-EBNA cells. These cells were also used to examine $PGF_{2\alpha}$ stimulated IP hydrolysis and the radioligand binding of [^{3}H]$PGF_{2\alpha}$. As predicted by the absence of TM7, there was no significant stimulation of IP hydrolysis or binding of [^{3}H]$PGF_{2\alpha}$ (data not shown).

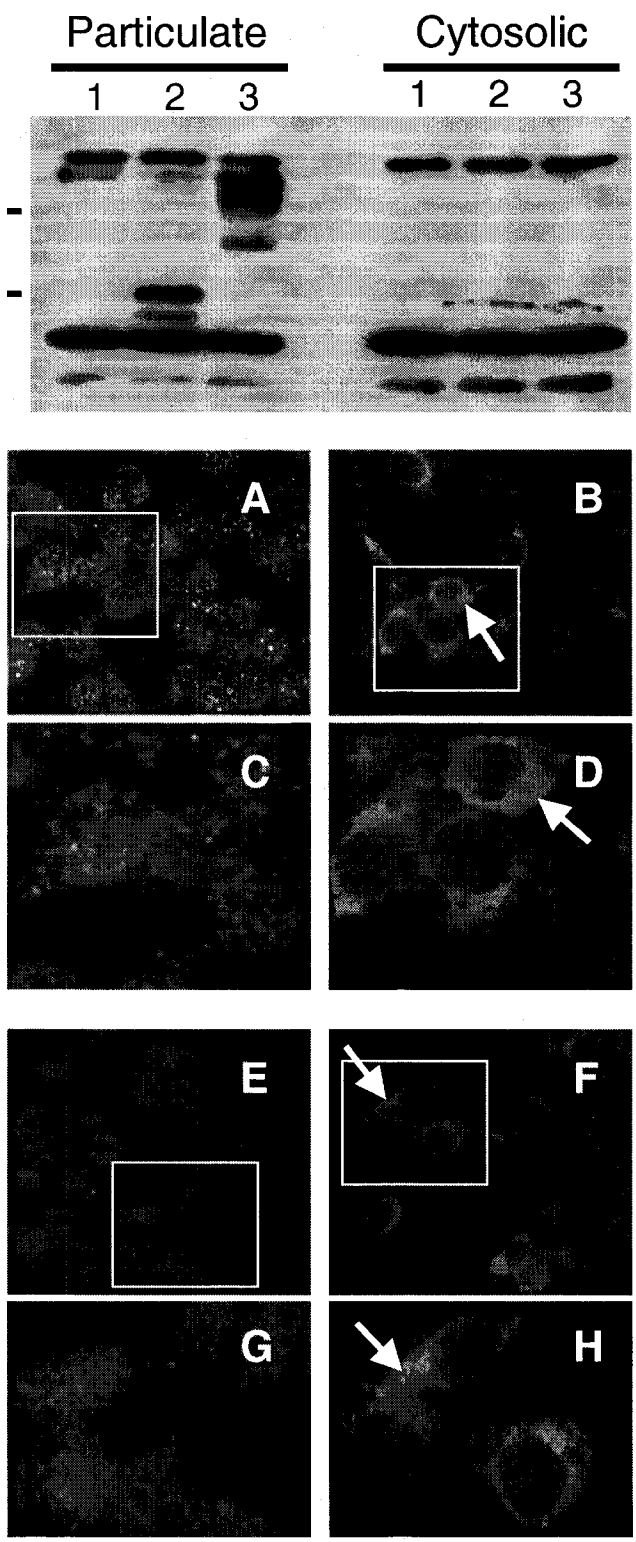
Particulate
Cytosolic
1 2 3
1 2 3
A
B
C
D
E
F
G
H

Figure 3.5 Immunoblotting (*top panel*) and immunofluorescence microscopy (*bottom panels A-H*) of human embryonic kidney (293-EBNA) cells stably transfected with FLAG-hFP$_S$. For immunoblotting, 60 μg (protein) of the ovine FP$_A$ particulate fraction and 300 μg of all other fractions were immunoprecipitated with an anti-FLAG antibody. The following lanes represent the particulate and cytosolic fractions of the different cell lines utilized in this experiment: *lanes 1*, 293-EBNA; *lanes 2*, hFP$_S$; and *lanes 3*, ovine FP$_A$. The expected sizes of the hFP$_S$ and ovine FP$_A$ proteins are approximately 32.7 and 40.5 kilo Daltons (kDa), respectively. Tick marks indicate the positions of the 40 kDa protein standard (upper) and 28 kDa standard (lower). These results are representative of three independent experiments. For immunofluorescence microscopy, untransfected HEK cells (*panels A, C, E, G*) and HEK cells transfected with FLAG-hFP$_S$ (*panels B, D, F, H*) were labeled with either anti-FLAG-M2 antibodies (*panels A-D*) or anti-hFP$_S$ polyclonal antibodies (*panels E-H*) as described in Experimental Procedures. *Panels C, D, G* and *H* show a 3x magnification of the area inside the white boxes shown in *panels A, B, E and F*, respectively. These results are representative of three independent experiments with each antibody.

Polyclonal antibodies were generated to the 31 carboxyl terminal amino acids of hFP_S and were used for the immunohistochemical localization of hFP_S in the placenta. Figure 3.6 shows three sets of two separate fields (all at 170x magnification) of the immunohistochemical staining of human placenta with either control rabbit primary IgG isotype antibodies (top panels), hFP_S antibodies (middle panels) or hFP_S antibodies that had been preincubated overnight with hFP_S fusion protein to block specific labeling (bottom panels). As shown in the middle panels, positive hFP_S immunoreactivity (brown) was observed to endothelial cells (large arrows) and trophoblast cells (small arrows). This labeling was specific and was not observed with either the control primary rabbit isotype antibodies (top panel) or the hFP_S antibodies that had been pre-incubated with hFP_S fusion protein (bottom panel). Figure 3.7 shows four separate fields (all at 60x magnification) of the immunohistochemical staining of human placenta with hFP_S antibodies. Again, positive hFP_S immunoreactivity was observed to endothelial cells (large arrows) and trophoblast cells (small arrows). In addition, the arrowheads show hFP_S staining of decidual cells.

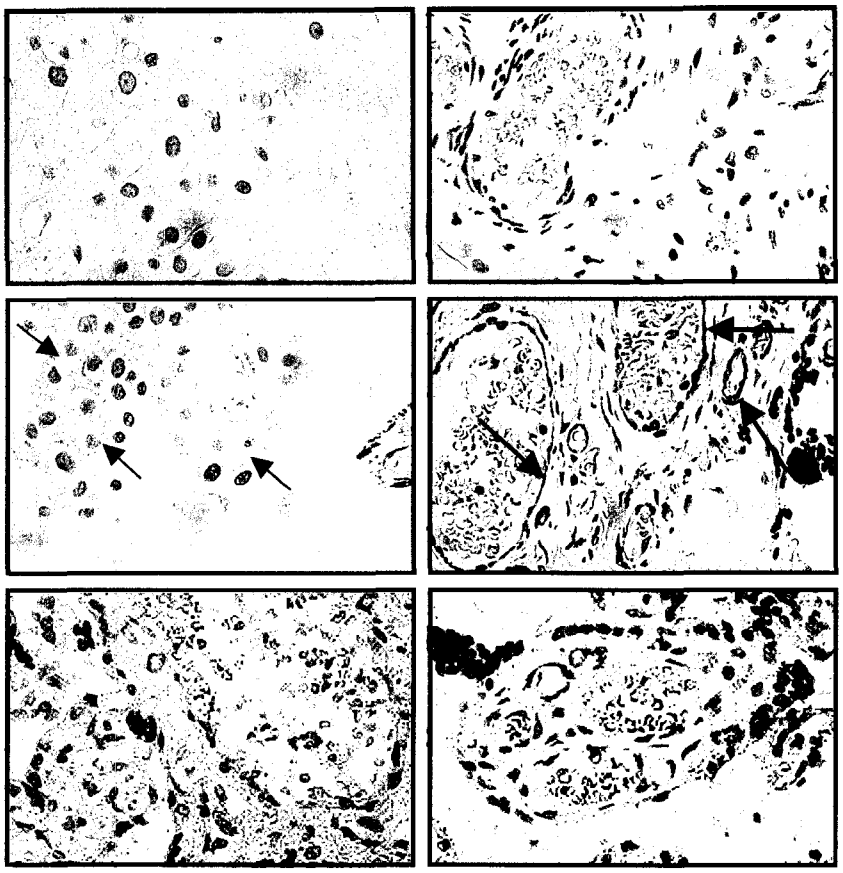

Figure 3.6 Photomicrographs of human placenta following immunohistochemical labeling with a hFP_S specific antibody (170x magnification). *Top panels* depict the negative controls that were prepared using a generic rabbit primary IgG isotype antibody. *Middle panels* are human placenta labeled with the hFP_S antibody (1:100 dilution). *Bottom panels* are human placenta labeled with the hFP_S antibody that had been preincubated overnight with the GST-hFP_S fusion protein. All slides were stained with hematoxylin to reveal cellular morphology. The *light blue color* indicates background while the *dark blue (or purple)* indicates nuclear staining. The *brown color* indicates positive immunoreactivity for the hFP_S protein. The *large arrows* point to endothelial cells while the *small arrows* point to trophoblast cells. These results are representative of three independent experiments.

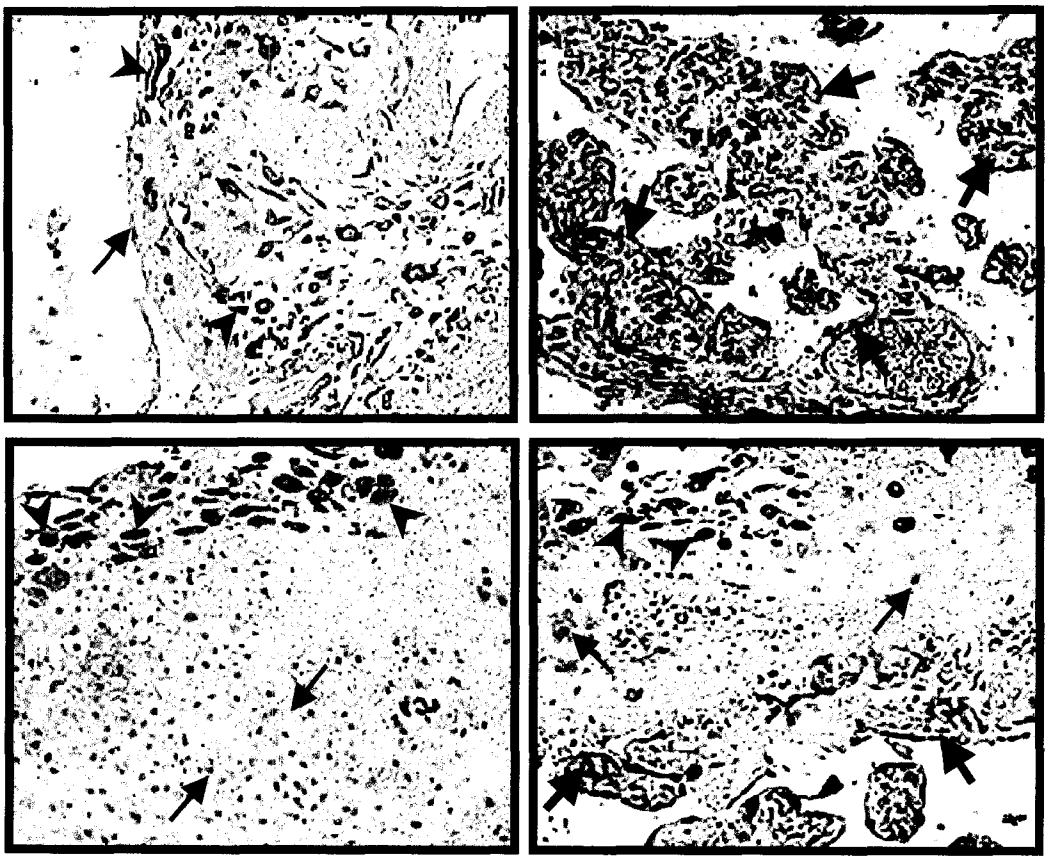

Figure 3.7 Photomicrographs of human placenta following immunohistochemical labeling with a hFP_S antibody (60x magnification). The four panels represent four separate fields of human placenta labeled with the hFP_S antibody (1:100 dilution). *Large arrows* point to endothelial cells, *small arrows* point to trophoblast cells, and *arrowheads* point to decidual cells. These results are representative of the same three independent experiments depicted in Figure 3.6.

RT-PCR using RNA from human umbilical vein endothelial cells (HUVEC) was done to corroborate the positive hFP_S immunostaining that was observed in endothelial cells from human placenta. For these experiments two sets of primers were used; one specific for hFP_S and a second generic set capable of amplifying both hFP_A and hFP_S (hFP_{gen}). Lane 1 in the top panel of Figure 3.8 shows that a product of the expected size (326 bp) was obtained with the hFP_S specific primers. Lane 1 of the middle panel shows that with the hFP_{gen} primers a major product of the size expected for hFP_S (631 bp) was observed, with no apparent product of the size expected for hFP_A (560 bp). Lane 1 in the bottom panel shows a product of the expected size (736 bp) was obtained using primers for GAPDH. Lanes 2 and 3 in all these panels represent negative controls in which either the HUVEC cDNA template was omitted from the reactions (lane 2) or the RT reactions were not performed (lane 3). These data support presence of mRNA encoding hFP_S, but no hFP_A, in HUVEC cells.

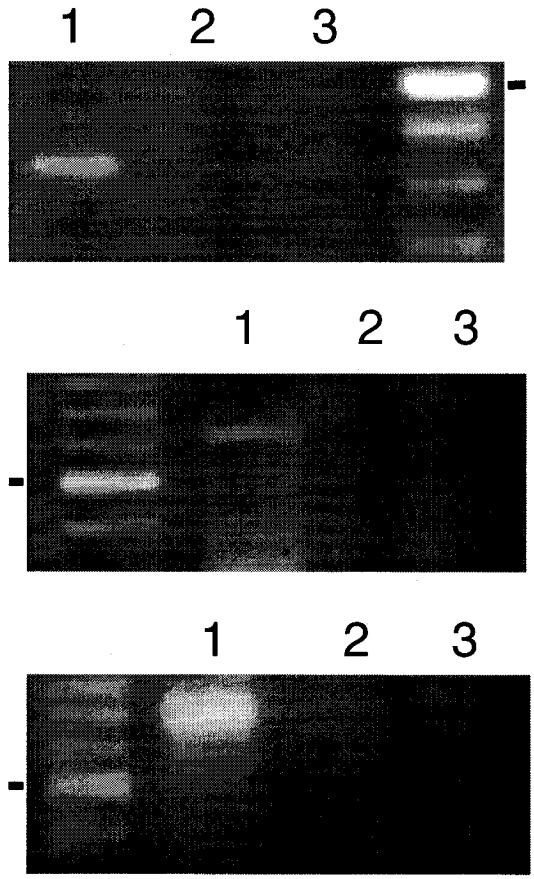

Figure 3.8 RT-PCR of human umbilical vein endothelial cell (HUVEC) RNA utilizing hFP_S (*top panel*), hFP_{gen} (*middle panel*) and GAPDH (*bottom panels*) specific primers. As described in Experimental Procedures, the hFP_S primers were designed to amplify hFP_S while the hFP generic (hFP_{gen}) were designed to amplify both hFP_A and hFP_S. The lanes are represented as follows: *lane 1*, cDNA prepared from RNA utilizing reverse transcriptase; *lane 2*; corresponding negative control lacking cDNA template; *lane 3*, RNA without reverse transcriptase after RNase treatment. The size of the expected PCR products are as follows: hFP_S, 326 bp; hFP_{gen}, 560 bp and 631 bp; and GAPDH, 736 bp. A 100 bp DNA ladder is shown at the right in the upper panel and at the left in the lower panels. Tick marks indicate the location of the 500 bp standard. These results are representative of three independent experiments.

3.4 Discussion

In the present study we have cloned an alternative mRNA splice variant of the human FP receptor that appears to encode a 6TM receptor with an extracellular carboxyl terminus. This receptor, named hFP_S, is generated by the insertion of a 71 bp exon into a well conserved splice site corresponding to the distal end of TM-6. Recently a similar 6TM-FP receptor variant was cloned from the bovine corpus luteum (Ishii and Sakamoto 2001). Like hFP_S, this bovine variant is generated by an insertion into the TM-6 splice site giving rise to a truncated receptor that lacks TM-7 and appears to have an extracellular carboxy terminus. Relative to the previously cloned FP receptors, the bovine 6TM-splice variant has 28 unique amino acids downstream of the splice site, whereas, hFP_S has 31. Despite this apparent structural similarity, however, there is no apparent homology in the amino sequence downstream of the splice site between these two receptors. Nevertheless, it is of interest to note that both of these 6TM variants have the dipeptide sequence, arginine-isoleucine, almost immediately downstream of the splice site. Basic residues are often found at the ends of transmembrane segments and in this case may demarcate the distal end of TM-6. Similarly, three other cDNA sequences were also reported as 6TM bovine FP receptor splice variants. One of these isoforms was the previously reported 6TM-FP-variant described above while the other two were unique 6TM FP receptor isoforms, named FP-δ and FP-ε (Sakamoto, Ishii et al. 2002). Relative to the hFP_S receptor, the bovine FP-δ and FP-ε share very little amino acid homology.

Previously, it has been reported that the intron located between exon two and what was previously exon three on the human FP gene was similar to that reported in the

mouse, 6.1 and 7.5 kb, respectively (Ishikawa, Tamai et al. 1996; Betz, Lagercrantz et al. 1999). Utilizing in-silico analysis, we were able to identify the unique hFP_S sequence as the third exon on the human prostaglandin FP receptor gene. Exon three is flanked by two introns, 4.3 and 38.5 kb, respectively. Collectively, these two introns as well as exon three (42.8 kb) are similar in size corresponding to the bovine gene, 33 kb (Ezashi, Sakamoto et al. 1997). In light of this and the presence of 6TM variants in the bovine and human, it seems reasonable that the bovine FP gene is more similar to the human than the mouse and possibly the ovine FP gene. Therefore, it is possible to hypothesize that more than one human 6TM and quite possible 7TM FP alternative splice variant exists warranting future cloning experiments.

We have good evidence that hFP_S is expressed both at the mRNA and protein levels in recombinant cells and human tissues. First, cDNAs encoding hFP_S were cloned separately from both the human heart and placenta and the presence of mRNA encoding hFP_S was confirmed by RT-PCR in both of these tissues. Second, Northern blot analysis showed the presence of hFP_S transcripts in human heart and skeletal muscle. Third, immunohistochemistry with hFP_S specific antibodies showed positive hFP_S immunoreactivity in several cell types from the human placenta. Finally, Western blot analysis and immunofluorescence microscopy of a cell line stably transfected with hFP_S showed the *de novo* expression of a protein of the appropriate size and localized in a membrane fraction of the cell lysate. Immunofluorescence microscopy showed that hFP_S was highly expressed in the perinuclear region of the cell in possible association with the endoplasmic reticulum and/or Golgi apparatus. This suggests that hFP_S might not be

processed correctly in 293-EBNA cells and that it is accumulating in these intracellular compartments. Further studies will be needed to determine if this is true or whether it simply reflects slow processing of hFP_S during transit to the plasma membrane.

Our failure to detect a clear hFP_S transcript in the Northern blot analysis of human placenta is probably because of the very limited expression of hFP_S in this tissue. Thus as shown by immunohistochemistry (Figures 3.6 and 3.7), the number of cells labeled in the placenta was small relative to the total cellular mass of this tissue. Although the presence of an hFP_S transcript could be detected by sensitive techniques such as RT-PCR (Figure 3.3) and by immunohistochemistry, the amount of hFP_S mRNA was insufficient for detection by Northern blot analysis. The presence of hFP_S message in highly vascularized tissue, such as the heart, placenta, and skeletal muscle, is interesting especially given the selective immunohistochemical identification of hFP_S in endothelial cells, trophoblast, and decidual cells.

Given that trophoblast and decidual cells were intensely stained for the hFP_S protein, it is important to understand the function of these cells as it may be useful for the functional characterization of hFP_S. Due to the apparent high expression level of hFP_S in these cells it can be hypothesized that hFP_S serves an important physiological function.

Trophoblasts are the first cells to undergo differentiation in the embryo being derived from the trophoectoderm of the developing bastocyst and are essential for the maintenance as well as inception of a successful pregnancy (Goldman-Wohl and Yagel 2002). In the nonpregnant state, the uterine vessels carry less than 1% of the maternal cardiac output, while in pregnancy the uteroplacental blood flow increases to about 25%

of total cardiac output (Kliman 2000). Trophoblasts are thought to displace the endothelial cell lining of the spiral arteries participating in degradation of smooth muscle and the elastic coat which maintains vessel integrity (Goldman-Wohl and Yagel 2002). This process of loosening maternal spiral arteries, called conversion, forms a vessel of low resistance and high capacitance in order to meet the demands of increased blood flow to the placenta (Goldman-Wohl and Yagel 2002). Trophoblasts have been shown to express angiogenic, anti-angiogenic, and vasoactive factors, including the most widely known angiogenic factor, vascular endothelial growth factor (VEGF) (Cross, Hemberger et al. 2002). Dysfunction of trophoblast is thought to contribute to preeclampsia which is a condition characterized by proteinuria as well as edema and is believed to occur due to shallow trophoblast invasion leading to unremodeled spiral arteries (Kliman 2000; Debra Goldman-Wohl 2002).

Decidualization involves the transformation of endometrial stromal fibroblasts to decidual cells following pregnancy and these cells play important roles in implantation, nutritional support for the embryo as well as protecting the mother and embryo from their respective invading cells (Kliman 2000; Fazleabas and Strakova 2002). The decidua interact with the trophoblast, restricting their movement by providing a physical barrier and generating a local cytokine environment that promotes trophoblast attachment rather than invasion (Kliman 2000). Interestingly, both these cells as well endothelial cells that we have identified to express hFP_S have been demonstrated to interact and play important roles in the reproductive process. It will be interesting to determine the extent to which hFP_S is involved in these physiological processes.

Recently, a study involving prostaglandin FP receptor gene knockout mice was published describing apoptosis and related proteins in placenta and decidual tissue (Mu, Kanzaki et al. 2003). In wild type mice fetuses were delivered to term, while FP knockout mice were incapable of parturition at any point in the pregnancy resulting in reabsorption of the fetuses. The authors noticed that FP knockout mice had a higher percent apoptotic index in placenta and decidua tissue when compared to wild type mice. This result was attributed to increased activated caspase-3 proapoptotic protein expression and decreased Bcl-2 anti-apoptotic protein expression in FP knockout mice that was not observed in wild type mice. The Bcl-2 family of proteins is known to regulate caspase activity. The expression of the Bax: Bcl-2 ratio increased approximately 3.4 fold in placenta and 2.3 fold in decidua of the knockout mice compared to wild type. Similarly, increases in trophoblast apoptosis were found in placenta tissue from women with pregnancies complicated by preeclampsia and intrauterine growth restriction compared to controls (Smith, Baker et al. 1997; Allaire, Ballenger et al. 2000). Our immunohistochemical data utilizing hFP_S and FP_A specific antibodies demonstrate positive hFP_S as well as negative FP_A immunoreactivity in human decidual and trophoblast cells. These data indicate that the hFP_S receptor, and not the hFP_A receptor, is present in these cells. Supporting this data is the lack of $PGF_{2\alpha}$ signaling determined in trophoblasts treated with $PGF_{2\alpha}$ that was observed in myometrium known to express the hFP_A receptor, unpublished data (Mu, Kanzaki et al. 2003). These studies suggest that at least some of the effects observed in FP knockout mice and pregnancy are mediated by a FP receptor gene product that does not bind $PGF_{2\alpha}$, possibly a hFP_S ortholog. Currently,

a murine ortholog of the hFP_S receptor does not exist but the data published by Mu et al. implicates the exact cell types, decidual as well as trophoblast cells, positive for hFP_S immunoreactivity. Therefore, it is tempting to speculate that the effects seen in these cells as it relates to pregnancy and apoptosis could be a result of knocking out a murine hFP_S ortholog. If this were proven true, hFP_S may function in a proto-oncogene capacity as a result of its direct involvement with Bcl-2 by inhibiting apoptosis.

Unfortunately, a biochemical function of hFP_S has yet to be identified. hFP_S does not bind $[^3H]PGF_{2\alpha}$ with any significant affinity and $PGF_{2\alpha}$ did not stimulate phosphoinositol hydrolysis in cells stably transfected with hFP_S. This is not too surprising given the importance of TM-7 in the binding of prostanoids. Thus, it is generally accepted that arginine-291, which is universally conserved in prostanoid receptors, is the counter ligand for binding of the C-1 carboxylate group of prostanoids (Narumiya, Sugimoto et al. 1999; Neuschafer-Rube, Engemaier et al. 2003). $PGF_{2\alpha}$ stimulation of the bovine FP 6-TM splice variant also failed to activate PKC, although it appeared to suppress $PGF_{2\alpha}$ mediated activation of PKC by the bovine FP_A receptor (Ishii and Sakamoto 2001). In our hands, coexpression of the hFP_S with hFP_A did not appear to modulate the $PGF_{2\alpha}$ stimulation of inositol phosphate hydrolysis by the hFP_A isoform; however, we did not examine $PGF_{2\alpha}$ activation of PKC. It is significant that alternative mRNA splicing involving the TM-6 splice site, to yield a truncated FP receptor, appears to have been conserved across species. It has, likewise, been conserved across at least two subtypes of prostanoid receptors. Thus, in addition to the 6TM-FP receptor splice variants, a 6TM splice variant of the rat EP_1 receptor has also been characterized (Okuda-

Ashitaka, Sakamoto et al. 1996). The rat 6TM-EP_1 splice variant has 49 unique amino acids downstream of the splice site and the authors hypothesize that it is capable of forming TM-7 even though it is not homologous to the 7TM domain of other prostanoid receptors. Unlike the 6TM-FP splice variants, the rat 6TM-EP_1 variant does appear to bind an endogenous ligand, prostaglandin E_2 (PGE_2), although it fails to activate a known second messenger response. Similarly, like the bovine 6TM-FP variant, the rat 6TM-EP_1 variant suppresses Ca^{2+} signaling by the EP_1 receptor when they are co-expressed. Based on PCR, Northern blot analysis and western blot analysis, the 6TM-EP_1 variant appears to be expressed endogenously, especially in the rat kidney.

Although the bovine FP and rat EP_1 receptors are known to be single copy genes, their genomic organization is unknown, as it concerns the formation of their corresponding 6TM-splice variants. On the other hand, we have specifically identified the exon that gives rise to hFP_S. It is a 71 bp sequence that is separated from exon-2 by 4.3 kb and from exon-4 by 38.5 kb. Exon-2 encodes some 5'-UTR and the coding sequence up to the 6TM splice site. Exon-4 encodes the sequence downstream of the 6TM splice site including TM-7, the carboxyl terminus and the 3'-UTR. hFP_A lacks exon-3, while hFP_S contains all four exons. Previously, it was thought that only 6.1 kb separated exon-2 and exon-4 and that the human FP gene consisted of only three exons (Betz, Lagercrantz et al. 1999). It is obvious that the FP gene has at least four exons and if carboxyl terminal splice variants exist there will be at least five exons. In this regard, it has been recently reported that there is two additional 6TM and three additional carboxy terminal splice variants of the bovine FP receptor (Sakamoto, Ishii et al. 2002). The

biochemical function of hFP_S is presently unknown, but its localization in endothelial cells and in highly vascularized tissues suggests a role in cardiovascular function.

CHAPTER FOUR:

PHARMACOLOGICAL CHARACTERIZATION OF THE SIX-TRANSMEMBRANE ORPHAN RECEPTOR, hFP_S

4.1 Introduction

GPCRs have historically been established to be valuable drug targets. It is estimated that 40-50% of marketed drugs are modulators of GPCR activity. To date, public databases demonstrate approximately 110 orphan GPCRs (oGPCRs) for which a natural ligand has yet to be identified, including hFP_S. Analysis of the human genome sequence is estimated to discover an additional 200 GPCRs, which will represent new drug targets for a wide variety of medical needs. Traditional methods for investigating orphan receptors have involved signal transduction assays that analyze a specific aspect of a signaling pathway, i.e. cAMP accumulation. However, these methods have proven to be narrow minded, time consuming and laborious with respect to identifying an endogenous ligand. To adapt orphan receptors, not only oGPCRs, into drug targets methods are needed that allow ligand occupancy to be turned into generalized robust assays that are acquiescent to high throughput screening (HTS) analysis. One approach is utilization of a fluorescence imaging plate reader (FLIPR) that gives a robust signal upon increased intracellular calcium binding to a FLOURO-4 fluorescent dye that has been loaded into experimental cells. Intracellular calcium accumulation is a product of several signaling pathways that results from release of intracellular stores and/or from the opening of a membrane calcium channel allowing an influx of extracellular calcium. FLIPR calcium assays have recently been used as a generalized high throughput screening method for characterizing GPCR agonist activity. To further expand this high throughput screening process, promiscuous G-proteins can be transfected into specific cell lines acting as an adaptor protein to funnel GPCR signal transduction to a common

pathway. Promiscuous G-proteins can be naturally occurring G-proteins (G_{16}), a member of the G_q family, or a chimera of two separate G-proteins, G_{qs}. The G_{qs} protein replaces the five C-terminal residues of G_q with the corresponding G_s sequence and directs some G_s-linked receptors to stimulate PLC-β resulting in calcium mobilization. Several oGPCRs have undergone "deorphaning" utilizing the FLIPR instrument along with G_{16} (Milligan and Rees 1999; Chambers, Macdonald et al. 2000; Elshourbagy, Ames et al. 2000). While these are only two examples of promiscuous G-proteins, there are several others that are beyond the scope of this dissertation. However, using the FLIPR and promiscuous G-protein technology does have its limitations. First, potential high throughput screening (HTS) hits will be overlooked if the orphan receptor does not couple to a G-protein or does not signal through a calcium-mediated pathway. Second, the mammalian cell line used in these experiments is of importance because differences in promiscuous G-protein function exist between cells lines. To address these limitations, we will attempt to utilize different FLIPR assays that measure endpoints other than intracellular calcium. In addition to measuring calcium, FLIPR instruments are also capable of measuring changes in intracellular pH and membrane potential.

The Na^+/H^+ exchanger (NHE) contributes to the pH stability of the cytoplasm by exporting protons out of the cells and importing sodium ions. BCECF is a pH sensitive dye with a high extinction coefficient in an alkaline environment and low coefficient in an acid atmosphere. This dye can be used to monitor the NHE activity by measuring changes in intracellular pH following an artificial acid-load of the cells. The activation of

many GPCR causes acid excretion, mostly via NHE activity, and it is therefore plausible to measure the response of these receptors to ligand by observing NHE activity.

Thus far, most membrane potential experiments have used a DiBAC dye indicator with the FLIPR instrument. DiBAC is a lipophillic, anionic, bis-oxonol dye that partitions slowly across the cytoplasmic membrane of live cells, depending on the membrane potential across the plasma membrane. DiBAC dye fluorescence intensity increases when the dye is bound to cytosolic proteins. Therefore, equilibrium is produced at a basal level when the dye is loaded into the cells. Upon addition of ligand, the cells may become depolarized or hyperpolarized for an unspecified amount of time. When the cells are depolarized, more DiBAC enters the cells and the increased concentration of DiBAC binding to intracellular lipids and proteins results in an increased fluorescence signal. Conversely, if a hyperpolarized state exists, the opposite effect occurs with DiBAC exiting the cells resulting in a decreased signal.

Previously, only a narrow focus has been achieved into the pharmacological characterization of hFP_S. It had been established that hFP_S does not bind $PGF_{2\alpha}$ and is not capable of mobilizing inositol phosphate accumulation in a FLAG-hFP_S stably transfected cell line. However, these experiments were not performed with the wildtype hFP_S protein. Since our data represent the first identification of this protein with its function still pending, we hypothesize that the addition of the FLAG tag sequence to the hFP_S protein could hinder its ability to elicit a functional response. With respect to the radioligand binding data, only whole cell radioligand binding was performed on the FLAG-hFP_S stably transfected cell line. Considering the previously reported

immunofluorescence microscopy of FLAG-hFP_S stably transfected cell line, it appears that the hFP_S protein may be expressed primarily perinuclear. One concern is that whole cell radioligand binding experiments would inhibit the transport of agonist across the cell membrane thereby preventing agonist binding to an intracellular expressing receptor. To circumvent this problem, we will utilize crude membrane fractions from the wildtype hFP_S cell line in radioligand binding assays. Additionally, we further hypothesize that the hFP_S receptor may function differently than traditional GPCRs and that non-traditional methods should be employed in attempts to identify its function. Herein, we report the attempts made to elucidate a function for hFP_s utilizing a newly created wildtype hFP_S expressing stable cell lines in 293-EBNA cells.

4.2 Experimental procedures

4.2.1 Creation of a wildtype hFP_S stable cell line in 293-EBNA cells

Utilizing the restriction enzymes *BamHI* and *XhoI*, a 1330 bp fragment was isolated from $hFP_S/pcDNA_3$. The fragment was isolated and subcloned into a $pCEP_4$ expression vector that had been digested with the same enzymes listed above. The resulting plasmid, wildtype $hFP_S/pCEP_4$, was then used to stably transfect 293-EBNA cells by limiting dilution and hygromycin selection as previously described (Fujino, Srinivasan et al. 2000). Simultaneously, 293-EBNA cells were also transfected with empty $pCEP_4$ plasmid and subjected to the same selection process for the purpose of a negative control cell line. This cell line will be utilized along side the hFP_S stably transfected cell line in all experiments and will be designated (-)293-EBNA.

4.2.2 Transient transfection protocol and cell culture

293-EBNA cells used for radioligand binding and IP accumulation were all transfected in the same fashion. Cells were split into 10 cm dishes and the next day were transiently transfected using FuGENE-6 (Roche Molecular Biochemicals) with the respective cDNA plasmid for each of the individual experiments. Untransfected as well as transiently transfected 293-EBNA cells were maintained in DMEM (Life Technologies, Inc.) containing 10% fetal bovine serum (FBS), 250 μg/ml Geneticin and 100 μg/ml gentamicin. 293-EBNA cells stably expressing the wildtype hFP_S receptor or $pCEP_4$ vector alone were maintained in the same media as untransfected 293-EBNA cells only hygromycin (200 μg/ml) was included to maintain receptor expression.

4.2.3 Membrane fraction radioligand binding

Cells were first washed three times using cold MES buffer consisting of 10 mM MES (pH 6.0), 0.4 mM EDTA, and 10 mM $MnCl_2$, then subjected to probe sonication (three seconds). Following sonication, cells were centrifuged and the resulting pellet collected, resuspended in ice-cold MES buffer at a concentration of 10^7 cells/ml, and 100 μl was added to a final assay volume (200 μl) containing 2.5 nM $[^3H]PGF_{2\alpha}$ (total binding) or $[^3H]PGF_{2\alpha}$ plus 10 μM unlabeled $PGF_{2\alpha}$ (nonspecific binding). Incubations were for 1 hr at room temperature and were terminated by filtration through Whatman GF/C glass filters using a cell harvester (M-24R, Brandel). Filters were washed five times with ice-cold MES buffer, and radioactivity determined by liquid scintillation counting.

4.2.4 Inositol phosphate (IP) assay

293-EBNA cells were transfected with either the human FP_A or FP_S receptor plasmid and grown to a confluence of approximately 90-100%. Cells were maintained as previously described. The night before the experiment, 0.2 μM myo-[2-^{3}H]inositol (Amersham, 16.6 Ci/mmol) were added to the cells in antibiotic free regular DMEM media containing no serum. The following morning, cells were washed once with 1x PBS then trypsinized and 10^6 cells were aliquoted per sample. Cells were then centrifuged at 2,100 RPM for 5 min in a tabletop centrifuge. The media were aspirated then resuspended in DMEM media containing 10 mM LiCl (Sigma). Cells were allowed to equilibrate for 10 min at 37°C/5% CO_2. Treatment groups were performed in triplicate with each sample receiving either vehicle (0.002% $NaCO_3$) or 1 μM $PGF_{2\alpha}$ for 1 hr. After 1 hr, samples were centrifuged for 5 min at 2,100 RPM. Cells were washed with PBS and then total inositol extracted by adding 2.5 ml of methanol/chloroform/water (1:1:0.5). Samples were then vortex and centrifuged at 4°C for 15 min, 2,100 RPM. Poly-Prep chromatography columns 0.8 x 4 cm (Bio-Rad) were loaded with 10% AG 1-X8 resin (Bio-Rad) and washed with H_2O. After 4°C spin, the aqueous phase was added to two milliliter H_2O and loaded onto the elution columns. The columns were then washed three times with H_2O and two times with 5 ml of 5 mM sodium tetraborate (borax, Sigma)/60 mM sodium formate (Sigma). The ^{3}H-IPs were eluted with 0.2 M ammonium formate/0.1 M formic acid (Sigma) and radioactivity determined by liquid scintillation counting. Data were analyzed using prism software.

4.2.5 Immunoprecipitation and immunoblot analysis

Cells were plated at a low density and grown to confluence then washed with PBS. The cells were scraped and sonicated in a lysis buffer consisting of 20 mM Tris-HCl (pH 7.5), 10 mM EDTA, 2 mM EGTA, 2 mM phenylmethylsulfonyl fluoride, 0.1 mg/ml leupeptin, and 2 mM sodium vanadate. Samples were centrifuged (16,000 x g) for 15 min at 4°C, the supernatant (cytosolic fraction) was removed and the pellet (particulate fraction) was solublized with lysis buffer containing 0.05% Triton X-100 and centrifuged again to remove insoluble debris as previously described (Fujino and Regan 2001). Protein concentrations were determined using a Bio-Rad assay kit (Bio-Rad Laboratories) and samples were immunoprecipitated overnight utilizing a hFP_S polyclonal antibody (1:100). Samples were then centrifuged for 3 min at 3000 rpm and washed with lysis buffer. Laemmli buffer (5x) was added and the samples were heated for 10 min at 55°C then placed on ice for 5 min and centrifuged. Samples were then separated on a 10% SDS-polyacrylamide gel, transferred to nitrocellulose membranes, and blocked with 1.5% nonfat milk in TBS containing 0.1% polyoxyethylenesorbitan monolaurate (TBST) for 1 hr at room temperature with rotation. The membrane was then incubated with hFP_S polyclonal antibodies (1:1000) overnight at 4°C with rotation. The membranes were washed in TBST and incubated with anti-rabbit secondary antibodies conjugated to horseradish peroxidase (1:10,000, Jackson Laboratories) for 1 hr at room temperature. The membranes were washed, and visualized by enhanced chemiluminescence (SuperSignal; Pierce).

4.2.6 cAMP accumulation assay

Cells were grown to 80% confluence in 10 cm plates, washed with Opti-MEM (Invitrogen) solution (37°C) containing isobutylmethylxanthine (0.1 mg/ml, Sigma). Cells (1 x 10^6 cells/ml^{-1}) were harvested and resuspended in Opti-MEM containing isobutylmethylxanthine and were treated with either vehicle or various concentrations of the respective agonists for 1 hr at 37°C and 5% CO_2. Cells were centrifuged in a Beckman tabletop centrifuge at 3000 rpm for 5 min (room temperature). Cells were resuspended in ice-cold TE buffer [50 mM Tris-HCl, 4 mM EDTA (pH 7.5)] and transferred to microcentrifuge tubes, subsequently reactions were terminated by boiling and placed on ice followed by centrifugation at 14,000 rpm for 2 min. Supernatants (representing ~10^6 cells) were transferred to new tubes wherein an equal volume of [^{3}H]cAMP (PerkinElmer Life Sciences) and twice the volume 0.06 mg/ml protein kinase A (PKA) [Sigma, product P5511] were added. After vortexing, samples were incubated on ice for 2 hr and reaction halted by addition of TE buffer containing 2% bovine serum albumin (BSA) and 26 mg/ml activated charcoal. Following a brief vortex and centrifugation at 14,000 rpm for 1 min, supernatants were added to scintillation vials, briefly vortex and radioactivity determined by liquid scintillation counting. The quantification of cAMP (expressed as pmol per 10^6 cells) accumulated in the samples was done utilizing a standard cAMP curve. The data was analyzed by Graphpad Prism software.

4.2.7 Fluorescence imaging plate reader (FLIPR) assay

Utilizing a FLIPR^{384} Fluoremetric Imaging Plate Reader System (Molecular Devices), experiments were performed measuring intracellular calcium mobilization, pH exchange, and membrane potential fluctuations. In all FLIPR assays, unless otherwise noted, experiments were conducted per Molecular Devices manufacturer protocol.

Ninety-six well drug plates for dose response (DR) and high throughput screening (HTS) of intracellular calcium mobilization and membrane potential fluctuations were comprised of experimental drugs (duplicate) as well as negative (duplicate) and positive control drugs (quadruplicate). These drugs were diluted in a solution of 1x Hanks Balanced Salt solution containing 20 mM HEPES (HBSS-HEPES) at concentrations of 30 μM (experimental drugs) and 3 μM (positive control drugs), respectively. A total of 44 experimental drugs were tested per plate.

Ninety-six well dose response plates were prepared by serial dilution and each drug plate contained negative and positive controls in quadruplicate as well as four experimental drugs, each in duplicate, serially diluted from 30 μM to 0.029 nM.

Promiscuous G-proteins, G_{16} or G_{qs} were transiently transfected into hFP_S, (-)293-EBNA, and positive control cells (hFP_A or ovine FP_B) 72 hrs before the experiment. For the transfection, 25,000 cells were plated into each well and allowed to attach to the 96-well plate. Utilizing FuGENE-6 transfection reagent, each well was transfected with 0.1 μg of either G_{16} or G_{qs} plasmid per manufacturer protocol. Cells were maintained at 37°C in 5% CO_2 for 72 hrs and FLIPR assay were subsequently performed.

FLIPR intracellular calcium assays were performed utilizing manufacturer protocol. Briefly, 96-well plates containing either hFP_S stably transfected cells or (-)293-EBNA cells were plated the night before the experiment. On each 96-well plate, six wells contained hFP_A stably transfected cells. Four of these hFP_A wells served as positive control wells, while two wells served as negative controls receiving only buffer. In some experiments promiscuous G-proteins, G_{16} or G_{qs}, were transfected into the hFP_S, (-)293-EBNA, as well as the hFP_A cells. The number of cells per well varied between experiments, ranging from 12,500 cells to 100,000 cells per well. Within each experiment, however, each plate containing the hFP_S or (-)293-EBNA cells had the same number of cells per well. The 96-well plates were allowed to grow overnight in regular media described above, and were maintained at 37°C in 5% CO_2. The next day the 96-well plates were washed (2x) using a cell washer and an equal volume of Fluo-4 working dye solution (Molecular Probes) buffer was loaded into each well. Cells were returned to 37°C in 5% CO_2 and incubated for 45 min. Following dye loading, cells were washed again (3x) then placed into the FLIPR instrument. Drugs were added from the HTS drug plate at one-third the final volume with the final concentration being 10 μM and 1 μM for the experimental and positive control drugs, respectively. Intracellular calcium accumulation was measured over five min. The data were exported using the FLIPR software and analyzed in Microsoft Excel.

FLIPR intracellular pH assays were performed utilizing manufacturer protocol. Briefly, ninety-six well plates were set up containing hFP_S cells or the (-)293-EBNA cells. As before, in each 96 well plate, six wells were set up for positive and negative

controls (4 wells and 2 wells, respectively) but in these experiments the ovine FP_B stably expressing cell line was utilized. For these experiments, 50,000 cells per well were routinely used and in some experiments promiscuous G-proteins, G_{16} or G_{qs}, were transfected into the hFP_S, (-)293-EBNA cells and ovine FP_B cell lines as previously described. Cells were plated and maintained as previously described in FLIPR intracellular calcium assay. Drug plates were prepared at 1.25x (12.5 μM) the final concentration in the same diluent and fashion as described above. The day of the experiment cells were washed (2x) in HBSS-HEPES buffer then loaded with an equal volume of BCECF working dye solution (7.2 μM, Molecular Probes #B-1150). Cells were incubated for 45 min at 37°C in 5% CO_2. After 45 min, one-tenth volume an acid load solution (200 mM NH_4CL_2 in 1x HBSS-HEPES) was added to each well followed by a 15 min incubation at 37°C in 5% CO_2. Subsequently, cells were washed 3x with wash buffer (20 mM NH_4Cl_2 in HBSS-HEPES). Cell plates were placed in FLIPR instrument and drug was added to each well at a final concentration of 10 μM. Changes in intracellular H^+ ions were measured over ten min. The data were exported the using FLIPR software and analyzed using Microsoft Excel.

FLIPR membrane potential assays were performed utilizing manufacturer protocol. In all membrane potential experiments 96 well plates contained hFP_S or (-)293-EBNA cells that were prepared and maintained as previously described in the intracellular pH assay. For these experiments the ovine FP_B stably expressing cells were used as positive control cells. Drug plates for HTS screening were prepared as previously described. In some experiments, promiscuous G-proteins, G_{16} or G_{qs}, were

transfected into the hFP_S, (-)293-EBNA cells and ovine FP_B cell lines as previously described. The day of the experiment, cells were washed (2x) and an equal volume of DiBAC (molecular probes, #B-438) working dye solution, final concentration 5 μM was added to each well and allowed to equilibrate for 60 min at 37°C in 5% CO_2. During the incubation, DiBAC dye was added to the drug plate at a final concentration of 5 μM and allowed to incubate at 37°C. After incubation, FLIPR experiments were performed at 36°C and one-third volume of drug (10 μM final concentration) was added to each well. Membrane potential experimental data were collected over ten min. The data were exported using the FLIPR and analyzed using Microsoft Excel software.

4.3 Results

To scrutinize further the functional expression of hFP_S, 293-EBNA cells were stably transfected with a wildtype hFP_S. A clonal cell line was identified for hFP_S expression based upon immunofluorescence staining (data not shown) and immunoblot analysis (Figure 4.1) with hFP_S polyclonal antibodies. Figure 4.3.1 depicts differential hFP_S protein expression, corresponding to the expected size of 32.7 kDa, in the particulate (lanes 2-5) but not cytosolic fraction of isolated clonal cell lines. Additionally, this band was absent in the control (-)293-EBNA cell line (lane 1). For the purpose of future experiments, unless otherwise stated, hFP_S clone 18 (lane 3) will be the primary cell line utilized to characterize the function of hFP_S. Interestingly, while is appears from immunofluorescence staining that this receptor is endogenously expressed, it still remains in a membrane fraction inside the cell.

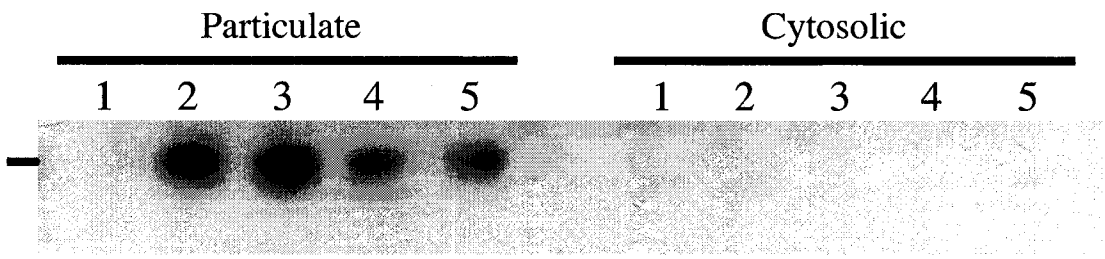

Figure 4.1 Immunoblotting of (-)293-EBNA and wt hFP_S stable cell line clones 24, 18, 21, and 2 corresponding to *lanes 1, 2, 3, 4, and 5*, respectively. For immunoblotting, 180 μg of clone 18 and 280 μg of all other clones particulate and cytosolic protein were immunoprecipitated with polyclonal hFP_S antibodies. The expected size of hFP_S is approximately 32.7 kDa. Tick Mark indicates the position of the 25 kDa standard. These results are representative of two independent experiments.

Figure 4.2 shows [^{3}H]PGF$_{2\alpha}$ (right) and [^{3}H]PGE$_2$ (left) membrane radioligand binding of stably transfected FLAG-hFP$_S$, hFP$_S$, (-)293-EBNA, and hFP$_A$ cell lines. The two highest expressing wt hFP$_S$ stable cell lines (clones 18 and 24) were utilized in these binding experiments. PGE$_2$ radioligand binding was determined as a result of a serendipitous discovery that suggested PGE$_2$ activation of adenylate cyclase in this cell line. Only the hFP$_A$ cell line demonstrated significant PGF$_{2\alpha}$ and PGE$_2$ binding in these experiments, while it appeared that wt hFP$_S$ (clone 18) as well as the FLAG-hFP$_S$ did demonstrate a small amount of PGE$_2$ binding, initially, these results could not be reproduced. These data indicate that whether hFP$_S$ is expressed in the cell membrane or an intracellular membrane it is not capable of binding PGE$_2$ and PGF$_{2\alpha}$.

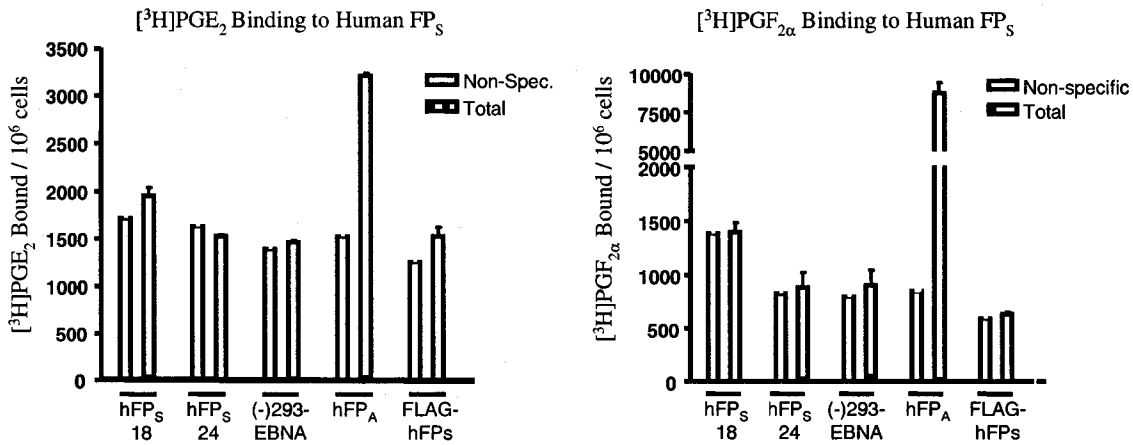

Figure 4.2 [^{3}H]PGE$_2$ (left) and [^{3}H]PGF$_{2\alpha}$ (right) membrane fraction radioligand binding of stably transfected FLAG-hFP$_S$, hFP$_S$, (-)293-EBNA, and hFP$_A$ cell lines. Total (*checkered boxes*) and nonspecific binding (*open boxes*) is reported for each cell line. The specific binding is the total binding minus the non-specific binding. The data for PGF$_{2\alpha}$ and PGE$_2$ binding are representative of a single independent experiment.

Functional studies to determine PLC mediated IP hydrolysis as well as cAMP accumulation through activation of adenylate cyclase were also performed with the wildtype hFP_S cell line. As predicted by the binding data, no significant stimulation of IP hydrolysis was observed with either PGE_2 or $PGF_{2\alpha}$ (data not shown). Likewise, no agonist dependent adenylate cyclase activity could be determined by measuring cAMP accumulation in the hFP_S cell line using BW245C (DP agonist), illoprost (IP agonist), PGE_2, $PGF_{2\alpha}$, PGJ_2, 8-iso-PGE_2, and oxytocin (data not shown).

High throughput screening of the hFP_S cell line versus the (-)293-EBNA cell line was achieved utilizing a FLIPR instruments measuring changes in intracellular calcium mobilization, pH change, and fluctuations in membrane potential. In some experiments promiscuous G-proteins were also exploited in these assays for agonist dependent stimulation of hFP_S cells not observed in (-)293-EBNA cells. Table one list the various compounds used in the calcium, pH, and membrane potential FLIPR assays, respectively.

Functional FLIPR HTS experiments measuring intracellular calcium and pH changes using the compounds from table one demonstrated no observable activation of the hFP_S cell line versus (-)293-EBNA control cells. Transient transfection of promiscuous G-proteins, G_{16} and G_{qs}, into the hFP_S and (-)293-EBNA cells followed by HTS screening also revealed no agonist dependent activation in these cells. In both FLIPR assays, positive as well as negative control cell lines demonstrated appropriate functional responses, as expected, indicating experimental technique and strongly suggesting significant results.

Wells	Drug Name	Concentration (log M) *		Wells	Drug Name	Concentration (log M) *	
A1-B1	Buffer /experimental cells	NC	=negative control	A1-B1	Buffer /experimental cells	NC	=negative control
C1-D1	Buffer /ovine FPB cells	NC	=negative control	C1-D1	Buffer /ovine FPB cells	NC	=negative control
E1-H1	17-phenyl-PGF2a/ ovine FPB cells	-6.0	=positive control	E1-H1	17-phenyl-PGF2a/ ovine FPB cells	-6.0	=positive control
A2&B2	9-deoxy-9-methylene PGE2	-5.0		A2&B2	R-2 methanandamide	-5.0	
C2&D2	16,16-dimethyl PGE2	-5.0		C2&D2	PGH2	-5.0	
E2&F2	Arachidonyl ethanolamide	-5.0		E2&F2	unoprostone	-5.0	
G2&H2	PGE2	-5.0		G2&H2	PGB2	-5.0	
A3&B3	11-B-PGF2a ethanolamide	-5.0		A3&B3	AL8810	-5.0	
C3&D3	11-deoxy-16,16-dimethyl PGE2	-5.0		C3&D3	Lingnoceric ceramide	-5.0	
E3&F3	11-deoxy-PGE1	-5.0		E3&F3	AH6809	-5.0	
G3&H3	PGJ2	-5.0		G3&H3	PGF2a alcohol methyl ester	-5.0	
A4&B4	15-keto-PGE2	-5.0		A4&B4	PGG2	-5.0	
C4&D4	Nervonic Ceramide	-5.0		C4&D4	Pinane TXA2	-5.0	
E4&F4	15-deoxy-delta 12,14-PGD2	-5.0		E4&F4	R-1 methanandamide	-5.0	
G4&H4	Arachidonyl serotonin	-5.0		G4&H4	I-BOP	-5.0	
A5&B5	Arachidonyl dopamine	-5.0		A5&B5	SQ 29,548	-5.0	
C5&D5	16,16-dimethylPGF2a	-5.0		C5&D5	11-deoxy-PGE2	-5.0	
E5&F5	CAY 10399	-5.0		E5&F5	TXB2	-5.0	
G5&H5	Butaprost	-5.0		G5&H5	5-trans-U46619	-5.0	
A6&B6	PGF2a ethanolamide	-5.0		A6&B6	PGK2	-5.0	
C6&D6	PGE2 ethanolamide	-5.0		C6&D6	Misoprostol	-5.0	
E6&F6	8-iso-PGE2	-5.0		E6&F6	Carbocyclic TXA2	-5.0	
G6&H6	PGF2a 1,3-gycerol ester	-5.0		G6&H6	15-deoxy-delta 12,14-PGJ2	-5.0	
A7&B7	PGE2 1,3-glycerol ester	-5.0		A7&B7	delta 12-PGJ2	-5.0	
C7&D7	Cloprostenol	-5.0		C7&D7	AGN195699	-5.0	
E7&F7	11-B-PGF2a	-5.0		E7&F7	AGN202698	-5.0	
G7&H7	PGA1	-5.0		G7&H7	AGN202622	-5.0	
A8&B8	(19) R-hydroxy PGF2a	-5.0		A8&B8	AGN195854	-5.0	
C8&D8	1a, 1b dihomo PGF2a	-5.0		C8&D8	AGN193261	-5.0	
E8&F8	8-iso-PGF2a	-5.0		E8&F8	AGN198267	-5.0	
G8&H8	17-trans-PGE3	-5.0		G8&H8	AGN202521	-5.0	
A9&B9	6-15-diketo-13,14,-dihydro PGF1a	-5.0		A9&B9	AGN192185	-5.0	
C9&D9	PGF1B	-5.0		C9&D9	AGN198518	-5.0	
E9&F9	15-keto-PGF1a	-5.0		E9&F9	AGN198013	-5.0	
G9&H9	15-deoxy-delta 12,14-PGA1	-5.0		G9&H9	AGN203892	-5.0	
A10&B10	15-epi-PGA1	-5.0		A10&B10	AGN198058	-5.0	
C10&D10	8-iso-PGE1	-5.0		C10&D10	AGN198421	-5.0	
E10&F10	16,16-dimethyl PGF2a	-5.0		E10&F10	AGN192022	-5.0	
G10&H10	15(s)-15-methyl PGD2	-5.0		G10&H10	Angiotensin II	-5.0	
A11&B11	Leukotriene B4 ethanolamide	-5.0		A11&B11	Oxytocin	-5.0	
C11&D11	S-1 methanandamide	-5.0		C11&D11	AGN204361	-5.0	
E11&F11	PGF3a	-5.0		E11&F11	AGN191995	-5.0	
G11&H11	5-trans-PGE2	-5.0		G11&H11	AGN193179	-5.0	
A12&B12	PGE1 alcohol	-5.0		A12&B12	AGN191837	-5.0	
C12&D12	U-46619	-5.0		C12&D12	AGN192066	-5.0	
E12&F12	Carboprostacyclin	-5.0		E12&F12	AGN193181	-5.0	
G12&H12	PGF1a	-5.0		G12&H12	15-keto-PGE1	-5.0	

Table 4.1 High throughput screening compounds utilized in FLIPR Ca^{2+}, pH, and membrane potential assays. Each column represents one 96 well plate identifying the location on the plate (wells), drug name, and drug concentration used in the experiments. Each drug was done in duplicate and experimental cells were either hFP_S or (-)293-EBNA stably transfected cells.

Utilizing hFP_S, (-)293-EBNA and ovine FP_B cell lines, FLIPR HTS membrane potential analysis demonstrated four potential ligands that appeared to have selective activity in hFP_S expressing cells that was not observed in (-)293-EBNA cells. These ligands include a naturally occurring agonist, oxytocin, as well as the synthetic compounds, PGB_2 (Cayman), AGNA9B9, and AGNA10B10 (Allergan Inc.). These experiments were repeated twice and demonstrated similar reproducibility. However, these are preliminary data and further work is required to determine the potency and selectivity of these compounds for the hFP_S receptor as well as further defining the specific signaling pathway.

4.4 Discussion

Herein, we describe the methods used to elucidate the pharmacological characterization for the hFP_S orphan receptor. Previously, functional characterization of hFP_S had been determined utilizing a FLAG-hFP_S cell line, for which, $PGF_{2\alpha}$ binding and IP hydrolysis were not observed. Concerned about the effects the FLAG epitope might have on the functional activity of this novel receptor, we generated a stably expressing wildtype hFP_S receptor cell line in (-)293-EBNA cells. Figure 4.1 demonstrates the different magnitude of expression for the hFP_S clones that is not observed in (-)293-EBNA cells. From these experiments, we selected the highest expressing clone 18 to be used in a variety of pharmacological assays. Radioligand binding of $PGF_{2\alpha}$ and PGE_2 as well as IP hydrolysis could not be achieved using the wildtype hFP_S cell line. The rationale for the binding of PGE_2 developed from a serendipitous discovery using the FLAG-hFP_S cell line in an adenylate cyclase assay. We intended to measure only the

basal levels of cAMP accumulation utilizing these cells compared to (-)293-EBNA to investigate the possibility of hFP_S possible coupling to the G_s pathway. However, FLAG-hFP_S cells accidentally received PGE_2 treatment and upon analysis it initially appeared to stimulate a small but significant increase in cAMP accumulation that was not observed in vehicle treated FLAG-hFP_S cells or (-)293-EBNA cells. When this result was more closely scrutinized by measuring cAMP accumulation utilizing a PGE_2 dose response the data were unremarkable and the PGE_2 radioligand binding data appeared to support these studies (Figure 4.3.2). Utilizing specific signaling assays and different prostaglandins, we were unable to identify any functionality for the hFP_S receptor and decided further investigations would require more widespread methodology.

Three different FLIPR HTS assays were performed using an array of agonists on hFP_S and (-)293-EBNA cells measuring intracellular calcium, pH changes and membrane potential fluctuations. While the calcium and pH experiments yielded no functional data, the membrane potential assays revealed agonist stimulated results from four compounds, three synthetic compounds and one naturally occurring. Interestingly, the oxytocin receptor has been shown to have a direct relationship with the FP receptor gene as demonstrated in FP knockout mice (Sugimoto, Yamasaki et al. 1997).

It is well established that FP knockout mice demonstrate an absence of parturition, wherein the fetuses die *in utero* and undergo reabsorption. However, fetuses could be rescued by ovariectomy or cesarean operation from these mice before or at the expected term (Sugimoto, Segi et al. 1998). Additionally, Sugimoto et.al. observed the level of oxytocin receptor mRNA expression to be markedly decreased, days 17-20 of

pregnancy, in homozygous FP receptor knockout mice versus wildtype and heterozygous mice and that this effect could be reversed by ovariectomy. It has been reported that oxytocin receptors are the suspected triggers for parturition (Soloff and Hinko 1993). Interestingly, FP wildtype mice demonstrated progressively decreased plasma concentrations of progesterone between days 19 and 21 of pregnancy that was not observed in FP knockout mice while estrogen levels between the two remained virtually unchanged (Sugimoto Y, Segi K, Ichikawa A, 1998). From these studies, there appears to be a direct relationship between FP and oxytocin receptors that may also be inversely related to serum progesterone levels in mice. The fact that we observe a possible oxytocin membrane potential stimulation in the hFP_S expressing cells that is not seen in the (-)293-EBNA cells suggest the hypothesis that hFP_S is directly up-regulating the G_q-coupled oxytocin receptor. Clearly, additional experiments directly measuring oxytocin mediated IP hydrolysis in hFP_S cells versus (-)293-EBNA cells should be examined. If this hypothesis is proven to be valid, then this data along with that published in the literature suggests the presence a murine hFP_S ortholog, which would support a possible function for the hFP_S receptor. Currently, although we have established a few potential agonists for hFP_S, however, a pharmacological function has yet to be determined.

CHAPTER FIVE:

SUMMARY, CONCLUSIONS AND FUTURE STUDIES

5.1 Summary and conclusions

In this dissertation, I have described the cloning and characterization of a human cDNA ortholog of the ovine FP_B receptor isoform as well as a novel human FP receptor mRNA alternative splice variant. Prostanoid receptor gene alternative splicing has been demonstrated to exist around the middle of TM6 and in the carboxyl tail downstream of TM7. Previously, 7TM mRNA alternative splice variants were first identified for FP receptors from an ovine mid-cycle corpus luteum library (Graves, Pierce et al. 1995; Pierce, Bailey et al. 1997). To date, these FP receptor isoforms represent the most distinguished FP splice variants with regard to their pharmacological differences and significance. More recently, bovine FP receptor gene splicing has been demonstrated at both the TM6 and carboxyl tail splice donor sites. In the bovine corpus luteum, mRNA alternative splicing produces three 6TM and three carboxyl tail FP receptor isoforms (Ishii and Sakamoto 2001; Sakamoto, Ishii et al. 2002). With respect to their pharmacological and physiological characterization, the bovine 6TM and 7TM splice variants are poorly defined compared to the ovine FP receptor isoforms.

Utilizing RACE PCR, we identified two clones from placenta and CX-1 colon adenocarcinoma cDNA libraries that appear to be putative human orthologs of the ovine FP_B receptor. These hFP_B orthologs were discovered to have DNA inverted repeat sequences common to the hFP receptor that were responsible for their unique cDNA sequence. Interestingly, the cDNA sequence splice site for the hFP_B placenta clone is located exactly where it would be predicted in relation to the ovine FP isoforms and results in a truncated receptor much like the ovine FP_B. It is hard to believe that a cloning

artifact could be produced with cDNA sequence modifications at the exact location that is observed across species. We attempted to functionally characterize the placenta hFP_B clone using a variety of pharmacological methods and transient transfections. However, while initial experiments in these assays appeared to be successful, efforts are required to determine their reproducibility. We later attempted to characterize the CX-1 adenocarcinoma cell line from which a second hFP_B clone was identified. Employing a RT-PCR strategy using hFP_A as well as hFP_{gen} primers, we demonstrated PCR products for the hFP_{gen} primer sets but not the hFP_A primer set. This data suggests the presence of an FP receptor isoform that is not hFP_A, supporting the RACE PCR CX-1 cloning data. Consequently, we attempted to gain a $PGF_{2\alpha}$ functional response in these cells to confirm the presence of an FP receptor isoform. Again, utilizing a variety of pharmacological methods and transient transfections, we were able to gain some initial results that suggested this possibility but these results could not be reproduced. The effect the inverted repeat DNA sequence has on protein expression is not clear but it could be one explanation for the lack of replication in the pharmacological experiments. One obvious conclusion that can be made is that if these hFP_B cDNA sequences are not cloning artifacts, which we believe to be the situation, then these receptor isoforms are generated by a means independent of mRNA alternative splicing. However, significant scientific data will be required to prove this theory.

Prostanoid receptor 6TM alternative mRNA splicing had been previously reported for the rat EP_1 and bovine FP receptors. For the rEP_1, one isoform exists (rEP_1-variant) and has been shown to bind PGE_2 subsequently suppressing the actions of EP_1 and EP_4

when coexpressed in CHO cells. Bovine FP receptors demonstrate three 6TM receptor isoforms (FP-δ, FP-ε, and 6TM-FP-variant), all three have been reported as cDNA sequence but only one is moderately characterized. This isoform, (6TM-FP-variant) when coexpressed with the bovine FP receptor demonstrates a decrease in PKC activity while $PGF_{2\alpha}$ binding data is not reported. We have identified a human 6TM FP receptor alternative splice variant, termed hFP_S that is generated by an insertion of a 71 bp exon into the TM6 splice site corresponding to the distal end of TM6. The bovine 6TM-FP-variant and hFP_S are produced by the same mechanism; an insertion that gives rise to truncated receptors lacking TM-7 resulting in an extracellular carboxy terminus. We have demonstrated mRNA expression of hFP_S in heart, placenta as well as skeletal muscle and confirmed protein expression with the use of antibodies in decidual, endothelial and trophoblast placenta cell lineages. Interestingly, immunofluorescence microscopy of hFP_S expressing stable cell lines demonstrates intracellular localization of a majority of the receptor suggesting it may not be expressed in the plasma membrane or has additional requirements to be expressed in the plasma membrane. Additionally, RT-PCR of HUVEC cells with hFP_S specific and hFP_A specific primers reveals only PCR products with the hFP_S specific primers suggesting that these receptors may demonstrate differential cellular expression.

Pharmacological characterization of wildtype hFP_S has demonstrated a lack of $PGF_{2\alpha}$ and PGE_2 binding in addition to $PGF_{2\alpha}$ mediated IP hydrolysis. Adenylate cyclase assays with various prostaglandin analogs as well as FLIPR assays measuring intracellular calcium and pH changes generated no discernible data. However, FLIPR

HTS membrane potential assays did yield four potential agonist for hFP_S activation that were not observed in (-)293-EBNA cells, namely oxytocin, PGB_2, AGNA9B9, and AGNA10B10. The latter two agonists are synthetic compounds produced by Allergan Inc. The effects of oxytocin my not be a direct result of hFP_S activation but rather activation of an hFP_S induced oxytocin receptor (OTR). Previous data reported demonstrates FP knockout mice to be deficient in OTR (Sugimoto, Segi et al. 1998). The membrane potential agonists need to be further scrutinized for hFP_S selectivity in addition to their potency and until such data is determined hFP_S must be considered an orphan receptor.

In conclusion, I have demonstrated that at least one FP receptor alternative splice variant, of the 6TM nature, exists in humans but is currently lacking pharmacological function. In addition, I also present evidence for the possible existence of a human FP_B receptor isoform that may be generated from a mechanism other than traditional mRNA alternative splicing and could play a role in the development of colon cancer.

5.2 Future studies

As described earlier, FP knockout mice are incapable of delivering their fetus to term without the assistance of a cesarean section or an ovariectomy implicating a dysfunction in or lack of OTR. Compared to wildtype mice, FP knockout mice are deficient in OTR and ovariectomy of FP knockout mice seems to partially restore the OTR expression that is not observed in sham-operated mice (Sugimoto Segi 1998). FLIPR HTS analysis demonstrates oxytocin activation of an hFP_S expressing cell line but not observed in control cells. We hypothesize from the FLIPR and knockout mice data

that hFP_S could potentially up regulate the expression of OTR. Since the OTR is coupled to the G_q protein signal transduction pathway, total IP mobilization can be performed using oxytocin on (-)293-EBNA, hFP_S and hFP_A expressing cell lines to test this hypothesis.

Numerous receptors display a degree of basal activity in the absence of agonist stimulation. It is not uncommon to observe this basal activity in a functional assay when comparing cell lines stably over expressing a given receptor to control cells. While most receptors are held largely in the inactive state, basal activity is thought to occur from the receptor bouncing in and out of an active conformation. Therefore, it is plausible to hypothesize that this basal activity has an effect on the gene expression within the cell it is expressed. We believe that microarray analysis of hFP_S stably expressing cells compared to (-)293-EBNA cells will display a unique pattern of gene expression that is related to the basal activity of the hFP_S receptor. Identifying the unique genes that are regulated by hFP_S may give valuable information as to defining its pharmacological and physiological function.

One concern regarding the functional characterization of hFP_S that has developed from the immunofluorescence staining (figure 3.5) is a large percentage of the receptor appears to be localized around a perinuclear intracellular compartment. Interestingly, olfactory receptors (ORs) are difficult to functionally express in heterologous cells and traffic poorly to the plasma membrane remaining trapped in the endoplasmic reticulum or Golgi apparatus, similar to the hFP_S receptor. Recently, it has been shown that expressing ORs in mature as well as differentiated olfactory cell lines versus

undifferentiated cell lines results in receptor trafficking to the plasma membrane (Gimelbrant, Haley et al. 2001). Gimelbrant and colleagues also show that certain types of ORs require specific chaperone proteins for proper trafficking to the plasma membrane. Also, other examples of GPCR whose membrane trafficking in heterologous cells improves in the presence of specific accessory proteins have been described (Ferreira, Nakayama et al. 1996; Ferreira, Nakayama et al. 1997; McLatchie, Fraser et al. 1998). These chaperone proteins are only expressed in distinct cell types. Immunofluorescence staining of hFP_S transiently transfected cell lines that are more native or mature and of different lineage (endothelial, decidual and trophoblast) than 293-EBNA cells can be utilized to determine if differential receptor localization exists similar to ORs. Keeping in mind that the hFP_S receptor has been shown to be expressed in vascular endothelial cells and that the bovine species has demonstrated FP 6TM receptor splice variants similar to hFP_S, it is possible that these receptors are activated by the same endogenous agonist. hFP_S cells are maintained in 10% fetal bovine serum that is obviously collected from the fractioning of fetal bovine blood. If the bovine 6TM FP receptor agonist is present in this serum and is capable of activating hFP_S resulting in its internalization it would explain the intracellular localization of this receptor. Performing immunofluorescence staining in the presence of reduced serum, 0.1% and 1% versus 10% perhaps would relocalize the hFP_S receptor to the plasma membrane. If this hypothesis were proven true then high performance liquid chromatography could then be utilized to fractionate the FBS serum isolating the individual components to be used in HTS and pharmacological screening for identifying an hFP_S agonist.

An alternative to the FLIPR membrane potential assay would be performing electrophysiology experiments on xenopus oocytes. Two advantages appear by utilizing this system. First, ion channels targeted to intracellular compartments in mammalian cells have been characterized in oocytes because they have been shown to express in the plasma membrane. The intracellular expression of hFP_S may be overcome and plasma membrane expression achieved utilizing the oocyte experimental model subsequently resolving the problem of agonist diffusion across the plasma membrane for activation of hFP_S. Second, if oocyte hFP_S receptor expression remains intracellular then patch clamp electrophysiology experiments can also be utilized to deliver drug across the plasma membrane thereby alleviating the problem of agonist diffusion across the plasma membrane. Utilizing this system, various agonist can be screened for hFP_S activity including the positive agonists from the FLIPR HTS membrane potential assay.

FP knockout, but not wildtype, mice demonstrated a possible correlation of an increased apoptotic index and decreased Bcl-2 expression resulting in active caspase-3 activity in placenta and decidual tissue. Interestingly, the same cell types, decidual and trophoblast cells, that demonstrated the highest rate of apoptosis in FP knockout mice were the same cell types positively labeled for hFP_S immunoreactivity in human placenta. These data collectively suggest the possibility that hFP_S may have an anti-apoptotic function. Correspondingly, hFP_S appears to have an increased growth rate when compared to hFP_A and (-)293-EBNA cells (unpublished observation). In separate experiments conducted by two different investigators, the hFP_S expressing cells appeared to grow about 25% faster than the control cell lines. A series of experiments utilizing

flow cytometry can be conducted to investigate the possible function of the hFP_S receptor with respect to apoptosis. First, the growth phase of each of these cell lines can be performed to determine if hFP_S expressing cells are in a higher S-phase (DNA replication) versus the hFP_A and (-)293-EBNA cell lines. Second, differential expression of Bcl-2 in each of these cell lines could also be quantitated using flow cytometry and an antibody to Bcl-2. Additionally, if Bcl-2 is determined to be expressed in the hFP_S cell line, as well as the others, RNAi experiments can be conducted to knock down hFP_S and hFP_A receptor expression to measure the effects on Bcl-2 expression thereby establishing a direct link between the receptor and Bcl-2. Third, apoptotic index experiments can be performed by treating all three cell lines with staurosporine, a known general inducer of apoptosis, then subsequently measuring the different markers of apoptosis.

Recently, reverse pharmacology has become a popular method for identification of oGPCRs. These techniques are often fishing expeditions that use the oGPCR as bait in order to screen purified organ extracts or vast collections of previously identified signaling peptide or chemical compounds. Most of the agonists identified by this method are protein in nature. Reverse pharmacology can be performed on hFP_S expressing cells and protein sequence utilizing human and bovine tissue extract from placenta, heart and skeletal muscle. Bovine tissue is a logical choice because it is the only other species, beside human, that displays 6TM FP receptor heterogeneity.

REFERENCES:

Abramovitz, M., Y. Boie, et al. (1994). "Cloning and expression of a cDNA for the human prostanoid FP receptor." J Biol Chem **269**(4): 2632-6.

Adams, J. W., D. S. Migita, et al. (1996). "Prostaglandin F2 alpha stimulates hypertrophic growth of cultured neonatal rat ventricular myocytes." J Biol Chem **271**(2): 1179-86.

Allaire, A. D., K. A. Ballenger, et al. (2000). "Placental apoptosis in preeclampsia." Obstet Gynecol **96**(2): 271-6.

Anthony, T. L., H. Fujino, et al. (2002). "Differential regulation of Ca(2+)-dependent Cl- currents by FP prostanoid receptor isoforms in Xenopus oocytes." Biochem Pharmacol **63**(10): 1797-806.

Anthony, T. L., K. L. Pierce, et al. (1998). "Prostaglandin F2 alpha receptors in the human trabecular meshwork." Invest Ophthalmol Vis Sci **39**(2): 315-21.

Aoki, J., H. Katoh, et al. (1999). "Signal transduction pathway regulating prostaglandin EP3 receptor-induced neurite retraction: requirement for two different tyrosine kinases." Biochem J **340 (Pt 2)**: 365-9.

Bergstrom, S., and Sjovall, J. (1957). "The isolation of prostaglandin." Acta Chem Scand **11**: 1086.

Betz, R., J. Lagercrantz, et al. (1999). "Genomic structure, 5' flanking sequences, and precise localization in 1P31.1 of the human prostaglandin F receptor gene." Biochem Biophys Res Commun **254**(2): 413-6.

Breyer, R. M., C. K. Bagdassarian, et al. (2001). "Prostanoid receptors: subtypes and signaling." Annu Rev Pharmacol Toxicol **41**: 661-90.

Chambers, J. K., L. E. Macdonald, et al. (2000). "A G protein-coupled receptor for UDP-glucose." J Biol Chem **275**(15): 10767-71.

Chang, C., M. Negishi, et al. (1997). "Functional interaction of the carboxylic acid group of agonists and the arginine residue of the seventh transmembrane domain of prostaglandin E receptor EP3 subtype." Biochem J **322 (Pt 2)**: 597-601.

Chen, M. C., D. A. Amirian, et al. (1988). "Prostanoid inhibition of canine parietal cells: mediation by the inhibitory guanosine triphosphate-binding protein of adenylate cyclase." Gastroenterology **94**(5 Pt 1): 1121-9.

Coleman, R. A. and I. Kennedy (1985). "Characterisation of the prostanoid receptors mediating contraction of guinea-pig isolated trachea." Prostaglandins **29**(3): 363-75.

Coleman, R. A., W. L. Smith, et al. (1994). "International Union of Pharmacology classification of prostanoid receptors: properties, distribution, and structure of the receptors and their subtypes." Pharmacol Rev **46**(2): 205-29.

Crofford, L. J., S. R. Pillemer, et al. (1994). "Hypothalamic-pituitary-adrenal axis perturbations in patients with fibromyalgia." Arthritis Rheum **37**(11): 1583-92.

Cross, J. C., M. Hemberger, et al. (2002). "Trophoblast functions, angiogenesis and remodeling of the maternal vasculature in the placenta." Mol Cell Endocrinol **187**(1-2): 207-12.

Debra Goldman-Wohl, S. Y. (2002). "Regulation of trophoblast invasion: from normal implantation to pre-eclampsia." Mol Cell Endocrinol **187**: 233-238.

Ehrenpreis, S., J. Greenberg, et al. (1973). "Prostaglandins reverse inhibition of electrically-induced contractions of guinea pig ileum by morphine, indomethacin and acetylsalicylic acid." Nat New Biol **245**(148): 280-2.

Elshourbagy, N. A., R. S. Ames, et al. (2000). "Receptor for the pain modulatory neuropeptides FF and AF is an orphan G protein-coupled receptor." J Biol Chem **275**(34): 25965-71.

Euler, U.S. von. (1934). "Zur Kenntnis der Pharmakologischen Wirkungen von Nativsekreten und Extrakten Mannlicker Accessorischer Geschlechtsdrusen." Arch Exp Pathol Pharmakol **175**: 78-81.

Euler, U.S. von. (1935). "Uber die Spezifische Blutdrucksenkende Substanz des Menschlichen Prosta- und Samenblasensekretes." Klin Wochenschr **14**: 1182-83.

Euler, U.S. von. (1937). "On the specific vasodilating and plain muscle stimulating substances from accessory genital glands in man and certain animals (prostaglandin and vesiglandin)." J Physiol. (Lond) **88**: 213-34.

Ezashi, T., K. Sakamoto, et al. (1997). "Genomic organization and characterization of the gene encoding bovine prostaglandin F2alpha receptor." Gene **190**(2): 271-8.

Fazleabas, A. T. and Z. Strakova (2002). "Endometrial function: cell specific changes in the uterine environment." Mol Cell Endocrinol **186**(2): 143-7.

Ferreira, P. A., T. A. Nakayama, et al. (1996). "Cyclophilin-related protein RanBP2 acts as chaperone for red/green opsin." Nature **383**(6601): 637-40.

Ferreira, P. A., T. A. Nakayama, et al. (1997). "Interconversion of red opsin isoforms by the cyclophilin-related chaperone protein Ran-binding protein 2." Proc Natl Acad Sci U S A **94**(4): 1556-61.

Fujino, H., K. L. Pierce, et al. (2000). "Delayed reversal of shape change in cells expressing FP(B) prostanoid receptors. Possible role of receptor resensitization." J Biol Chem **275**(38): 29907-14.

Fujino, H. and J. W. Regan (2001). "FP prostanoid receptor activation of a T-cell factor/beta -catenin signaling pathway." J Biol Chem **276**(16): 12489-92.

Fujino, H. and J. W. Regan (2003a). "Prostaglandin F(2alpha) stimulation of cyclooxygenase-2 promoter activity by the FP(B) prostanoid receptor." Eur J Pharmacol **465**(1-2): 39-41.

Fujino, H. and J. W. Regan (2003b). "Prostanoid receptors and phosphatidylinositol 3-kinase: a pathway to cancer?" Trends Pharmacol Sci **24**(7): 335-40.

Fujino, H., D. Srinivasan, et al. (2000). "Differential regulation of prostaglandin F(2alpha) receptor isoforms by protein kinase C." Mol Pharmacol **57**(2): 353-8.

Fujino, H., D. Srinivasan, et al. (2002). "Cellular conditioning and activation of beta-catenin signaling by the FPB prostanoid receptor." J Biol Chem **277**(50): 48786-95.

Funk, C. D., L. Furci, et al. (1993). "Cloning and expression of a cDNA for the human prostaglandin E receptor EP1 subtype." J Biol Chem **268**(35): 26767-72.

Garcia-Perez, A. and W. L. Smith (1984). "Apical-basolateral membrane asymmetry in canine cortical collecting tubule cells. Bradykinin, arginine vasopressin, prostaglandin E2 interrelationships." J Clin Invest **74**(1): 63-74.

Gimelbrant, A. A., S. L. Haley, et al. (2001). "Olfactory receptor trafficking involves conserved regulatory steps." J Biol Chem **276**(10): 7285-90.

Goldblatt, M.W. (1933). "A depressor substance in seminal fluid." Chem Ind (Lond) **52**: 1056-57.

Goldman-Wohl, D. and S. Yagel (2002). "Regulation of trophoblast invasion: from normal implantation to pre-eclampsia." Mol Cell Endocrinol **187**(1-2): 233-8.

Goodman, L. S., A. Gilman, et al. (1996). Goodman & Gilman's the pharmacological basis of therapeutics. New York, McGraw-Hill Health Professions Division.

Graves, P. E., K. L. Pierce, et al. (1995). "Cloning of a receptor for prostaglandin F2 alpha from the ovine corpus luteum." Endocrinology **136**(8): 3430-6.

Hasegawa, H., H. Katoh, et al. (2000). "Different membrane targeting of prostaglandin EP3 receptor isoforms dependent on their carboxy-terminal tail structures." FEBS Lett **473**(1): 76-80.

Hirata, M., Y. Hayashi, et al. (1991). "Cloning and expression of cDNA for a human thromboxane A2 receptor." Nature **349**(6310): 617-20.

Ishii, Y. and K. Sakamoto (2001). "Suppression of protein kinase C signaling by the novel isoform for bovine PGF(2alpha) receptor." Biochem Biophys Res Comm **285**(1): 1-8.

Ishikawa, T. O., Y. Tamai, et al. (1996). "Mapping of the genes encoding mouse prostaglandin D, E, and F and prostacyclin receptors." Genomics **32**(2): 285-8.

Katoh, H., J. Aoki, et al. (1998). "Constitutively active Galpha12, Galpha13, and Galphaq induce Rho-dependent neurite retraction through different signaling pathways." J Biol Chem **273**(44): 28700-7.

Katoh, H., A. Watabe, et al. (1995). "Characterization of the signal transduction of prostaglandin E receptor EP1 subtype in cDNA-transfected Chinese hamster ovary cells." Biochim Biophys Acta **1244**(1): 41-8.

Kliman, H. J. (2000). "Uteroplacental blood flow. The story of decidualization, menstruation, and trophoblast invasion." Amer Jour Pathol **157**(6): 1759-68.

Kliman, H. J. (2000). "Uteroplacental blood flow. The story of decidualization, menstruation, and trophoblast invasion." Am J Pathol **157**(6): 1759-68.

Korinek, V., N. Barker, et al. (1997). "Constitutive transcriptional activation by a beta-catenin-Tcf complex in APC-/- colon carcinoma." Science **275**(5307): 1784-7.

Krall, J. F., J. D. Barrett, et al. (1984). "Interaction of prostaglandin E2 and beta-adrenergic catecholamines in the regulation of uterine smooth muscle motility and adenylate cyclase in the rat." J Endocrinol **102**(3): 329-36.

Kurzrok, R., and Lieb, C.C. (1930). "Biochemical studies of human semen. II. The action of semen on he human uterus." Proc Soc Exp Biol Med **28**: 268-72.

T. Maniatis, E.F. Fritsch, J. Sambrook, in: N. Ford, C. Nolan, M. Ferguson (eds), Molecular cloning: a laboratory manual, Cold Spring Harbor Laboratory Press, Cold Spring Harbor, N.Y, 1982, pp 9.31-9.62.

Masferrer, J. L., B. S. Zweifel, et al. (1994). "Selective inhibition of inducible cyclooxygenase 2 in vivo is antiinflammatory and nonulcerogenic." Proc Natl Acad Sci U S A **91**(8): 3228-32.

McLatchie, L. M., N. J. Fraser, et al. (1998). "RAMPs regulate the transport and ligand specificity of the calcitonin-receptor-like receptor." Nature **393**(6683): 333-9.

Milligan, G. and S. Rees (1999). "Chimaeric G alpha proteins: their potential use in drug discovery." Trends Pharmacol Sci **20**(3): 118-24.

Morin, P. J., A. B. Sparks, et al. (1997). "Activation of beta-catenin-Tcf signaling in colon cancer by mutations in beta-catenin or APC." Science **275**(5307): 1787-90.

Mu, J., T. Kanzaki, et al. (2003). "Apoptosis and related proteins in placenta of intrauterine fetal death in prostaglandin f receptor-deficient mice." Biol Reprod **68**(6): 1968-74.

Mukhopadhyay, P., P. Bhattacherjee, et al. (1999). "Expression of prostaglandin receptors EP4 and FP in human lens epithelial cells." Invest Ophthalmol Vis Sci **40**(1): 105-12.

Mukhopadhyay, P., L. Bian, et al. (2001). "Localization of EP(1) and FP receptors in human ocular tissues by in situ hybridization." Invest Ophthalmol Vis Sci **42**(2): 424-8.

Mukhopadhyay, P., T. E. Geoghegan, et al. (1997). "Detection of EP2, EP4, and FP receptors in human ciliary epithelial and ciliary muscle cells." Biochem Pharmacol **53**(9): 1249-55.

Namba, T., Y. Sugimoto, et al. (1992). "Mouse thromboxane A2 receptor: cDNA cloning, expression and northern blot analysis." Biochem Biophys Res Commun **184**(3): 1197-203.

Narumiya, S., Y. Sugimoto, et al. (1999). "Prostanoid receptors: structures, properties, and functions." Physiol Rev **79**(4): 1193-226.

Needham, L. K. and E. Rozengurt (1998). "Galpha12 and Galpha13 stimulate Rho-dependent tyrosine phosphorylation of focal adhesion kinase, paxillin, and p130 Crk-associated substrate." J Biol Chem **273**(23): 14626-32.

Negishi, M., Y. Sugimoto, et al. (1995). "Prostaglandin E receptors." J Lipid Mediat Cell Signal **12**(2-3): 379-91.

Neuschafer-Rube, F., E. Engemaier, et al. (2003). "Identification by site-directed mutagenesis of amino acids contributing to ligand-binding specificity or signal transduction properties of the human FP prostanoid receptor." Biochem J **371**(Pt 2): 443-9.

Ohia, S. E. and J. E. Jumblatt (1990). "Prejunctional inhibitory effects of prostanoids on sympathetic neurotransmission in the rabbit iris-ciliary body." J Pharmacol Exp Ther **255**(1): 11-6.

Okuda-Ashitaka, E., K. Sakamoto, et al. (1996). "Suppression of prostaglandin E receptor signaling by the variant form of EP1 subtype." J Biol Chem **271**(49): 31255-61.

O'Neill, G. P. and A. W. Ford-Hutchinson (1993). "Expression of mRNA for cyclooxygenase-1 and cyclooxygenase-2 in human tissues." FEBS Lett **330**(2): 156-60.

Peifer, M. and P. Polakis (2000). "Wnt signaling in oncogenesis and embryogenesis--a look outside the nucleus." Science **287**(5458): 1606-9.

Petiot, A., E. Ogier-Denis, et al. (2000). "Distinct classes of phosphatidylinositol 3'-kinases are involved in signaling pathways that control macroautophagy in HT-29 cells." J Biol Chem **275**(2): 992-8.

Phillips, W. A., F. St Clair, et al. (1998). "Increased levels of phosphatidylinositol 3-kinase activity in colorectal tumors." Cancer **83**(1): 41-7.

Pierce, K. L., T. J. Bailey, et al. (1997). "Cloning of a carboxyl-terminal isoform of the prostanoid FP receptor." J Biol Chem **272**(2): 883-7.

Pierce, K. L., H. Fujino, et al. (1999). "Activation of FP prostanoid receptor isoforms leads to Rho-mediated changes in cell morphology and in the cell cytoskeleton." J Biol Chem **274**(50): 35944-9.

Pierce, K. L. and J. W. Regan (1998). "Prostanoid receptor heterogeneity through alternative mRNA splicing." Life Sciences **62**(17-18): 1479-83.

Raychowdhury, M. K., M. Yukawa, et al. (1994). "Alternative splicing produces a divergent cytoplasmic tail in the human endothelial thromboxane A2 receptor.[erratum appears in J Biol Chem 1995 Mar 24;270(12):7011]." J Biol Chem **269**(30): 19256-61.

Regan, J. W., T. J. Bailey, et al. (1994). "Cloning of a novel human prostaglandin receptor with characteristics of the pharmacologically defined EP2 subtype." Mol Pharmacol **46**(2): 213-20.

Richelsen, B., E. F. Eriksen, et al. (1984). "Prostaglandin E2 receptor binding and action in human fat cells." J Clin Endocrinol Metab **59**(1): 7-12.

Sakamoto, K., T. Ezashi, et al. (1994). "Molecular cloning and expression of a cDNA of the bovine prostaglandin F2 alpha receptor." J Biol Chem **269**(5): 3881-6.

Sakamoto, K., Y. Ishii, et al. (2002). "Cloning and characterization of the novel isoforms for PGF2 alpha receptor in the bovine corpus luteum." DNA Seq **13**(5): 307-11.

Smalley, W. E. and R. N. DuBois (1997). "Colorectal cancer and nonsteroidal anti-inflammatory drugs." Adv Pharmacol **39**: 1-20.

Smith, S. C., P. N. Baker, et al. (1997). "Increased placental apoptosis in intrauterine growth restriction." Am J Obstet Gynecol **177**(6): 1395-401.

Soloff, M. S. and A. Hinko (1993). "Oxytocin receptors and prostaglandin release in rabbit amnion." Ann N Y Acad Sci **689**: 207-18.

Srinivasan, D., H. Fujino, et al. (2002). "Differential internalization of the prostaglandin f(2alpha) receptor isoforms: role of protein kinase C and clathrin." J Pharmacol Exp Ther **302**(1): 219-24.

Srivastava, S., M. Verma, et al. (2001). "Biomarkers for early detection of colon cancer." Clin Cancer Res **7**(5): 1118-26.

Sugimoto, Y., K. Hasumoto, et al. (1994). "Cloning and expression of a cDNA for mouse prostaglandin F receptor." J Biol Chem **269**(2): 1356-60.

Sugimoto, Y., E. Segi, et al. (1998). "Female reproduction in mice lacking the prostaglandin F receptor. Roles of prostaglandin and oxytocin receptors in parturition." Adv Exp Med Biol **449**: 317-21.

Sugimoto, Y., F. Ushikubi, et al. (1999). "Prostanoid receptors: structures, properties, and functions." Physiol Rev **79**(4): 1193-226.

Sugimoto, Y., A. Yamasaki, et al. (1997). "Failure of parturition in mice lacking the prostaglandin F receptor." Science **277**(5326): 681-3.

Takeuchi, K., H. Ukawa, et al. (1999). "Impaired duodenal bicarbonate secretion and mucosal integrity in mice lacking prostaglandin E-receptor subtype EP(3)." Gastroenterology **117**(5): 1128-35.

Tanaka, T., H. Yokohama, et al. (1990). "Synergistic effect of prostaglandin E2 and ouabain on catecholamine release from cultured bovine adrenal chromaffin cells." J Neurochem **54**(1): 86-95.

Thierauch, K. H., H. Dinter, et al. (1994). "Prostaglandins and their receptors: II. Receptor structure and signal transduction." J Hypertens **12**(1): 1-5.

Thomas, D. W., R. B. Mannon, et al. (1998). "Coagulation defects and altered hemodynamic responses in mice lacking receptors for thromboxane A2." J Clin Invest **102**(11): 1994-2001.

Toh, H., A. Ichikawa, et al. (1995). "Molecular evolution of receptors for eicosanoids." FEBS Letters **361**(1): 17-21.

Woodward, D. F., C. E. Fairbairn, et al. (1995). "Radioligand binding analysis of receptor subtypes in two FP receptor preparations that exhibit different functional rank orders of potency in response to prostaglandins." J Pharmacol Exp Ther **273**(1): 285-7.

Zhou, C., Y. Yang, et al. (1990). "Mini-prep in ten minutes." Biotechniques **8**(2): 172-3.